2015

Polycyclic Aromatic Hydrocarbons Dynamics in the Northern Gulf of Mexico

Puspa Lal Adhikari
Louisiana State University and Agricultural and Mechanical College

POLYCYCLIC AROMATIC HYDROCARBONS DYNAMICS IN THE NORTHERN GULF OF MEXICO

A Dissertation

Submitted to the Graduate Faculty of the
Louisiana State University and
Agricultural and Mechanical College
in partial fulfillment of the
requirements for the degree of
Doctor of Philosophy

in

The Department of Oceanography and Coastal Sciences

by
Puspa Lal Adhikari
B.Sc., Tribhuvan University, 2003
M.Sc., Tribhuvan University, 2005
M.S., University of Arkansas at Pine Bluff, 2011
August 2015

ACKNOWLEDGEMENTS

I would like to take this opportunity to thank my advisor Dr. Kanchan Maiti for his endless guidance, insight, mentorship, friendship and encouragement to be the best I could be. He has provided me with an immeasurable amount of knowledge on chemical oceanography, oceanographic instrumentation, their successful deployment and recovery, and most importantly on how things work differently in oceanographic settings. I also owe a great deal of gratitude to my distinguished committee members Drs. Edward Overton, John White, Mark Benfield, Brian Marx, and Randy Duran for their time and guidance. Your invaluable suggestions guided me towards the successful completion of my dissertation. Special thanks to Dr. Edward Overton for providing significant insight on PAHs analysis and Dr. Brain Marx for statistical guidance. Sincere thanks to Dr. John White, for providing an opportunity to work in his lab for an additional project on 'phosphorous fractionation'.

I appreciate all help from the captain and crew of the *R/V Endeavor*, *R/V Walton Smith* and the *R/V Pelican.* This study would not have been possible without my lab mates Patrick Jones and Somiddho Bosu. Thank you for your support throughout the sample collection and analysis. I owe gratitude to Steve Jones, and Chris Cleaver for their support in instrumentation, and Dr. Malinda Sutor for her help with sampling, cruise planning and management. Also, I would like to thank Dr. Brad Rosenheim for inviting me to sample during the CARTHE cruise on board *R/V Pelican.* I am grateful to Drs. Hernando Bacosa, Jim McManus, Silke Severmann and William Berelson for their helping hands on sediment core collection and core slicing. Special thanks to Buffy Meyer, Heng Gao and Scot Miles for their time, support and guidance during lab analysis for PAHs. I also want to thank Charles Milan for his assistance with CHN analysis.

I would like to express my gratitude to all the faculty and staff of the Department of Oceanography and Coastal Sciences for their help with academic and non-academic issues, whenever needed. Also, I would like to thank all my friends, on and off-campus, and Nepali community members in Baton Rouge for being a part of my life for last four years. Thank you everyone.

I owe a depth of gratitude to my family whose support, encouragement and loving patience made this dissertation possible - my parents Giri P. Adhikari and Maya Adhikari, sister Sita, brother Subash, my wife Samikshya, my son Prasun and my extended family. I honestly could have not even started on this journey without your motivation. Thank you for caring so much, and most importantly for your patience during my graduate studies and always believing in my ability to achieve this dream.

Finally, this research would not have been possible without the funding support from the Gulf of Mexico Research Initiative (GoMRI) and the Bureau of Ocean Energy Management (BOEM).

TABLE OF CONTENTS

LISTS OF TABLES

LIST OF FIGURES

ABSTRACT

Polycyclic aromatic hydrocarbons (PAHs) are introduced into the marine environment via oil seeps/spills, riverine discharges, continental runoff, coastal erosion, and atmospheric deposition. An estimated 2.1 x 10^{10}g of PAHs entered into the northern Gulf of Mexico (GOM) during the Deepwater Horizon (DWH) oil spill in 2010. It became evident following the oil spill that accurate quantification of ultimate fate of these potentially carcinogenic and/or mutagenic organic pollutants is extremely challenging. In general, very little is known about PAHs fate, distribution and accumulation in the open ocean ecosystems. This study determines the upper ocean vertical fluxes and sedimentary PAHs accumulation rates in the GOM.

The concentrations of particulate and dissolved ΣPAH_{43} varied between 0.2-1.3 ng/L, and 24-58 ng/L, respectively during this study period in April 2012 and 2013. Dissolved ΣPAH_{43} were found to be orders of magnitude lower than the values reported during DWH oil spill. Sediment trap-based vertical fluxes of particulate ΣPAH_{43} varied between 2-8 μg m^{-2} d^{-1}. The vertical fluxes are found to be an important loss term for PAHs in the upper ocean with 3-7% of total particulate PAHs inventory in the euphotic zone being lost daily via this pathway. The trap-independent PAHs fluxes estimated via ^{238}U-^{234}Th disequilibria are similar to the trap-derived fluxes, within the factor of three. The ^{234}Th-based method provides a larger spatial coverage in relatively shorter time and thus can be more appropriate for upper ocean PAHs flux estimation in high traffic areas like the GOM.

The concentrations and sediment ΣPAH_{43} accumulation rates in sediment cores collected one to three years after DWH varied between 26-160 ng/g and 1.4-63 ng $cm^{-2}y^{-1}$, respectively. Observed ΣPAH_{43} concentrations are similar to the background pre-spill values, indicating long term impacts of the oil spill on sediment PAHs to be minimal. The source diagnostic analyses

suggest a noticeable change in PAHs composition in the last few years, towards lower molecular weight dominancy in PAHs profiles, attributed to the deposition of higher molecular weight PAHs byproducts by control combustion during the DWH oil spill. This study can serve as post-spill baseline PAHs concentrations and their accumulation rates in the GOM.

CHAPTER 1: INTRODUCTION

Polycyclic aromatic hydrocarbons (PAHs) are a group of ubiquitous organic pollutants, composed of 2-7 fused benzene rings in different arrangements (Albers, 2003; Haynes, 1968; Neff, 1979). They are typically present in nature as a complex mixture of hydrocarbons (Albers, 2003; Neff, 1979). PAHs can be introduced into the marine environments via natural oil seeps, accidental oil spills, riverine discharges, continental runoff, coastal erosion, and atmospheric deposition (Dachs et al., 2002; Mitra and Bianchi, 2003, Tsapakis et al., 2006). A number of PAHs such as naphthalene, benzo(a)pyrene, benzo(e)pyrene and their metabolic products are of major environmental health concerns because of their toxic, carcinogenic and mutagenic properties (Samanta et al., 2002; Yan et al., 2004).

The environmentally significant PAHs have molecular weights varying between 128.16 (naphthalene) to 300.36 g mol^{-1} (coronene) (Eisler, 1987; Haynes, 1968; Neff, 1979). Individual PAHs with 2-6 benzene rings are commonly identified and quantified for oil spill analyses (Table 1.1). In general, PAHs with 2-3 benzene rings are categorized as lower molecular weight PAHs (LMW-PAHs), with 4 rings as middle molecular weight PAHs (MMW-PAHs), while the PAHs with more than 4 rings are considered the higher molecular weight PAHs (HMW-PAHs) (Meador et al., 1995). Molecular weight determines physico-chemical properties of PAHs and controls their behavior, distribution and biological effects (Eisler, 1987). Aqueous solubility and volatility of PAHs decreases while boiling point, persistency, resistance to biodegradation, and partition coefficient increases with increasing molecular weight (Albers, 2003; Kanaly and Harayama, 2000; May et al., 1978). PAHs, especially the HMW-PAHs, are hydrophobic and tend to partition in non-polar compounds like lipids in organisms and are often referred to as lipophilic organic compounds (Meador et al., 1995; Wild and Jones, 1995). Most PAHs are

Table 1.1. Numbers of benzene rings, molecular weight and partition coefficients (Log Kow) of the polycyclic aromatic hydrocarbon (PAH) compounds commonly used in oil spill analysis.

PAH	Benzene rings	Molecular weight (g mol^{-1})*	Log Kow*
Naphthalene	2	128	3.36
C-1 Naphthalene	2	142	3.80
C-2 Naphthalene	2	156	4.20
C-3 Naphthalene	2	170	4.66
C-4 Naphthalene	2	184	5.10
Fluorene	3	166	4.21
C-1 Fluorene	3	180	4.72
C-2 Fluorene	3	194	5.20
C-3 Fluorene	3	208	5.70
Dibenzothiophene	3	184	4.53
C-1 Dibenzothiophene	3	198	4.96
C-2 Dibenzothiophene	3	212	5.42
C-3 Dibenzothiophene	3	226	5.89
Phenanthrene	3	178	4.57
C-1 Phenanthrene	3	192	5.05
C-2 Phenanthrene	3	206	5.46
C-3 Phenanthrene	3	220	5.92
C-4 Phenanthrene	3	234	6.32
Anthracene	3	178	4.53
Fluoranthene	4	202	5.08
Pyrene	4	202	4.92
C-1 Pyrene	4	216	5.48
C-2 Pyrene	4	230	6.15
C-3 Pyrene	4	244	6.60
Benzo(a)Anthracene	4	228	5.89
Chrysene	4	228	5.71
C-1 Chrysene	4	242	6.14
C-2 Chrysene	4	256	6.43
C-3 Chrysene	4	270	6.94
C-4 Chrysene	4	284	7.36
Benzo (b) Fluoranthene	5	252	6.27
Benzo (k) Fluoranthene	5	252	6.29
Benzo (e) Pyrene	5	252	6.44
Benzo (a) Pyrene	5	252	6.11
Perylene	5	252	6.44
Dibenzo (a,h) anthracene	5	278	6.71
Indeno (1,2,3 - cd) Pyrene	6	276	6.72
Benzo (g,h,i) perylene	6	276	6.71

*(*Source: Diercks et al., 2010; Haynes, 2013; Mackay and Shiu, 1977; Wang et al., 2006, and Dr. Edward Overton, Department of Environmental Sciences, Louisiana State University, Baton Rouge).*

biodegradable however, their rate of degradation is slow in aquatic environment and they can persist for a long time in anaerobic conditions (Albers, 2003; Bossert et al., 1984; Gutierrez, 2011). PAHs can bio-accumulate in some organisms but most of them have low tendency of bio-magnification due to their rapid metabolization in organisms (Eisler, 1987; Neff, 1979).

1.1. Human health effects of PAHs

Aromatic hydrocarbons were and, in some cases, are still being used in commercial products like dyes, plastics, pesticides and cosmetics (Bechtold and Mussak, 2009; Harvey, 1991; Mumtaz et al., 1996). PAHs like benzo[a]pyrene and dibenzo[a,h]anthracene were among the first few compounds declared to be carcinogenic to humans in early 20^{th} century. This made researchers realize that microorganisms were not the only cause of diseases but can also be caused by some relatively simple organic compounds like the PAHs (Harvey, 1991). A number of PAHs and their metabolic products have been found to be toxic, mutagenic and/or carcinogenic even at relatively low levels (Eisler, 1987; Samanta et al., 2002; Yan et al., 2004). PAHs are lipid soluble (lipophilic) and can be readily taken up by plants and animal tissues, where they either directly cause toxicity or are metabolized into reactive metabolites to bind with cellular proteins and DNA leading to deleterious effects such as mutations, malformation, tumors and cancer (Albers, 2003; Eisler, 2000; Santodonato, et al., 1981). The LMW-PAHs can cause acute toxicity but are not carcinogens, in contrast HMW-PAHs are less toxic but are carcinogenic, mutagenic and/or teratogenic (causing birth defects) to organisms (Eisler, 1987). The acute human health effects of PAHs can be respiratory impairment, eye irritation, nausea, vomiting, diarrhea, while the long term effects are reduced immunity, neurological disorders, genotoxicity, teratogenic effects, and risks of cancers (e.g., skin, lungs, respiratory tract, bladder, gastrointestinal) (Boffetta et al., 1997; Kim et al., 2013; Mumtaz et al., 1996; Olsson et al.,

2010). The toxic and persistent nature of PAHs have resulted in their listing as priority pollutants by various government agencies (e.g., US EPA) and are regularly monitored worldwide in different environmental matrices. The sixteen environmentally significant PAHs listed by the US EPA in the priority pollutant list are; Naphthalene, Acenaphthene, Acenaphthylene, Fluorene, Phenanthrene, Anthracene, Fluoranthene, Pyrene, Benzo[a]anthracene, Chrysene, Benzo[b]fluoranthene, Benzo[k]fluoranthene, Benzo[a]pyrene, Dibenzo[a,h]anthracene, Benzo[ghi]perylene, and Indeno[1,2,3-cd]pyrene (Figure 1.1).

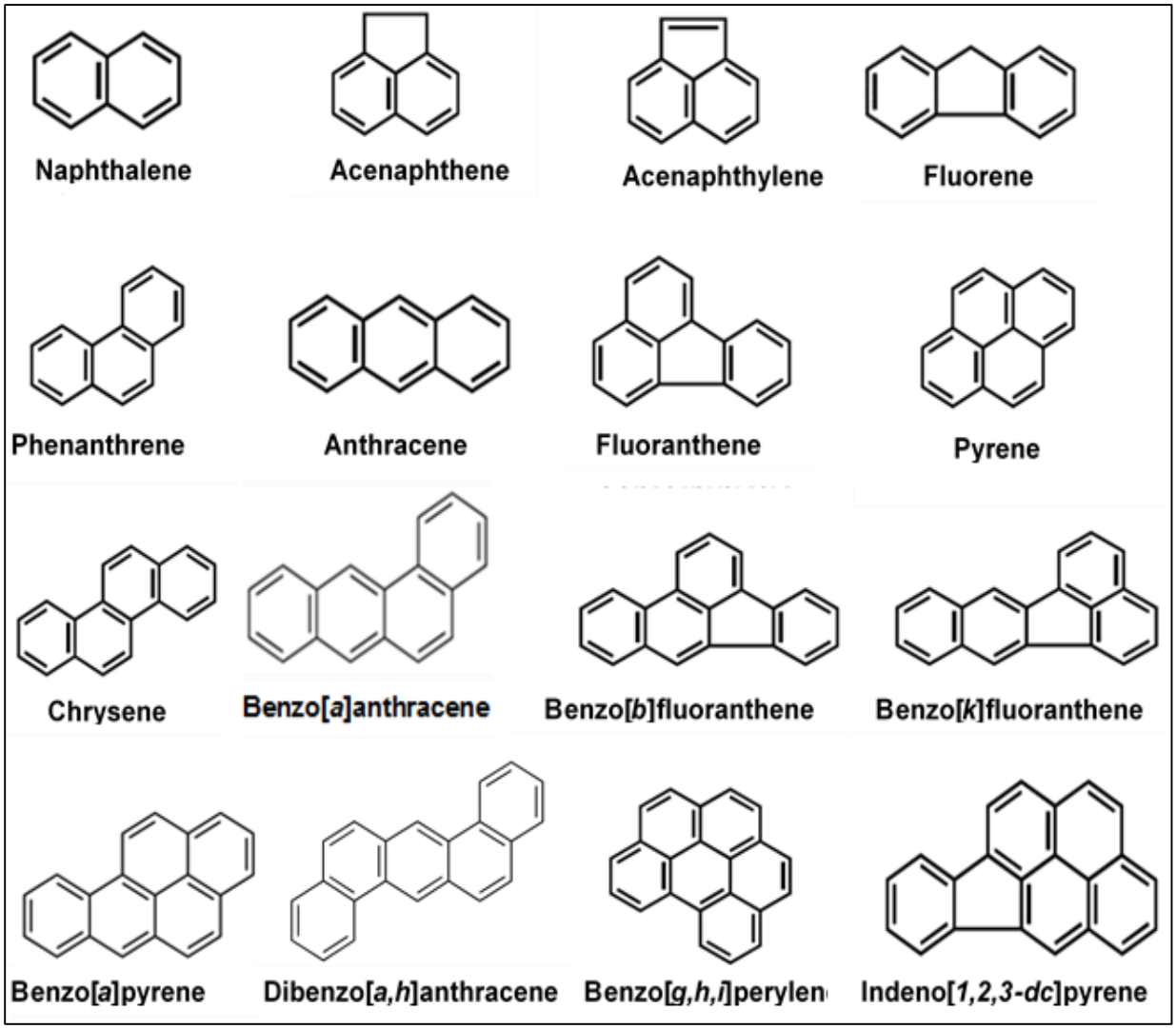

Figure 1.1. Molecular structures of the sixteen polycyclic aromatic hydrocarbons listed in the US EPA priority pollutant list (Bruzzoniti et al., 2010).

1.2. Sources of PAHs

The major processes responsible for PAHs formation are: i) high temperature incomplete thermal decomposition (pyrolysis) and subsequent recombination (pyrosynthesis) of organic compounds such as petroleum products, coal, wood, tobacco, agricultural wastes and other carbon containing materials (Albers, 2003; Mastral and Callen, 2000), ii) long term sediment diagenesis at low temperature within the sedimentary rock formations like the natural coal and oil deposits (Grimmer, 1983; Neff, 1979), and iii) biological activities of certain organisms (Eisler, 2000; Wilcke et al., 2000).

Natural oil seeps, forest fires, volcanoes and biosynthesis in plants, fungi and bacteria are the natural inputs of PAHs to the environment (Albers, 2003; Neff, 1979; Wild and Jones, 1995). Petroleum refining, accidental or intentional petroleum spills/leakage, fossil fuel combustion, residential firewood burning, industrial and domestic effluents, coal tar, asphalt, incineration, runoffs and atmospheric deposition are the major anthropogenic sources of PAHs (Eisler, 2000; Neff, 1985). Depending upon their origin, PAHs can be broadly categorized into two groups; petrogenic and pyrogenic PAHs. Petrogenic PAHs are those produced due to incomplete combustions of organic matters while the pyrogenic PAHs are from crude oil and other petroleum products (Budzinski et al., 1997; Yunker et al., 2002).

1.3. Sinks of PAHs in marine ecosystems

The environmental fate of PAHs released into the marine ecosystems is determined by various physical, chemical, and biological processes acting on them (Albers, 2003). Evaporation, photo-chemical oxidation, natural/artificial dispersion, dissolution, emulsion, biodegradation, vertical/lateral transports, and sedimentation play an important role in PAHs dynamics in marine environment (Albers, 2003; Berrojanbiz et al., 2011). The particle-mediated vertical transport

fluxes followed by burial in deep-sea sediments is one of the most important mechanisms of upper ocean PAHs removal (Dachs et al., 1997; Gustafsson, 1997a; Lipiatou et al., 1997).

The PAHs with low aqueous solubility and high partition coefficients readily sorbed onto marine particles, mainly organic rich particulate matter such as particulate organic carbon (POC), which are removed from water column via vertical sinking of particles and subsequently buried in the seafloor sediments (Dachs et al., 2002; Gustafsson et al., 1997a; Mackay and Shiu, 1977). Thus the seafloor is a final repository of PAHs where they can persist for a long time and this burial in deep-sea sediments is considered to be the major global sinks for PAHs entering the marine ecosystems (Gustafsson et al., 1997a; Marini and Frapiccini, 2013; Neff, 1979). In order to understand the ultimate fate of PAHs in marine environment, it is essential to quantify this critical pathway of PAHs removal, via sinking particles and their sedimentary burial. Such information can provide insights into the distribution, dispersal, and residence time of PAHs in the ocean and help to construct global mass-balance and transport models (Dachs et al., 1996; Gustafsson et al., 1997a; Lipiatou et al., 1993).

In the last two decades, a number of studies have shown that the large, rapidly sinking particles can account for a significant portion of the total flux of persistent organic pollutants (POPs) such as PAHs (Dachs et al., 1996; Deyme et al., 2011; Tsapakis et al., 2006). However, upper ocean PAHs flux estimates are globally scarce, primarily due to the absence of convenient/feasible method to quantify this mechanism (Gustafsson et al., 1997a). There are limited number of PAHs flux studies based on deep-sea sediment traps, dated bottom cores and/or numerical modeling (Bouloubassi et al., 2006; Lipiatou et al., 1997; Palm et al., 2004). These methods potentially integrate PAHs fluxes over time and space, and may not represent the actual upper ocean PAHs fluxes.

Surface-tethered drifting sediment traps deployed for relatively short period of time (2-3 days) provide a direct instantaneous measurement of upper ocean PAHs fluxes (Buesseler et al., 2007). These trap-based estimates however, do not provide enough spatial coverage, and are difficult to deploy and retrieve. An alternative technique of utilizing naturally occurring ^{238}U series radioisotopes as a tracer of particle-mediated sinking fluxes of PAHs has been used by few previous studies (Gustafson et al., 1997a). This method may provide reliable data with large spatial coverage in shorter time and lower costs. It can be a better approach of estimating upper ocean PAHs fluxes, especially in high traffic areas like the northern Gulf of Mexico (GOM), where drifting sediment traps are difficult to deploy due to the presence of numerous rigs, and traffic hazards from transportation and exploration activities (Adhikari et al., 2015; Buesseler et al., 2007).

The vertical fluxes of PAHs when coupled with their accumulations rates in the seafloor sediments can provide valuable information on the effects of biogeochemical processes on sinking PAHs in the water column. It helps to determine what fraction of the upper ocean PAHs inventory reaches to the bottom and what fraction ultimately get buried in sediments. The PAHs accumulation rates based on ^{210}Pb-dated sediment cores can provide an understanding of historic variations in PAHs inputs, effects of sediment diagenesis on PAHs and their long term sink in the marine systems. Such reconstruction of historic PAHs accumulation rates can provide an opportunity to see the effects of a particular PAHs input (e.g., Deepwater Horizon oil spill in the northern GOM) on sedimentary PAHs pollution trend (Santschi et al., 2001).

1.4. PAHs pollution in the northern Gulf of Mexico

The northern GOM is a major hub for oil and gas production, oil refineries, seafood production, commercial and recreational fishing, and marine transportation (NOAA, 2008). This

makes the northern GOM, an area of major ecosystem health concerns, before, and especially after the Deepwater Horizon (DWH) oil spill in 2010. The northern GOM represents an ideal location to investigate and understand the source, fate, transport and accumulation of PAHs, in water column and sediments. The Mississippi River discharge, coastal erosion, atmospheric deposition, numerous natural oil seeps, gas hydrates and accidental or intentional oil spill/leaks (over 1,500 oil spills reported per year) related to petroleum exploration/transportation are the sources of PAHs in the northern GOM (Mitra and Bianchi, 2003; Overton et al., 2004; Wang et al., 2011). In addition to these background sources, an estimated 4.1 million barrels of oil including 2.1×10^7 kg of PAHs entered into the northern GOM waters during the DWH oil spill in 2010 (Reddy et al., 2012). It has been estimated that 4-31% of the PAHs released during DWH oil spill were deposited in seafloor, covering an area of 3200 km^2 in the northern GOM (Valentine et al., 2014). Release of such an unprecedented amount of PAHs in a single event can substantially increase their concentrations and impair health of the marine ecosystems, both the pelagic and benthic communities. The toxic, carcinogenic, mutagenic and persistent nature of PAHs coupled with large seafood/fishing industry in the Gulf make them a critical group of organic contaminants that need to be monitored thoroughly in this region.

A number of studies have been conducted to assess PAHs distribution in the northern GOM, especially after the DWH oil spill, primarily focusing on surface sediments, dissolved PAHs, and their toxicity to aquatic organisms (Allan et al., 2012; Diercks et al., 2010; Turner et al., 2014; Xia et al., 2012). However, the exact fate of PAHs released in the water column and sediments remains a topic of debate. It became evident following the DWH oil spill that accurate quantification of the ultimate fate of the spilled oil was extremely challenging and baseline data on concentration and flux of petroleum-derived hydrocarbons in the water column are missing

for this region. In general, very little is known about how hydrocarbons and toxic byproducts like PAHs behave in the marine systems and what drives their fate and distribution in the open ocean. The longer the residence time of PAHs in a marine ecosystem, the higher their chance of getting into the food web and cause detrimental effects on marine organisms and human health. It is thus essential to study transports, residence time, sinks and long term fates of PAHs released into the marine ecosystems (Dachs et al., 2002; Gustaffson et al., 1997a; Lipiatou, et al., 1997).

1.5. Dissertation goals and objectives

The overarching goal of this study is to provide a comprehensive understanding of PAHs dynamics in the northern GOM in terms of their removal from upper ocean via vertical sinking and accumulation in bottom sediments. To the best of my knowledge, this is the first study to quantify the vertical flux and residence time of particulate PAHs, and to determine sedimentary PAHs accumulation rate in the northern GOM. In order to carry out this research, water column and sediments samples were collected from four different cruises during 2011 to 2013 in the northern GOM onboard *R/V Endeavor* in summer 2011 (40 days), *R/V Walton Smith* in spring 2012 (15 days) and 2013 (18 days), and *R/V Pelican* in summer 2013 (8 days).

This study also provided a rare opportunity to contrast the PAHs fluxes simultaneously estimated using two different techniques i.e. surface-tethered drifting sediments traps and ^{238}U-^{234}Th disequilibria, and compare it to the ^{210}Pb-based PAHs accumulation rates in sediments. The near absence of pre-DWH baseline PAHs data from deep-sea made it difficult to accurately assess the long-term impact of DWH oil spill. The results from this study thus can serve as post-spill baseline data on concentrations, vertical transport fluxes and accumulation rates of PAHs in the northern GOM.

The objectives of this study were to: 1) quantify the concentrations, vertical fluxes and residence times of particulate PAHs in the upper mesopelagic zone of the northern GOM; 2) utilize ^{234}Th-^{238}U disequilibrium as a possible proxy for measuring particulate PAHs fluxes in the northern GOM water column; and 3) quantify PAHs concentrations, distributions and ^{210}Pb-based PAHs accumulation rates in the northern GOM sediments, 1-3 years after the DWH oil spill. Each of these objectives are separately addressed in next three chapters.

CHAPTER 2: VERTICAL FLUXES OF POLYCYCLIC AROMATIC HYDROCARBONS IN THE NORTHERN GULF OF MEXICO[1]

2.1. Introduction

Petroleum-derived hydrocarbons can be introduced into the marine environment via oil seeps/spills, riverine discharges, continental runoff, coastal erosion, and atmospheric deposition (Albers et al., 2003; Dachs et al., 2002; Lipiatou et al., 1997; Mitra and Bianchi, 2003, Park et al., 2001, 2002; Tsapakis et al., 2006). Among these hydrocarbons, polycyclic aromatic hydrocarbons (PAHs) are of major environmental concern as some of the PAHs and their metabolic products are toxic, mutagenic and/or carcinogenic (Samanta et al., 2002; Yan et al., 2005). These hydrocarbons are readily taken up by plant and animal tissues, can bio-accumulated in some marine organisms and persistent in nature (Albers et al., 2003; Sverdrup et al., 2002, Tao et al., 2009). In general, PAHs have low aqueous solubility, with both solubility and volatility decreasing with increasing molecular weight (Albers et al., 2003; Mackay and Shiu, 1977; May et al., 1978). Due to their low solubility and high partition coefficients, PAHs entering into an aquatic environment get readily sorbed onto particles, mainly organic rich particulate matter (Dachs et al., 2002; Gustafsson et al., 1997a, 1997b, 2001; Ko et al., 2003; May et al., 1978). PAHs sorbed onto these particles in the open oceans are subsequently deposited to the sediments via vertical sinking which serves as a major mechanism for the removal and global cycling of particle reactive organic pollutants such as PAHs (Dachs et al., 2002; Lipiatou et al., 1997). The open ocean and the deep-sea sediments are thus considered the major global sinks for environmental releases of petroleum-derived hydrocarbons, and marine particles are thought to

[1] This chapter previously appeared as: Adhikari, P.L., Maiti, K., Overton, E.B., 2015. Vertical fluxes of polycyclic aromatic hydrocarbons in the northern Gulf of Mexico. Marine Chemistry 168, 60-68. It is reprinted by permission of Elsevier (see Appendix 1).

play a crucial role in the distribution, transport and fate of these hydrocarbons entering into ocean waters (Gustafsson et al., 1997a; NRC, 2003). However, other loss terms besides vertical sinking such as evaporation, biodegradation, photo-oxidation, dispersion, and lateral transport can also play an important role in PAHs dynamics in marine waters (Berrojalbiz et al., 2011). Researchers have long recognized the importance of quantifying vertical fluxes of such organic contaminants from surface to deep ocean in order to understand their dispersal and residence time in marine environment and construct global mass-balance fate models (Dachs et al., 1996; Lipiatou et al., 1993). Studies carried out during the last two decades have shown that large, rapidly sinking particles can account for a significant portion of the total flux of organic contaminants (Dachs et al., 1996; Elder and Fowler, 1977) and direct measurements of such particle-associated contaminant fluxes can be carried out using sediment traps (Bouloubassi et al., 2006; Dachs et al., 1996; Deyme et al., 2011; Lipiatou et al., 1993; Raoux et al., 1999; Tsapakis et al., 2006).

The northern Gulf of Mexico (GOM) provides an ideal location to investigate the role of marine particles in modulating vertical PAHs fluxes. This region receives hydrocarbons from many sources including spills/leaks (over 1,500 oil spills reported per year), numerous natural seeps, atmospheric deposits, and riverine input (Mitra and Bianchi, 2003; Park et al., 2001, 2002; Wade et al., 1989). An estimated 2.1×10^{10} g of PAHs also entered into the northern GOM waters during the 2010 Deepwater Horizon (DWH) oil spill (Reddy et al., 2012). A number of studies have been conducted to assess PAHs distribution in the northern GOM but they mainly focus on surface sediments, dissolved PAHs, and their toxicity to aquatic organisms (Allan et al., 2012; Diercks et al., 2010; Mitra et al., 2012; Sammarco et al., 2013; Xia et al., 2012). However, to date none of these studies addresses the vertical fluxes of particulate phase PAHs associated

with sinking particles in the GOM. The absence of flux measurements in the water column limits our understanding of the distribution, transport and fates of PAHs in this region.

The major objective of this study is to quantify the vertical fluxes of particulate PAHs for the first time in the upper mesopelagic zone of the northern GOM. The mesopelagic or the "twilight" zone located between the base of the euphotic zone and 1000 m, is the zone of highest particle and organic matter attenuation with depth, with particulate matter sinking through this zone in relative short time frame. The mesopelagic layer has been considered as the largest "heterotrophic digester" of the oceans (Benner, 2000) and accounts for 95% of the fish biomass in the ocean (Irigoien, et al., 2014). The nature, transformation and remineralization of organic matter through the mesopelagic layer affect the quantity and stoichiometry of material delivered to the bathypelagic zone and thus play a critical role in setting a limit on the amount of PAHs that can be transported to the deep-sea and seafloor sediments.

2.2. Materials and methods

2.2.1. Sample collection

Three types of samples (water for dissolved PAHs, suspended particles for particulate PAHs and settling particles for sinking PAHs) were collected from the vicinity of the DWH well head in the northern GOM aboard the *R/V Walton Smith* during April 2012 and 2013 cruises. In order to determine any spatial variability in PAHs concentrations and fluxes in this region, sampling were carried out at three different locations; near Deepwater Horizon spill site (DWH), north of DWH (NDWH), and south of DWH (SDWH). These locations were repeated again in 2013 to identify any trend in temporal variability. Sampling locations for 2012 are labeled as NDWH-12, DWH-12 and SDWH-12, while sampling locations for 2013 are NDWH-13, DWH-

13 and SDWH-13 (Figure 2.1). The stations are ~100 km from the mouth of Mississippi River and in water depths of 1200-2000 m.

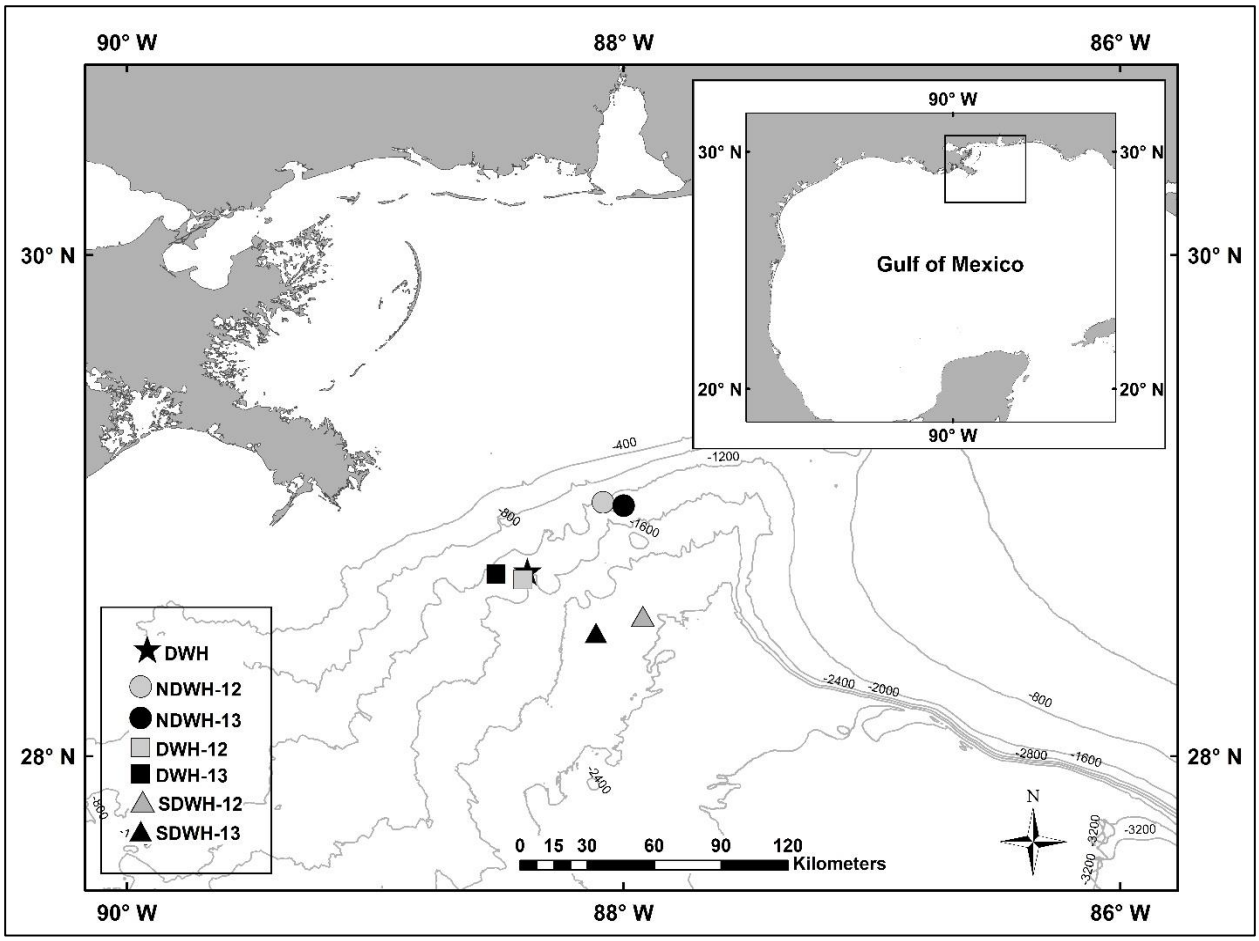

Figure 2.1. Sampling locations in the northern Gulf of Mexico, in the vicinity of Deepwater Horizon (DWH) oil spill site. Sampling stations are, NDWH-12 and NDWH-13; north of DWH for 2012 and 2013, DWH-12 and DWH-13; at DWH for 2012 and 2013, and SDWH-12 and SDWH-13: south of DWH for 2012 and 2013.

2.2.2. Dissolved

At each sampling station, vertical profiles of water samples were collected from 0-1000 m using shipboard CTD sampling rosette. At each depth, 20 L of water samples were collected for the analysis of dissolved PAHs. Immediately after collection, water in the Niskin bottles was directly passed through pre-conditioned Solid-phase extraction (SPE) disks with C-18 media (C.I. Agent® Storm-Water Solutions, WA, USA). The solid-phase extraction of PAHs on C-18

media has been previously used in number of studies (Kiss et al., 1996; Kootstra et al., 1995; Marce and Borrull, 2000). Flow rates during filtrations were kept constant at about 50 ml min^{-1} using Masterflex Peristaltic Pumps (Cole-Parmer, IL, USA). After the completion of filtration, the SPE disks were stored at -20 $^{\circ}$C until analysis. The PAHs concentration extracted from these disks represents total water column PAHs concentration. Given the expected low particle concentration in the open ocean, no additional pre-filters were added in line with the SPE disks. The particulate PAHs concentration were found to represent ~1% of total PAHs concentration (next section) which is well within the analytical errors of total PAHs concentrations measurements and hence considered negligible. For the practical purpose, these concentrations therefore were considered as dissolved PAHs.

2.2.3. Particulates

Particulate PAHs concentrations in the open ocean are very low (Dachs et al., 1997; Gustafsson et al., 1997a; Lipiatou et al., 1997) therefore it was essential to collect and filter large volumes of water samples in order to get concentrations well above the detection limits of the analytical instruments. Particle samples were collected by *in situ* filtration using battery-operated submersible pumps (McLane Research Laboratories, Inc., Falmouth, USA). The pump deployment consisted of a vertical array of four pumps at 100, 150, 250, and 350 m depths. Two such deployments were performed at each station, one immediately after the deployment of sediment traps and the other just before the recovery of the sediment traps. The average of these two deployments are presented here as a representative of the suspended particulate concentration in the water column, during the period the sediment traps were collecting sinking particles (see section below). Large-volume water samples (~500-800 L) were filtered at a flow rate of 4-6 L min^{-1} through acid washed 150 mm pre-filters (Nitex screen of 51 µm pore sizes) to

exclude swimmers and zooplanktons, and then onto pre-combusted (at 450 ºC for 8 hours) 1 µm nominal, 150 mm diameter Quartz Microfiber Filter (QMA) (Whatmann, Kent, U.K.) to capture operationally defined suspended particles. The filtration rate (4-6 L min^{-1}) used in this study minimizes the chances of over collection of larger particles and particle breakage during filtrations (Maiti et al., 2012). After the recovery of pumps, the filters were taken out and two 22 mm diameter subsamples were collected for particulate organic carbon (POC) analysis. The subsamples for POC analysis were dried onboard at 60 ºC while the rest of the filter was stored at -20 ºC for PAHs analysis. The particles captured onto the screens (>51 µm) were tested for PAHs signatures and found to be below the detection limits, therefore only QMA filters were used for the further analysis.

2.2.4. Settling particles

Direct measurements of PAHs fluxes were carried out using sediment traps. Surface-tethered drifting sediment trap arrays were utilized to minimize the hydrodynamic issue, which is caused by horizontal flow over the mouth of the trap and trap motion that may lead to under or over sampling of sinking particulate material (Buesseler, 2007; Gardner, 1985; Gust et al., 1996). This issue mostly affects traps in the upper few hundred meters of the water column, where current velocities are highest. The sediment trap arrays were deployed for 2.5 to 3.0 days at 150, 250 and 350 m below surface to capture sinking particles at two stations each year; stations DWH-12 and SDWH-12 in 2012, and DWH-13 and SDWH-13 in year 2013. Due to bad weather I was unable to deploy sediment traps at station NDWH-12 in 2012. In 2013, after the second deployment at DWH-13, I lost one of the trap arrays at 350 m due to interference from a seismic survey boat and could not deploy traps at station NDWH-13. The design, construction, pre-conditioning, deployment, recovery and sample processing of the sediment traps are available

elsewhere (Lamborg et al., 2008). Briefly, each sediment trap array, consisted of a surface float (supporting a flasher, radar target and Argos/GPS transmitter), enough line to deploy three frames holding trap tubes at target depths, a drogue at 10 m to reduce hydrodynamic slip that can occur with surface tethered systems as a result of wind forcing as well as bungee/floats to dampen wave/wind action. Each frame of sediment trap consist of eight cylindrical collection tubes (height = 60 cm, diameter = 12 cm; H/D ratio = 5) to capture the sinking particles and baffle at the top to prevent particle loss and to avoid swimmer in the tubes. The sediment trap tubes were fitted with time-triggered lids designed to close at the end of the deployment. Before every deployment, the sediment tubes were filled with freshly filtered (1 µm pore size) seawater collected from the same depth they were to be deployed. The trap-tubes were then poisoned immediately prior to deployment with 2% buffered formaldehyde solution (freshly prepared in brine) by slowly injecting about 500 ml of the solution directly into the bottom. Direct injection of the denser brine solution to the bottom of the collecting tubes helped to keep the formaldehyde solution at the bottom. Formaldehyde solution retards bacterial activities on the organic matter that settled at the bottom of the trap tubes (Bouloubassi et al., 2006; Deyme, et al., 2011; Lee et al., 1992). The sediment traps were deployed for short period of times ($\leq$ 3 days) and the sinking particles captured in trap tubes were immediately processed after their recovery which minimizes the solubilization bias of sediment traps (Buesseler, et al. 2007). After recovery of the traps, particles were allowed to settle in the tubes, by letting the traps to stand for at least 2 h. The excess seawater was then decanted using silicon tubing and a slow transfer pump. Out of the eight sediment trap tubes deployed at each depth, four tubes were allocated for PAHs analysis, two tubes for POC analysis, one for other analysis and one was treated as blank (lid of the blank tube remained closed throughout the deployment period). For PAHs analysis, the remaining

contents in four tubes from each depth were pooled together by passing them through an acid-washed nylon mesh (350 µm pore) in Teflon filter holder, to remove possible swimmers (Lamborg et al., 2008). The solution was then homogenized and filtered onto pre-combusted (at 450 $^{\circ}$C for 8 hours) Whatman GF/F filters (47 mm diameter, 0.7 µm pore size). The samples for POC and blank were also processed and collected on GF/F filters in same manner as mentioned above. The filters for PAHs analysis were then stored at -20 $^{\circ}$C while the POC samples were dried onboard at 60 ºC, folded, wrapped in pre-combusted aluminum foil and stored in petri-dishes at room temperature until analysis.

2.2.5. Sample extraction and PAHs analysis by GC/MS

In the laboratory, the samples were spiked with known concentrations of Phenathrene-d_{10} recovery standard prior to extraction. Particulate and trap samples were then Soxhlet extracted for 24 hours with dichloromethane (DCM), while the SPE disks for dissolved PAHs were extracted using method described for C.L.A.M (continuous low-level aquatic monitoring) SPE Disks elution (C.I.Agent® Storm-Water Solutions, WA, USA). The solvent extracts were then concentrated by rotary evaporation and nitrogen blowdown to 1 ml. A mixture of internal standards composed of Napthalene-d_8, Acenaphthene-d_{10}, Chrysene-d_{12}, and Perylene-d_{12} was added into the final sample extracts just prior to the instrumental analysis.

The sample extracts were analyzed for PAHs following standard EPA Method 8270. Chemical analyses were performed using an Agilent 7890A Gas Chromatograph (GC) (Santa Clara, CA) equipped with a Agilent 5975C inert XL mass selective detector (MSD) and fitted with a HP-5MS high resolution capillary column (30 m long, 0.25 mm diameter and 0.25 µm thick film). The carrier gas was ultrahigh purity helium (Air Liquide, Houston, TX) at a constant flow rate of 1 ml min^{-1}. The injection port was set at 250 $^{\circ}$C, run in splitless mode and was fitted

with a Hewlett-Packard single tapered deactivated borosilicate liner. The oven temperature program was as follows; the initial temperature was set to 60 $^{\circ}$C and was held for 3 minutes; the temperature was then increased to 280 $^{\circ}$C at a rate of 5 $^{\circ}$C min^{-1} and held for 3 minutes. The oven was then heated from 280 $^{\circ}$C to 300 $^{\circ}$C at a rate of 1.5 $^{\circ}$C min^{-1} and held at 300 $^{\circ}$C for 2 minutes. The temperature of the MSD interface to MS was set at 280 $^{\circ}$C. The MSD was operated in the selective ion monitoring (SIM) mode for quantifying specific PAHs.

The concentrations of specific target PAHs were determined by the response factors calculated using a combination of internal and calibration standards. The calibration standards were prepared at five different concentrations (5-point calibration curve) and contained each parent polycyclic aromatic hydrocarbon. The calibration curve resulted in instrument response factors that were used to calculate the concentrations of individual analytes in the extracted samples. Alkylated PAH homologues were quantified by response factors generated by the un-alkylated parent PAH compounds.

A total of 43 PAHs, including parents and the sum of their C1 to C3 or C4 alkylated homologues, were identified and quantified in the samples. They encompass a series of parent PAHs with 2-6 aromatic rings [naphthalene to benzo(g,h,i)perylene] and several associated alkyl-substituted homologues of each parent PAH. The individual PAH analytes were summed and presented in terms of ΣPAH_{43}. The list of the PAH compounds identified and quantified in this study and their corresponding abbreviations are presented in Appendix 2.

2.2.6. Quality assurance/quality control (QA/QC)

A commercially-prepared oil analysis standard (Oil Analysis Standard, Lot #121004, Absolute Standards), was used to prepare the five-point calibration standards. The solution of the calibration standards was stored in amber vials with PTFE-lined caps, checked frequently and

replaced in case of degradation. A continuing calibration standard (one point of the initial 5-point calibration standard) was analyzed in each batch of extracted samples or each 12-hour period during which analyses were performed. Acceptance criterion for the continuing calibration standard was ± 20% of the mean relative response factor calculated from the initial five-point curve. Field and procedural blanks were processed and found to be below 5% of the target analytes. The laboratory reference oil standard (MC252 Source Oil) was analyzed in each sample batch as an additional QA/QC sample. The recoveries for Phenanthrene-d_{10} ranged between 55% and 106%, with average recovery of 73 ± 9%, 74 ± 7%, and 76 ± 18% for particulate, sinking and dissolved PAHs, respectively. The reported concentrations of target analytes are recovery corrected.

2.2.7. Analysis of particulate organic carbon (POC)

The dried particulate samples in the filters (GF/F and QMAs) were placed in a desiccator with concentrated fuming hydrochloric acid for 36 hours to remove inorganic carbon (Hedges and Stern, 1984). After acid fumigation the samples were dried at 60 $^{\circ}$C and then analyzed for POC using Elemental Analyzer (PerkinElmer, 2400 Series II CHNS/O Analyzer). The analytical error associated with carbon analysis was less than 3%.

2.3. Results and discussion

2.3.1. Dissolved PAHs concentrations

Dissolved ΣPAH_{43} concentrations varied between 31.2 to 51.2 ng/L (mean = 40.3 ± 6.0 ng/L) and 24.2 to 58.0 ng/L (mean = 35.5 ± 9.0 ng/L) in year 2012 and 2013, respectively. Dissolved PAHs did not show a clear spatial variation among sampling stations (Figure 2.2a and 2.2b). Vertical profiles of dissolved PAHs showed a general pattern of low concentrations at 100 m followed by elevated concentrations at 150 m and then decreased or remain constant with

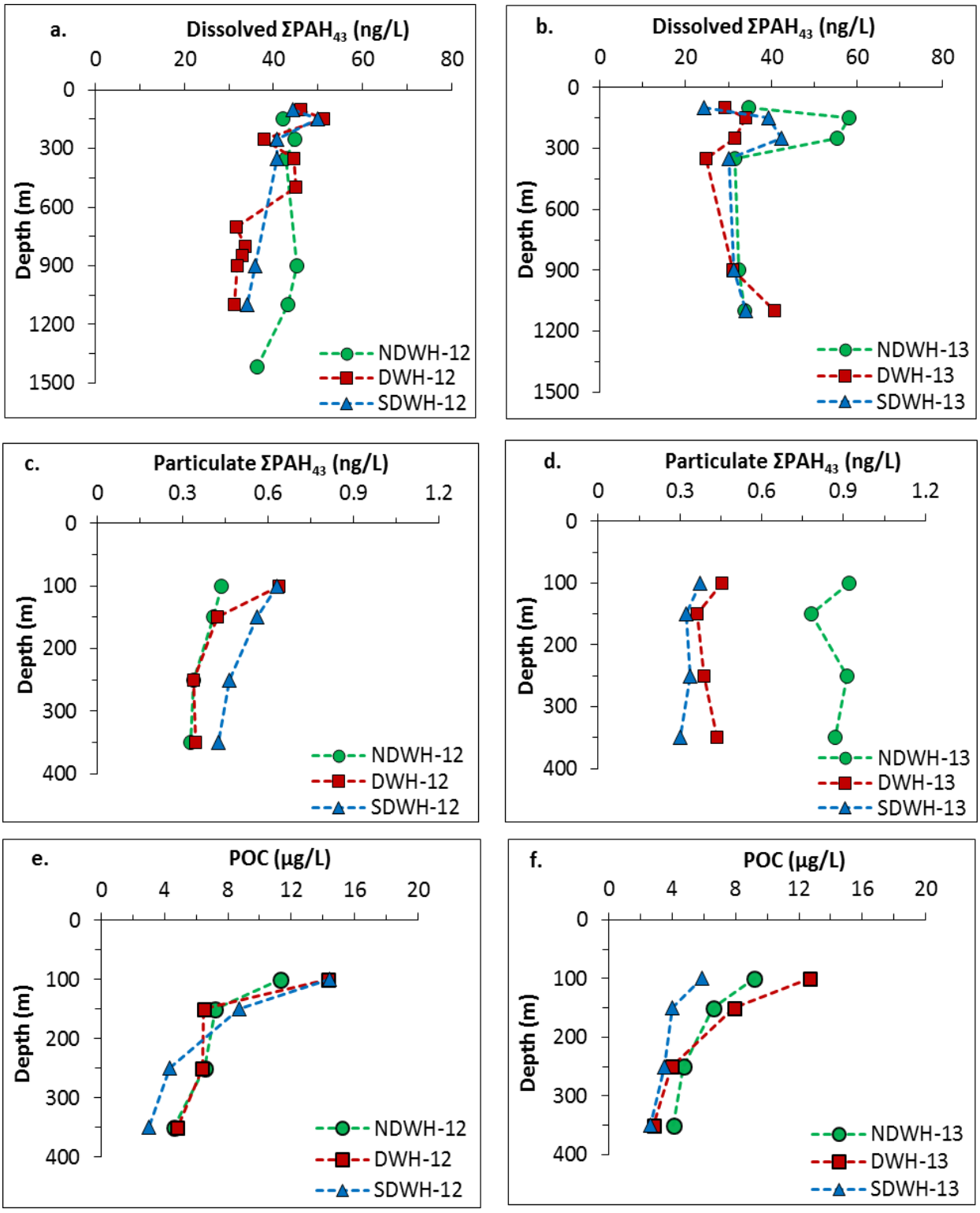

Figure 2.2. Dissolved ΣPAH_{43} concentrations (a) and (b) for 2012 and 2013, particulate ΣPAH_{43} concentrations (c) and (d) for 2012 and 2013, and POC concentrations (e) and (f) for 2012 and 2013, in the northern Gulf of Mexico water column.

depth. The change in concentrations in upper 350 m of water column was more pronounced in 2013 than in 2012 (Figure 2.2a and 2.2b). There are no comparable dissolved PAHs data from the open waters of the GOM with an exception of the concentrations reported by Diercks et al. (2010) during the DWH oil spill. Although it may not be directly comparable, the observed values are within the range of reported post-spill concentrations of available PAHs (ΣPAH_{33} 16-170 ng/L) from various locations along the Gulf coasts (Allan et al., 2012), while the values are higher than the reported pre-spill concentrations (ΣPAH_{33} 3.8-9.1 ng/L) from coastal GOM (Allan et al., 2012) (Table 2.1). The dissolved ΣPAH_{43} concentrations from this study are found to be an order of magnitude higher than values reported from other oceanic settings like the semi-enclosed Mediterranean Sea (Berrojalbiz et al., 2011; Dachs et al., 1997; Lipiatou et al., 1997) and the oligotrophic North Atlantic Ocean (Lipiatou et al., 1997) (Table 2.1). As mentioned earlier, given the multiple sources of PAHs present in this region, these higher values are not surprising. Dissolved ΣPAH_{43} in this study are found to be similar between the two sampling years and over three orders of magnitude lower than the concentrations observed in the same area during the DWH oil spill in 2010 (Diercks et al., 2010) (Table 2.1). The results indicate that there is a large degree of attenuation of DWH oil inputs in the 2-3 years following the spill and the PAHs concentrations might be approaching background levels for this region.

2.3.2. Particulate PAHs concentrations and its relation to POC distribution

Particulate ΣPAH_{43} concentrations varied between 0.33 to 0.64 ng/L (mean = 0.44 ± 0.1 ng/L) in year 2012, and 0.30 to 0.92 ng/L (mean = 0.54 ± 0.2 ng/L) in 2013. Particulate PAHs data from coastal Louisiana (< 100 m water depth, around the MR delta) during and one year after the oil spill are reported to be in the range of 83-252 ng/L and 7.2-83 ng/L (Liu et al., 2014) (Table 2.1). These values from coastal sites are not directly comparable to my study sites. To the

Table 2.1. Comparison of dissolved and particulate PAHs concentrations (ng/L), and particulate PAHs fluxes (μg m^{-2} d^{-1}) in various locations of the global oceans, ranging from coastal settings to the open seas. The data are reported as the ranges of concentrations and fluxes.

Location	Compounds	Concentrations (ngL^{-1})	Fluxes ($\mu gm^{-2}d^{-1}$)	Reference
Dissolved PAHs				
Southern Mediterranean Sea	ΣPAH_{19}	0.4-0.9	-	Dachs et al., 1997
Western Mediterranean Sea	ΣPAH_{10}	0.78	-	Lipiatou et al., 1997
North Atlantic Ocean	ΣPAH_{10}	0.62	-	Lipiatou et al., 1997
Open Mediterranean Sea	ΣPAH_{19}	0.16-8.80	-	Berrojalbiz et al., 2011
Gulf of Mexico*	ΣPAH_{41}	29,400-1,89,000	-	Diercks et al., 2010
Gulf of Mexico**	ΣPAH_{33}	16-170	-	Allan et al., 2012
Gulf of Mexico***	ΣPAH_{33}	3.8-9.1	-	Allan et al., 2012
Gulf of Mexico	ΣPAH_{43}	24.2-58.0	-	This study
Particulate PAHs				
Southern Mediterranean Sea	ΣPAH_{19}	0.21-0.77	-	Dachs et al., 1997
Western Mediterranean Sea	ΣPAH_{10}	0.27	-	Lipiatou et al., 1997
North Atlantic Ocean	ΣPAH_{10}	0.012	-	Lipiatou et al., 1997
Open Mediterranean Sea	ΣPAH_{19}	0.03-0.37	-	Berrojalbiz et al., 2011
Gulf of Mexico$^{\gamma}$	ΣPAH	83-252	-	Liu et al., 2014
Gulf of Mexico$^{\gamma\gamma}$	ΣPAH	7.2-83.3	-	Liu et al., 2014
Gulf of Mexico	ΣPAH_{43}	0.30-0.92	-	This Study
PAHs Fluxes				
Chesapeake Bay	ΣPAH_{13}	-	13.7	Ko and Baker, 2003
Mediterranean Sea	ΣPAH_{25}	-	0.006-0.24	Colombo et al., 2006
Mediterranean Sea	ΣPAH_{15}	-	0.22-0.24	Dachs et al., 1996
Mediterranean Sea	ΣPAH_{12}	-	0.3-0.9	Lipiatou et al., 1993
Eastern Mediterranean Sea	ΣPAH_{35}	-	0.022-0.028	Tsapakis et al., 2006
NW Mediterranean Sea	ΣPAH_{24}	-	0.12-10.5	Raoux et al., 1999
NW Mediterranean Sea	ΣPAH_{35}	-	0.04-4.74	Deyme et al., 2011
Gulf of Mexico	ΣPAH_{43}	-	1.95-7.78	This Study

*During Deepwater Horizon Oil Spill in 2010

** Post-spill coastal concentrations

***Pre-spill coastal concentrations

γ Coastal concentrations during Deepwater Horizon Oil Spill in 2010

γγ Coastal concentrations in May 2011

best of my knowledge, there are no published studies of particulate PAHs in the region that could directly be compared with these values from open waters. However, my results are within the range of ΣPAHs reported in the suspended particulate matter in the Mediterranean Sea (Berrojalbiz et al., 2011; Dachs et al., 1997; Lipiatou et al., 1997), and are order of magnitude higher than the values reported from the North Atlantic (Lipiatou et al., 1997) (Table 2.1). The vertical profiles of particulate PAHs show a trend of maximum at 100 m (Figure 2.2c and 2.2d). Dachs et al. (1997) have reported similar patterns of particulate PAHs with concentrations maxima at 100 m which is immediately below the depth of the biomass maxima. The concentrations of particulate PAHs are usually expected to decrease with increase in depth (Dachs et al., 1997; Lipiatou et al., 1997) of the water column due to decrease in marine particles with depth as well as the degradation and desorption of PAHs during vertical transport (Dachs et al., 1996, 1997; Lipiatou et al., 1993, 1997; Raoux et al., 1999). However, in this study the concentrations remain similar throughout the upper 350 m of the water column (Figure 2.2c and 2.2d). Particulate PAHs showed similar spatial variations both years except NDWH-13, which had higher concentration of particulate PAHs than the other two sites (Figure 2.2c and 2.2d). The concentrations of particulate PAHs also did not show significant temporal variation between the sampling years with an exception of NDWH station. The concentrations of particulate ΣPAH_{43} at station NDWH were approximately factor of ~2 higher in 2013 than in 2012 (Figure 2.2c and 2.2d). However, the exact reason for this variability is unknown.

Average particulate PAHs concentration remained similar between 2012 and 2013, contributing 1.0% and 1.5% to the total water column PAHs pool, respectively. In general, due to their high ocatanol-water (Kow) and organic carbon sorption partition coefficients (Koc) (Means et al., 1980), PAHs tends to partition more favorably in the particulate phase than the dissolved

phase (Bouloubassi and Saliot, 1993). The lower percent contribution of particulate PAHs to total PAHs concentration in the water column can thus be attributed to the lower availability of particulate matter in the water column (Bouloubassi and Saliot, 1993). The oligotrophic nature of open GOM (Wawrik and Paul, 2004) thus results in PAHs phase distribution comparable to that of the North Atlantic (Lipiatou et al., 1997) and open Mediterranean Sea (Berrojalbiz et al., 2011), which also represent similar low particle oligotrophic setting.

Particulate organic carbon concentrations from all the sampling locations varied between 2.0 to 17.4 µg/L (mean = 7.5 ± 4.0 µg/L) in 2012 and 2.3 to 15.7 µg/L (mean = 6.0 ± 3.6 µg/L) in 2013. The pattern of change in POC concentrations with depth was similar to that of particulate PAHs (except NDWH-13); maxima at 100 m followed by lower concentration at depths in all stations both the years (Figure 2.2e and 2.2f). However, decrease in POC concentration with depths was more pronounced than that of PAHs (Figure 2.2c, 2.2d, 2.2e and 2.2f). PAHs and POC concentration from individual station were positively correlated (Pearson Correlation Coefficient between 0.88 to 0.98), except for stations NDWH-13 and DWH-13. The positive correlation between particulate PAHs and POC points to the preferential sorption of PAHs onto organic particles shown by number of previous studies (Means et al., 1980; Wang et al., 2001).

2.3.3. Vertical fluxes of particulate PAHs and its relation to POC fluxes

Particle mediated vertical fluxes of ΣPAH_{43} at 150 m varied between 5.21 to 6.25 µg m^{-2} d^{-1} in 2012 and 2.04 to 2.40 µg m^{-2} d^{-1} in 2013. The vertical fluxes of particulate PAHs showed a little to no change with depths (Figure 2.3a). The PAHs fluxes in 2012 were 2.5 to 4.0 times higher than in 2013 (Figure 2.3a). To the best of my knowledge, this is the first study to estimate trap based vertical fluxes of PAHs in the mesopelagic zone of the northern GOM. Therefore,

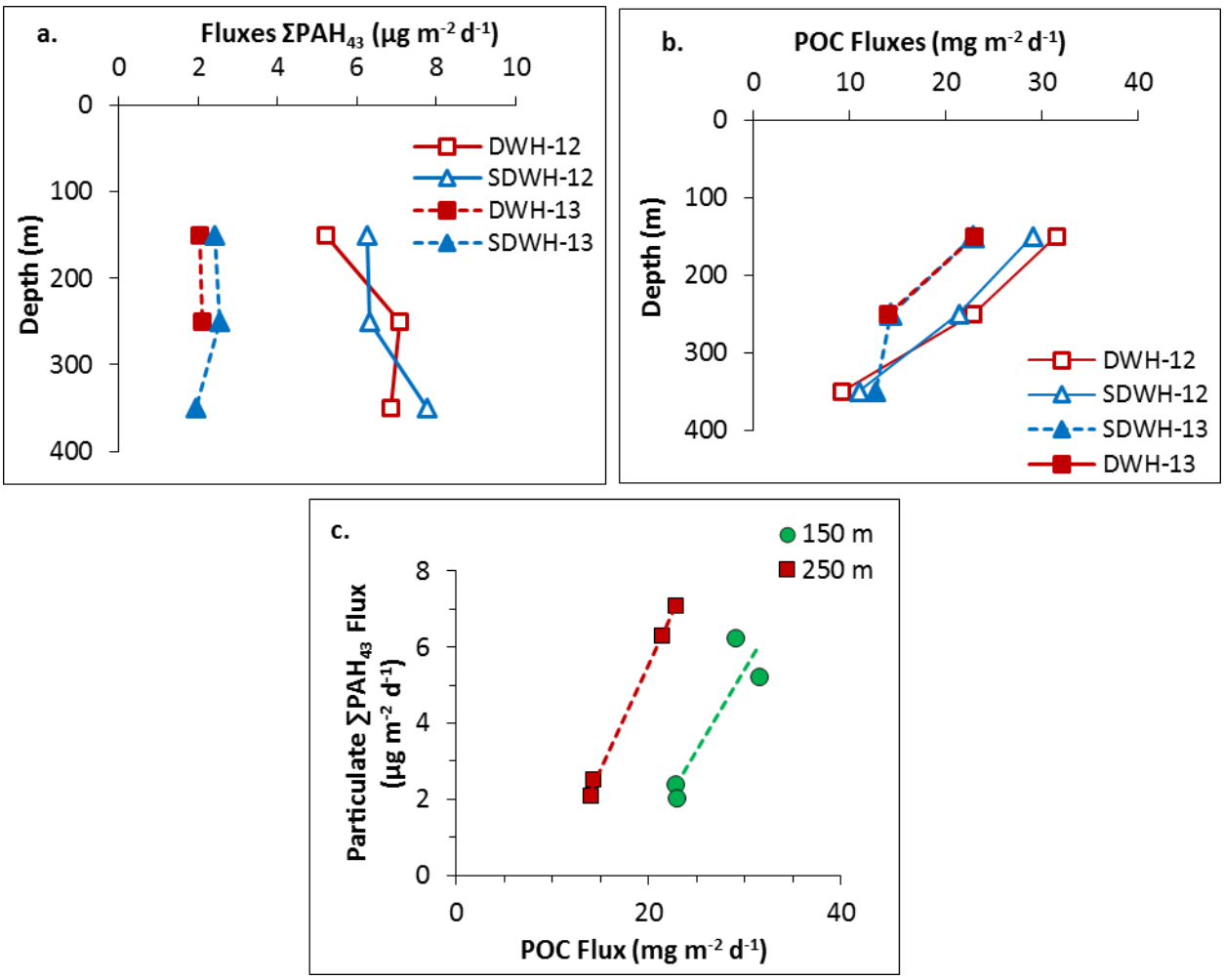

Figure 2.3. Particulate ΣPAH_{43} fluxes (a), POC Fluxes (b), and vertical fluxes of particulate ΣPAH_{43} vs vertical fluxes of POC (c) in the northern Gulf of Mexico water column.

there are no comparable published data on PAHs fluxes for this region. Previous studies from other locations, coastal and open oceans, have reported PAHs fluxes varying over orders of magnitude (Bouloubassi et al., 2006; Deyme et al., 2011; Raoux et al., 1999) (Table 2.1). Although it is not directly comparable, the observed values of PAHs fluxes in this study are lower than the Chesapeake Bay (Ko et al., 2003) while they are higher than the PAHs fluxes reported from different locations of the open Mediterranean Sea (Bouloubassi et al., 2006; Dachs et al., 1996; Lipiatou et al., 1993; Tsapakis et al., 2006) (Table 2.1). However, the fluxes are

within the range of PAHs fluxes reported for the Northwestern Mediterranean Sea (Deyme et al., 2011; Raoux et al., 1999) (Table 2.1).

The sediment trap based POC fluxes at 150 m were comparatively higher in 2012 (29.04-31.52 mg C m^{-2} d^{-1}) than 2013 (22.79-22.95 mg C m^{-2} d^{-1}) (Figure 2.3b). However, unlike PAHs fluxes which did not show significant flux attenuation between 150 m and 350 m, the POC fluxes followed a typical oceanic profile with 70-45% of the POC fluxes at 150 m being remineralized by 350 m. This is probably related to the preferential remineralization of organic matter by zooplankton grazing and bacterial respiration. In spite of the differences in flux attenuation with depth, both PAHs and POC fluxes showed a similar pattern of higher fluxes in 2012 than 2013 (Figure 2.3a and 2.3b) and found to be strongly correlated at 150 m (R^2 = 0.998) and 250 m (R^2 = 0.814) (Figure 2.3c). No such correlation was observed for fluxes at 350 m which is likely due to preferential removal of POC by remineralization compared to PAHs, however the loss of one trap at 350 m in 2013 makes it difficult to make such interpretation with high degree of confidence. The strong correlation between PAHs and POC fluxes indicates preferential sorption of PAHs onto these organic particles (Means et al., 1980; Wang et al., 2001) followed by subsequent downward fluxes. Thus processes controlling POC fluxes in the upper ocean like biological productivity, plankton community, zooplankton grazing can be directly responsible for modulating PAHs fluxes in the open ocean in conjunction with other factors like atmospheric input, and the nature of PAHs available in the water column. The dominancy of PAHs profiles by lower molecular weight (LMW) and middle molecular weight (MMW) PAHs in the sediment traps, which are preferentially scavenged via sorption on organic-rich particles and packaging of larger rapidly sinking particles (Bouloubassi et al., 2006; Dachs et al., 1996, 2002), further support the role of POC in modulating PAHs fluxes observed in this study.

Therefore, the higher PAHs flux in 2012 was possibly due to larger POC fluxes in 2012 than in 2013. Similar correlation between POC and PAHs fluxes have been observed in few other studies from the Mediterranean Sea (Dachs et al., 1996; Deyme et al., 2011). However, almost none of these studies are exclusively focused on the upper mesopelagic zone where POC fluxes undergoes most dynamics changes and are often tightly related to production, plankton community, zooplankton gazing and vertical migration.

2.3.4. Rate of loss of particulate PAHs via vertical fluxes

This is the first instance where both particulate PAHs concentrations and sinking PAHs fluxes from the upper mesopelagic zone (< 500 m) were measured simultaneously in the same study using large volume *in situ* pumps and the drifting sediment traps, respectively. This provides the unique opportunity to directly estimate the loss of the particulate PAHs from the water column via vertical fluxes and hence understand the role of vertical sinking in PAHs cycling in open oceans. The fraction of water column particulate PAHs inventory that is lost from the upper ocean per day due to vertical sinking can be calculated from PAHs flux estimates and water column particulate PAHs inventories as follows.

$$\text{Daily loss} = \frac{(\text{PAHs fluxes } (\text{ng m}^{-2}\ \text{d}^{-1}) * 100\ \%}{(\text{Total particulate PAHs inventory } (\text{ng m}^{-2})} \qquad (2.1)$$

The PAHs flux at a particular depth can be calculated from corresponding sediment traps while the particulate PAHs inventories can be estimated by integrating particulate PAHs concentrations over that water column depth. Particulate PAHs inventories were calculated using depth-weighted integration, and assuming the particulate PAHs concentrations to be constant between two sampling points. Since sediment trap from 350 m at station DWH-13 was lost, the particulate PAHs loss could not be estimated from this station.

The rate of loss of particulate PAHs from the upper 350 m of the water column via vertical sinking, are shown in the Figure 2.4a for years 2012 and 2013. The results show that approximately 3.1-6.7%, 2.0-5.5%, and 1.6-4.2% of the total particulate PAHs in the water column is lost daily from upper 150, 250, and 350 m of the water column, respectively (Figure 2.4a). The loss of particulate PAHs via vertical sinking is found to be higher in 2012 compared to 2013, indicating more efficient transport in 2012 (Figure 2.4a).

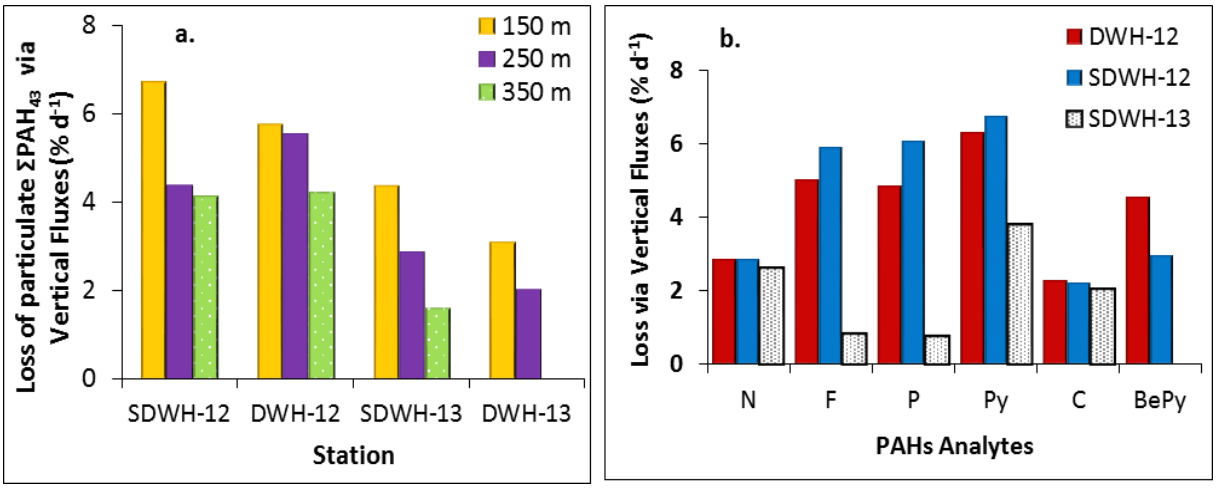

Figure 2.4. Rate of loss of particulate ΣPAH_{43} via vertical fluxes (a) rate of loss of selected particulate PAHs, (b) from upper 350 m of the water column via vertical transport. Note Benzo(e)pyrene was not detected in both pumps and traps samples at SDWH-13.

Despite the variability between two years, it is important to note that the daily loss of PAHs via sinking fluxes represent a substantial portion of the particulate PAHs stock in the water column. This loss term can provide us with some understandings about the cycling of particle bound PAHs in the upper ocean from this region where such data are lacking. If we assume the vertical transport as the sole process by which particle bound PAHs can be lost from the water column, then the daily loss of 3.1% to 6.7% of particulate PAHs inventory calculated at 150 m (approximate depth of the euphotic zone ~120 m) implies that the entire particulate PAHs inventory in the euphotic zone will be lost within 15-32 days in this region. Similarly, if

we consider the entire 350 m of the upper ocean, we can expect the particulate PAHs inventory of this water column to be lost due to vertical sinking between 24-62 days. The faster removal rate in the upper 150 m indicates the availability of more particles in the euphotic zone for PAHs to attach and sink. However, this estimate should be treated with caution, as a number of other loss terms like evaporation, biodegradation, photo-oxidation, dispersion and lateral transport can reduce the residence times of particulate PAHs in the water column to varying degree. This estimate assumes steady-state and ignores all the above mentioned processes. Thus, the residence times estimated in this study can only be regarded as an upper limit. Moreover, the residence times will be sensitive to any processes that change the particle size distributions in the water column such as biological production, atmospheric deposition and/or riverine input.

In order to obtain further insight on vertical transport, I selected six PAHs with contrasting molecular weights; naphthalene [N], fluorene [F] and phenanthrene [P] (LMW; ≤3 rings), pyrene [Py] and chrysene [C] (MMW; 4 rings), and benzo(e)pyrene [BePy] [higher molecular weight (HMW); 5 rings]. Then their rates of loss from upper 350 m of the water column were estimated as shown in Figure 2.4b. Pyrene, phenenthrene and fluorene were found to be more efficiently scavenged than benzo(e)pyrene, naphthalene and chrysene (Figure 2.4b). Particle fluxes in the open GOM is mainly dominated by POC fluxes associated with biological productivity and LMW-MMW PAHs such as fluorene, phenanthrene and pyrene are more efficiently scavenged by uptake into organic rich particulate matter like fecal pellets (Bouloubassi et al., 2006; Dachs et al., 1996; Lipiatou et al., 1993). The lower rate of removal of naphthalene via particulate fluxes is possibly due to higher solubility of naphthalene than the other PAHs (Mackay and Shiu, 1977; May et al., 1978). Removal of chrysene in the form of particulate flux was considerably lower than other PAHs for both stations in both years

(Figure 2.4b), which was derived by comparatively lower concentrations of chrysene in settling particles than the suspended particles. The lower vertical transport efficiency of chrysene in the water column could be due to its preferential sorption onto finer particles which do not readily sink and get captured in the traps. This could result in a longer half-life of chrysene in the water column, similar to those reported by another study (2-5 years) in the GOM (Tansel et al., 2011).

2.3.5. Molecular profiles and sources of PAHs

Abundance of lower molecular weight (LMW; ≤ 3 rings) compounds dominated the PAHs profiles in all samples (dissolved, particulate and sinking), followed by middle molecular weight (MMW; 4 rings) compounds, with irregular appearances of compounds with higher molecular weight (HMW; > 4 rings) in some of the samples. About 72 ± 11% of the total PAHs was contributed by LMW PAHs, while MMW and HMW PAHs contributed about 26 ± 10%, and 2 ± 2% of the total PAHs, respectively. Similar distributions of PAHs with abundance of LMW and MMW compounds have been reported from different locations of the global oceans (Allan et al., 2012; Colombo et al., 2006; Dachs et al., 1996, 1997; Deyme et al., 2011; Diercks et al., 2010; Lipiatou et al., 1993, 1997). The molecular profiles of individual PAHs concentrations and particulate PAHs fluxes at 150 m, from all three stations are presented in Appendix 3.

Isomeric ratios of PAHs have been used by various authors (Budzinski et al., 1997; Yunker et al., 2002) to recognize sources of PAHs: e.g., anthracene to anthracene plus phenanthrene [An/(An+Phe)], fluoranthene to fluoranthene plus pyrene [Flu/(Flu+Pyr)] and benzo(a)anthracene to benzo(a)anthracene plus chrysene [BaA/(BaA+Ch)]. The An/(An+Phe), Flu/(Flu+Pyr) and BaA/(BaA+Ch) ratios less than 0.1, 0.4, and 0.2, respectively, indicate petroleum sources whereas values higher than 0.1, 0.4, and 0.35, respectively, generally indicate

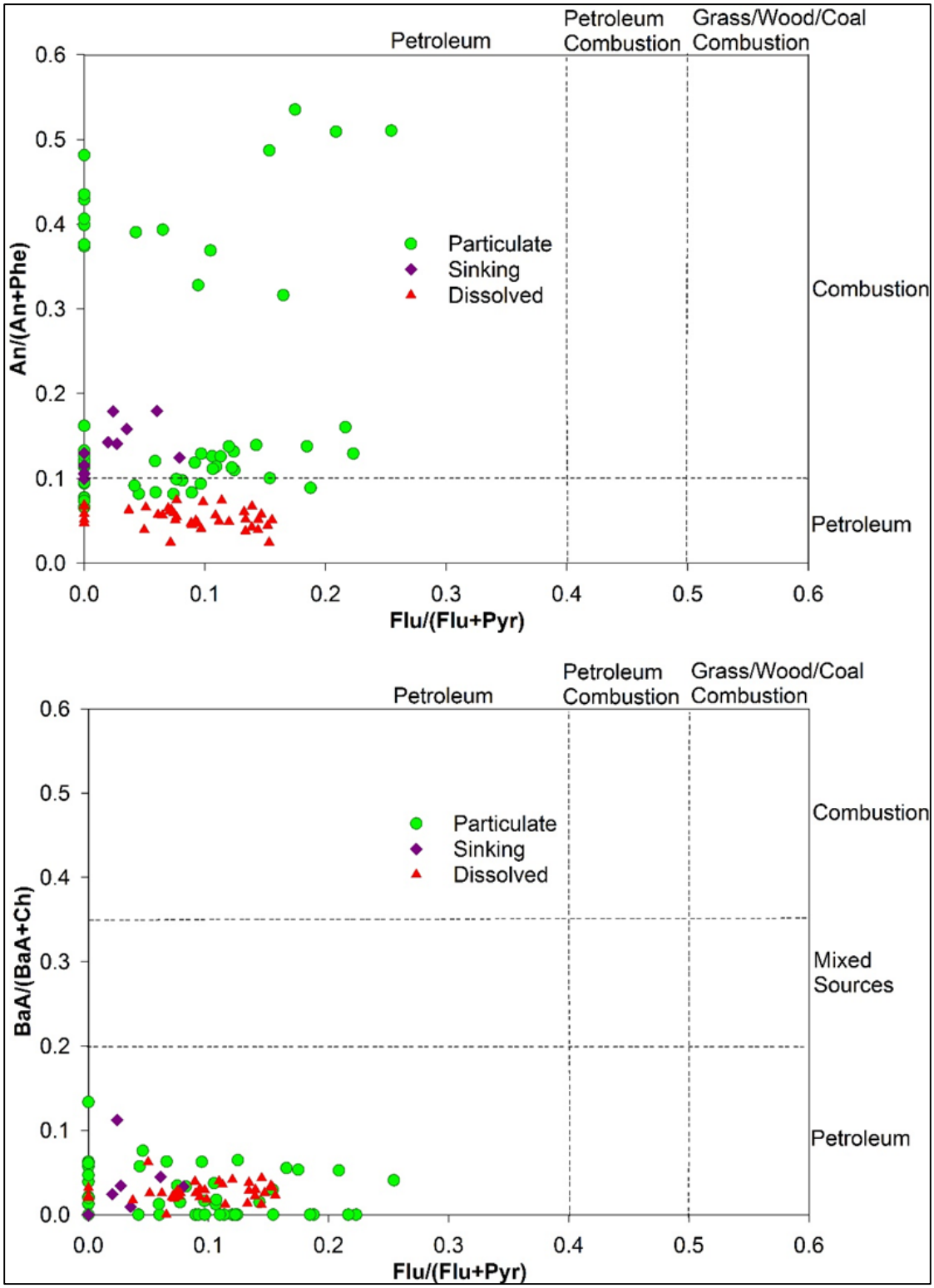

Figure 2.5. Anthracene to anthracene plus phenanthrene [An/(An+Phe)], fluoranthene to fluoranthene plus pyrene [Flu/(Flu+Pyr)], and benzo(a)anthracene to benzo(a)anthracene plus chrysene [BaA/(BaA+Ch)] ratios for the source recognition of particulate, sinking and dissolved PAHs (Yunker et al., 2002).

combustion sources (Budzinski et al., 1997; Yunker et al., 2002). The particulate and settling samples showed mixed PAHs sources with An/(An+Phe) ratios >0.1 in about 60% of the samples (Figure 2.5a), while Flu/(Flu+Pyr) and BaA/(BaA+Ch) were less than 0.4 and 0.2 respectively in all the samples (Figure 2.5a and 2.5b), indicating predominantly petroleum sources. The dissolved PAHs were also of petroleum origin, as indicated by the PAHs ratios (Figure 2.5a and 2.5b). The ratios of ΣMethylphenanthrenes to phenanthrene were always >0.5, which further characterizes the PAHs of petroleum origin (Sporstol et al., 1983). Alkylated homologues contributed approximately 76 ± 7% (ranged between 55 to 90%) of the total PAHs. The abundance of LMW PAHs and the dominance of alkylated homologues over parent compounds (except napthobenzothiophene and chrysene) further reflect a major contribution of unburned fossil sources (Bence et al., 2007; Laflamme and Hites, 1978; Sporstol et al., 1983; Yunker et al., 2002). There is no noticeable temporal and spatial variation in PAHs sources implying petroleum origin as the dominant input source of PAHs in the GOM throughout the study periods.

2.4. Conclusion

This study, for the first time, reports the concentrations and vertical fluxes of particle-bound PAHs from the mesopelagic zone of the northern GOM. Concentrations of dissolved and particulate PAHs remained similar between two study years, 2012 and 2013. The concentrations of dissolved PAHs were observed to have gone down by over 1000 times from concentrations reported during and immediately after DWH oil spill (Diercks et al., 2010). In absence of any available pre DWH baseline data on PAHs (dissolved or particulate) from the open GOM, these values can be considered as post DWH base line concentrations. The source diagnostic analyses indicated that the PAHs in the northern GOM water column were predominant due to petroleum

origin (Bence et al., 2007; Laflamme and Hites, 1978; Sporstol et al., 1983; Yunker et al., 2002). The PAHs fluxes are found to vary by factor of 2-4 between the two years in spite of similar dissolved and particulate concentrations in the water column, indicating the important role of marine particles, especially POC, in mediating such fluxes. The strong correlation between PAHs and POC fluxes and the dominancy of LMW-MMW PAHs in the sediment traps, which are preferentially sorbed and scavenged on organic-rich particles, support the role of POC in modulating PAHs fluxes observed in this study. The vertical fluxes are found to be an important loss term for particle bound PAHs in this region with 3.1-6.7% of total particulate PAHs inventory in the euphotic zone being lost daily via this pathway. Efficient removal of particulate PAHs from the upper water column via marine particle settling supports the theory that the deep-sea sediments are the major global sinks of PAHs (Gustafsson et al., 1997a). Hence, it can be of significant importance for the benthic organisms living in/on those deep-sea surficial sediments.

To the best of my knowledge, this work represents the first instance of utilizing surface-tethered drifting sediment traps for direct estimation of particle mediated PAHs fluxes in upper mesopelagic zone. Typically moored sediment traps with their longer collection period are utilized to determine PAHs fluxes in the ocean (Table 2.1). The short deployment length for these traps (2-3 days) posed the challenge as to whether enough particles can be collected to quantify PAH fluxes. These traps were found to be sufficient for collection and characterization of PAHs fluxes in this region which will open doors to future research on further understanding the role of various biogeochemical processes in controlling PAHs fluxes in the mesopelagic zone. The measurement of fluxes and the rate of loss of particulate PAHs in the water column, presented in this study, provides us with a necessary first step to better constrain related models

of pollutant cycling which will be valuable for understanding the fate and cycling of PAHs in the mesopelagic region of northern GOM (Dachs et al., 2002; Palm et al., 2004).

CHAPTER 3: ^{238}U-^{234}TH DISEQUILIBRIA AS A TRACER OF VERTICAL FLUX OF POLYCYCLIC AROMATIC HYDROCARBONS IN THE NORTHERN GULF OF MEXICO

3.1. Introduction

The radioactive disequilibrium between naturally occurring radioisotope ^{238}U ($t_{1/2}$ = 4.5 billion years) and its daughter ^{234}Th ($t_{1/2}$ = 24.1 days) has been extensively used to estimate the vertical flux of particles in marine systems (Buesseler et al., 2006). ^{234}Th is particle-reactive, with a much higher distribution coefficient (K_d~10^6-10^7 L/kg; Moran and Buesseler, 1993), than ^{238}U (K_d ~10^2 L/kg; Anderson, 1982) which is regarded as a conservative element under oxic conditions. The ^{234}Th, because of its high partition coefficient, is preferentially 'sorbed' on to the particles in water column and if those particles are sinking, thus get removed from the water column (Figure 3.1). This results in a relative deficiency of ^{234}Th with respect to ^{238}U in the upper ocean (Bhat et al., 1969; Buesseler et al., 2006). Quantitative estimation of this deficiency between ^{238}U and ^{234}Th activities in the water column allows us to quantify the rate of ^{234}Th removal via vertical sinking of particles from the upper ocean (Figure 3.1) (Buesseler et al., 2006; Maiti et al., 2012; Savoye et al., 2006). High particle affinity, well-constrained source, relative ease of analysis, and short half-life of ^{234}Th make it suitable scavenging tracer of particles in the upper oceans, integrated over a time scale of 3-4 weeks (Buesseler, et al., 2006; Waples et al., 2006). This approach has been increasingly used in past two decades to quantify the vertical fluxes of particulate organic carbon (Buesseler et al., 2006; Moran et al., 2003), particulate inorganic carbon (Bacon et al., 1996), biogenic silica (Buesseler et al., 2001; Rutgers van der Loeff et al., 2002) and particle reactive organic pollutants (Gustafsson et al., 1997a, 1997c, 1998; Palm et al., 2004) in the marine systems.

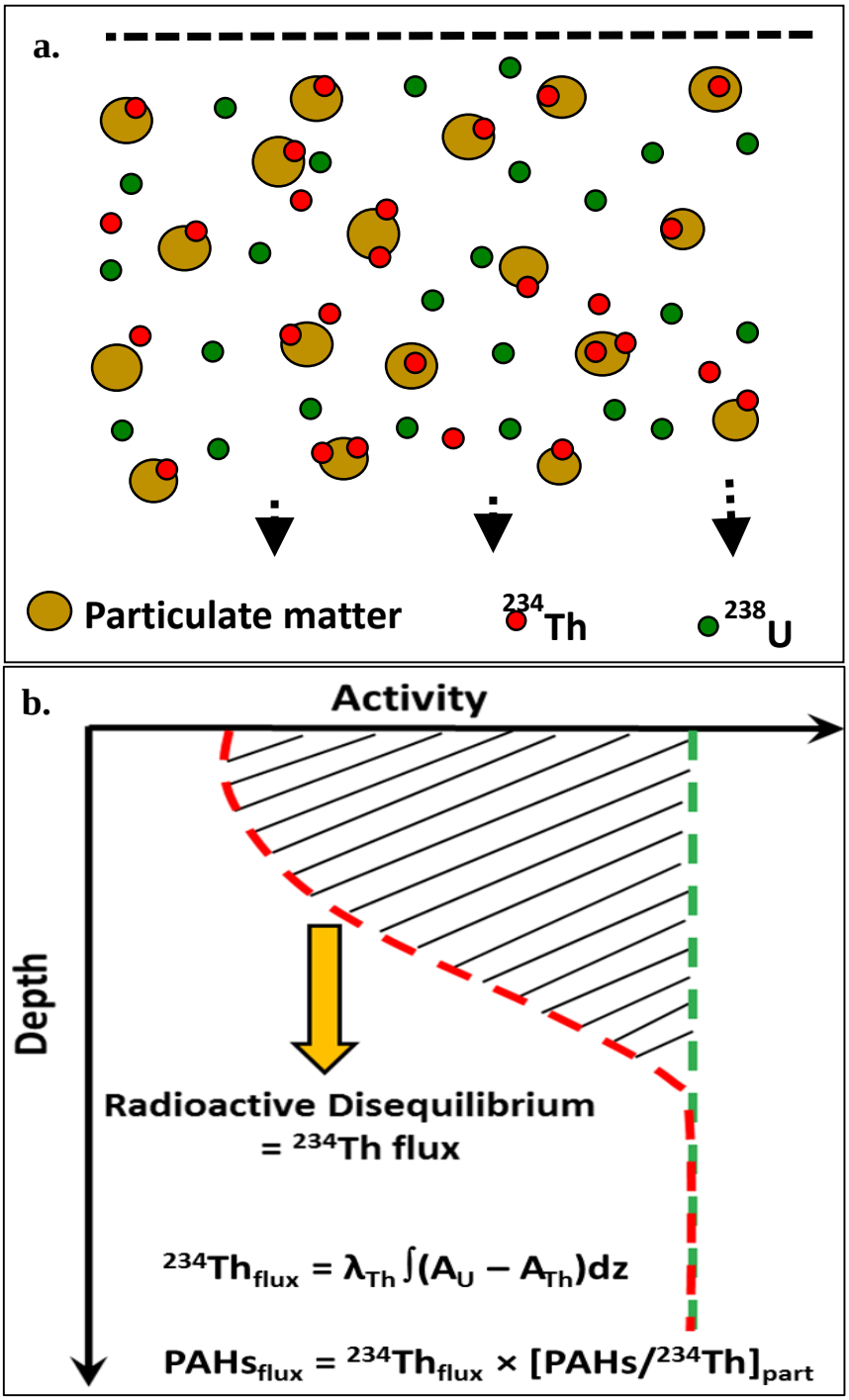

Figure 3.1. A conceptual model showing the principal on how the upper ocean ^{238}U-^{234}Th disequilibria can be utilized as a tracer of vertical fluxes of polycyclic aromatic hydrocarbons (PAHs) from upper mesopelagic zone; a) particle reactive nature and vertical scavenging of ^{234}Th, and b) ^{234}Th deficiency in upper oceans due to particle mediated vertical sinking of ^{234}Th (while ^{238}U remain conservative) and its application to estimate PAHs fluxes.
(Graphic source: Dr. Kanchan Maiti, Department of Oceanography and Coastal Sciences, Louisiana State University, Baton Rouge)

The particle-mediated vertical transport followed by burial in deep-sea sediments is an important mechanism of polycyclic aromatic hydrocarbons (PAHs) removal from the water column which plays a fundamental role in the marine biogeochemical budget of PAHs (Dachs et al., 1997; Gustafsson, 1997a; Lipiatou et al., 1997; Palm et al., 2004). Therefore, it is important to quantify this critical pathways of PAHs removal in order to understand their residence time and long term fate in marine systems. However, the data on upper ocean PAHs flux are rare, primarily due to lack of feasible method to quantify this mechanism. There are limited number of open ocean PAHs flux data based on deep-sea sediment traps (>350 m), dated bottom cores and/or numerical modeling; with little to no such data for the upper mesopelagic zone. The mesopelagic zone is considered as the largest "heterotrophic digester" and accounts for 95% of the fish biomass in the ocean (Benner, 2000; Irigoien, et al., 2014). This is the zone with highest particle and organic matter attenuation with depth. The aggregation-disaggregation processes and remineralization of sinking particles in the mesopelagic zone play a critical role in setting a limit on the amount of PAHs that can be transported to the deep-sea and their burial in seafloor sediments (Buesseler et al., 2007). Thus, the PAHs flux estimated via deep sediment traps and the dated bottom cores may not always represent the actual PAHs fluxes in the upper mesopelagic zone (Buesseler et al., 2007).

Surface-tethered drifting sediment traps, when designed and deployed following proper protocols, can provide direct instantaneous measurements of the upper ocean PAHs fluxes integrated over 2-3 days (Adhikari et al., 2015). However, such trap data are limited in the global ocean and almost non-existent in the Gulf of Mexico (GOM). The major reason for such limited data is probably a combination of expensive set up cost, long ship time requirement, difficulties and risks associated with successful deployment and retrieval of the drifting sediment traps,

especially in an area prone to bad weather and high traffic like the northern GOM (Adhikari et al., 2015; Buesseler et al., 2007). Most of these issues can be overcome by applying ^{238}U-^{234}Th disequilibria as a tracer of particulate PAHs fluxes from the upper mesopelagic zone. Moreover, the ^{238}U-^{234}Th technique requires only water column samples for ^{234}Th and particulate samples for PAHs/^{234}Th ratios which can be collected relatively quickly, allowing vertical flux quantification at higher spatial resolution. PAHs have relatively low aqueous solubility, high octanol partition coefficient and high affinity for marine particles (Albers et al., 2003; May and Shiu, 1977; Means et al., 1980). Like thorium, PAHs get readily partitioned onto solid phase in marine water column, primarily on particulate organic matter such as particulate organic carbon (POC), which is followed by subsequent downward settling (Dachs et al., 2002; Gustafsson, 1997a; Means, 1995; Windsor and Hites, 1979). Thus, it is fair to assume that they both are coupled through the same particle dynamics and the ^{234}Th can be successfully applied as a tracer of vertical PAHs fluxes in the upper ocean. However, till date only one study has utilized this method to quantify PAHs fluxes in the open ocean and there is no direct comparison between ^{234}Th-derived PAHs flux estimates with the more established sediment trap-based estimations to verify the feasibility of the method (Gustafsson et al., 1997a).

The objective of this study is to utilize ^{238}U-^{234}Th disequilibria to derive particulate PAHs fluxes from the upper mesopelagic zones in the northern GOM and compare them with the sediment trap-based flux estimates. The northern GOM has numerous sources of PAHs including river discharge, coastal erosion, atmospheric deposition, natural oil seeps, gas hydrates and accidental or intentional oil spills related to petroleum exploration and transportation (Mitra and Bianchi, 2003; Overton et al., 2004; Wang et al., 2011). In addition to these background sources, an estimated 2.1 x 10^{10} g of PAHs also entered into this region during the 2010 Deepwater

Horizon (DWH) oil spill (Reddy et al., 2012). Thus, it is an area with major environmental health concerns in terms of PAHs pollution and provides an ideal location to study PAHs dynamics in the upper ocean.

3.2. Materials and methods

3.2.1. Sampling locations

Water column profiles of total and particulate ^{234}Th and PAHs were collected from the vicinity of DWH oil spill sites in the northern GOM aboard the *R/V Walton Smith* (Figure 3.2).

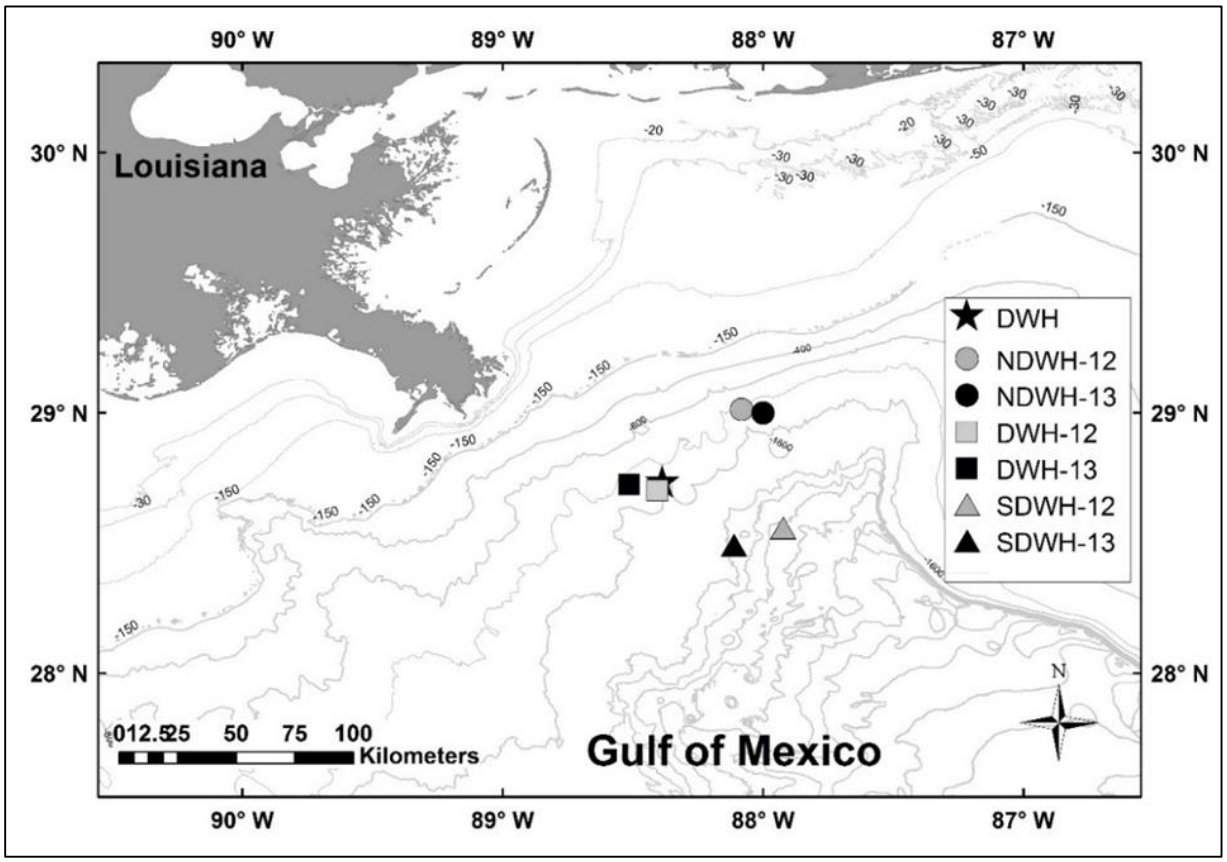

Figure 3.2. Sampling locations in the northern Gulf of Mexico, in the vicinity of the Deepwater Horizon (DWH) oil spill site. Sampling stations for 2012 are labelled as DWH-12 (Deepwater Horizon), NDWH-12 (North of Deepwater Horizon) and SDWH (South of Deepwater Horizon). While the sampling stations DWH-13, NDWH-13, and SDWH-13 represent same locations for 2013.

The sampling stations were all located in the open ocean with water depths varying between 1200-2000 m. In order to identify spatial-temporal variability in ^{234}Th-derived PAHs

fluxes in this region, samples were collected from three different locations during April 2012 and April 2013. The sampling locations for 2012 were labeled as DWH-12 (near Deepwater Horizon spill site in 2012), NDWH-12 (north of DWH in 2012), and SDWH-12 (south of DWH in 2012). Same locations were repeated again in 2013; DWH-13, NDWH-13 and SDWH-13 (Figure 3.2). At each of these three locations, two sets of samples (except sediment traps) were collected two days apart and are designated by letter 'a' and 'b' at the end of their station i.d. (e.g. NDWH-12a and NDWH-12b).

3.2.2. Sample collection

Water column samples were collected from 0-500 m at 12 depths using shipboard CTD sampling rosette. At each depth, 4 L of water samples were collected in acid washed HDPE bottles directly from the CTD Niskins through acid cleaned silicon tubes. Suspended particles for the analysis of particulate ^{234}Th and PAHs were collected by *in situ* filtration, using battery-operated submersible pumps (McLane Research Laboratories, Inc., Falmouth, USA). The suspended particles collected using these pumps are assumed to be representative of sinking particles (Buesseler et al., 2006; Lepore et al., 2009). At each station, an array of four pumps at 100, 150, 250 and 350 m depths were deployed for ~4 h to filter 500-800 L of water onto acid cleaned 51 µm polycarbonate screen followed by pre-combusted 1 µm QMA filters (Quartz Micro-fiber, Whatman International Ltd., England) to capture size-fractionated particles. The filtration rates varied between 4-6 L min^{-1} in order to minimize the chances of over collection of larger particles, particle breakage during filtration, and to exclude swimmers (Maiti et al., 2012). After the recovery of the pumps, the QMA filters were taken out of the filter holder, a sub-sample of 22 mm diameter was collected from each sample, dried onboard at 60 ºC and stored

for particulate ^{234}Th analysis. While the rest of the QMA filter was stored at -20 ºC for particulate PAHs analysis.

Surface-tethered drifting sediment trap arrays were deployed for 2.5-3.0 days at 150, 250 and 350 m below surface to capture sinking particles at two stations each year; stations DWH-12a and SDWH-12a in 2012, and DWH-13a and SDWH-13a in 2013. No trap data are available for NDWH for both years; due to bad weather in 2012, and damaged and loss of a part of the sediment trap array by the interference with a seismic survey boat at station DWH in 2013. The design, construction, pre-conditioning, deployment, recovery and sample processing of the sediment traps, and PAHs analysis on the settling particles captured by the traps are available in Adhikari et al. (2015) and Lamborg et al. (2008).

3.2.3. ^{238}U and ^{234}Th analysis

The conservative nature of ^{238}U allows estimation of ^{238}U activities in seawater by multiplying a constant 0.0704 dpm PSU^{-1} with salinity (Chen et al., 1986; Owens et al., 2011). The ^{238}U and salinity can show a non-conservative behavior in estuarine and coastal water (Baskaran and Swarzenski, 2007). All the samples collected for this study were from deep water therefore, the assumption of conservative behavior of ^{238}U is reasonable (Baskaran et al., 1996; Hung et al., 2004). For determining ^{234}Th activity in the water column, each 4 L sample was spiked with a known activity of ^{230}Th (10 dpm g^{-1}) using a weight calibrated pipette, immediately after collecting the samples in the HDPE bottles. Acidification helps taking out organic molecules in the sample, which can retain thorium in sample solution. After >8 hours, pH was brought back to 8 by adding NH_4OH. Then the thorium was co-precipitated with MnO_2 by addition of $KMnO_4$ and $MnCl_2$ into the bottles (Pike et al., 2005). The precipitate was allowed to form for another >8 hours and then was filtered using 25 mm diameter 1 μm QMA filters. For

the analysis of β-emission in RISØ analyzer (developed by the Center for Nuclear Technologies, Technical University of Denmark), the filters with precipitate were dried and fixed on RISØ cups, below one layer of Mylar and two layers of regular aluminum foil. Then the samples were analyzed in RISØ counter for estimating beta emission from ^{234}Th via ^{234}mPa (E_{max} = 2.19 MeV). After the first count, the samples were stored for six months and then recounted to estimate background emission from long lived radioisotopes (Maiti et al., 2012).

A number of factors might cause loss of thorium from the samples during analysis, viz., imperfect precipitation, breaking of filters, leakages and spills, which are potential sources of underestimation (Pike et al., 2005). Hence, it is important to quantify the loss of thorium during analysis in order to estimate original ^{234}Th activity in the samples. The filters (after recounting for thorium) were used to estimate method-recovery of thorium, following "2-spike" method (Rodriguez y Baena et al., 2006). After recounting in RISØ counter, filters were dismounted from RISØ cups, spiked with 1 gm ^{228}Th standard and sonicated in 10% H_2O_2:8M HNO_3 solution. Ion-exchange chromatography was carried out to separate thorium, followed by plating and final counting in Canberra Alpha-analyst. Method-recovery was estimated from the ratio of ^{230}Th and ^{228}Th activities. The method recovery ranged between 70-95%, excluding outliers. Reported values for ^{234}Th are recovery corrected using the recoveries of ^{230}Th yield monitor and decay corrected to the time of collection. Propagated errors include uncertainties related to counting, sample volume, and other measurement errors.

3.2.4. PAHs/^{234}Th ratios in particulate samples

The 22 mm QMA subsamples from pump filters dried at 60 °C were mounted onto RISØ cups and analyzed for particulate ^{234}Th activity in RISØ analyzer, using the same procedure explained above for dissolved ^{234}Th analysis. The rest of the QMA filters stored at -20 ºC were

analyzed for particulate PAHs using GC/MS, following the protocol used by Adhikari et al. (2015). Briefly, the particulate samples in filter QMAs were spiked with known concentrations of recovery standard, Soxhlet extracted for 24 hours with dichloromethane, the solvent extracts were concentrated to 1 ml, spiked with internal standards, and then the samples were analyzed using an Agilent 7890A GC interfaced with an Agilent 5975C inert XL mass selective detector (MSD) (EPA SW-846 method 8270). In order to ensure low level detection of the target PAHs, the MSD was operated in the selective ion monitoring (SIM) mode, targeting for 43 PAHs; 18 parent PAHs with 2-6 aromatic rings [naphthalene to benzo(g,h,i)perylene] and 25 C1-C3 or C4 alkyl-substituted homologues of the parent PAHs. The concentrations of the sum of all 43 ($\sum PAH_{43}$) individual PAHs identified and quantified in this study (Appendix 2) were used to calculate $\sum PAH_{43}/^{234}Th$ ratios.

3.2.5. Calculating ^{234}Th-based particulate PAHs fluxes

One-dimensional steady-state model has been used by a number of previous studies in different oceanographic settings to estimate particulate ^{234}Th fluxes in the water column (Buesseler et al., 1992, Gustafsson et al., 1997a, c; Maiti et al., 2009; Savoye et al., 2006). The basic principle of this model is that the total activity of ^{234}Th in water column is balanced between its source from the radioactive decay of its parent ^{238}U, loss due to its own decay, advective and diffusive source/sinks of ^{234}Th, and removal of particulate ^{234}Th via vertical transport. It can be described by the following activity balance equation (Buesseler et al., 1992; Maiti et al., 2009),

$$\frac{\delta[^{234}Th_{tot}]}{\delta t} = \lambda_{Th}(^{238}U_{tot} - ^{234}Th_{tot}) - F_{Th} + V \qquad (3.1)$$

where $^{238}U_{tot}$ is the total activity of ^{238}U (dpm L^{-1}), $^{234}Th_{tot}$ is the observed activity (dpm L^{-1}) of total ^{234}Th, λ_{Th} is the radioactive decay constant for ^{234}Th (0.029 d^{-1}), F_{Th} is the particle

mediated vertical flux of ^{234}Th (dpm m^{-2} d^{-1}), $\delta[^{234}Th_{tot}]/\delta t$ is the change in total ^{234}Th activity with time, and V represents the sum of advective and diffusive processes (Buesseler et al., 1992; Maiti et al., 2009). Most of the previous open ocean as well as coastal studies have assumed a steady-state conditions ($\delta[^{234}Th_{tot}]/\delta t = 0$) and negligible advective and diffusive processes (Buesseler et al., 1992; Gustafsson et al., 1997a; Maiti et al., 2009, 2012). Therefore, the equation (1) can be reduced to,

$$F_{Th} = \lambda_{Th}(^{238}U_{tot} - ^{234}Th_{tot}) \qquad (3.2)$$

The total particle mediated fluxes of ^{234}Th (dpm m^{-2} d^{-1}) can be calculated by integrating equation (2) over the water column depth of interest.

$$(F_{Th})_z = \lambda_{Th} \int_0^z (^{238}U_{tot} - ^{234}Th_{tot})\, dz \qquad (3.3)$$

Where $(F_{Th})_z$ is the depth integrated ^{234}Th flux at the lower depth boundary, 'z'.

The ^{234}Th flux estimated in equation (3) can be combined with the PAHs/^{234}Th ratios in suspended particles to estimate particulate PAHs fluxes,

$$(F_{PAHs})_z = \left(\frac{PAHs}{^{234}Th}\right)_z \times (F_{Th})_z \qquad (3.4)$$

Where $(PAHs/^{234}Th)_z$ is the ratio of particulate PAHs concentrations and ^{234}Th activities at depth 'z'.

In order to accurately translate water column derived ^{234}Th fluxes into PAHs fluxes, both the ^{234}Th and PAHs must be coupled to same sinking particles. Previous studies have shown that ^{234}Th and hydrophobic organic compounds like PAHs are associated with the same settling particles (Gustafsson et al., 1997a, 1998). Adhikari et al. (2015) concluded that the suspended PAHs are likely associated in finer particulate matter (<51 μm) including POC, therefore in this study reports ^{234}Th-derived PAHs fluxes only for that particle size ranges.

3.3. Results and discussion

3.3.1. Total ^{234}Th activities and ^{238}U-^{234}Th disequilibria

Total ^{234}Th activities varied between 1.15-2.75 dpm L^{-1} in 2012 and between 1.65-2.75 dpm L^{-1} in 2013. These values are within the range of previously reported total ^{234}Th activity concentrations in the northern GOM (Baskaran et al., 1996; Hung et al., 2004). Salinity derived ^{238}U activities remained similar throughout the water column; 2.50 ± 0.02 dpm L^{-1} and 2.51 ± 0.01 dpm L^{-1}, respectively in 2012 and 2013. The upper 150 m of the water column were depleted in ^{234}Th activities, however in some cases (NDWH-13a, NDWH-13b and DWH-13a) the ^{238}U-^{234}Th disequilibria could be observed up to 200 m (Figure 3.3 and 3.4). The stations NDWH and DWH had higher ^{238}U- ^{234}Th disequilibria than SDWH in 2012, while it remained similar in 2013 (Figure 3.3 and 3.4). In some of the stations, ^{234}Th activities were found to be more than ^{238}U, especially below 200 m which is due to particle remineralization (Maiti et al., 2009). In general, ^{238}U- ^{234}Th equilibrium was regained at depths >250 m in both years (Figure 3.3 and 3.4).

The magnitude of ^{238}U-^{234}Th disequilibria, quantified by the ^{234}Th/^{238}U ratio (= 1 at radioactive equilibrium and lower values implying higher disequilibria) varied between 0.44 -1.0 in 2012 and between 0.66 -1.0 in 2013 (Figure 3.3 and 3.4). Similar, ^{238}U/^{234}Th ratios have been previously reported for the northern GOM water column (Hung et al., 2004). The ^{234}Th/^{238}U ratio is an excellent tracer of chemical scavenging, lower the ratio higher is the removal by particles and thereby more vertical transport (Gustafsson et al., 1997c; Maiti et al., 2013). The higher ^{238}U-^{234}Th disequilibria in upper 150 m of the water column (Figure 3.3 and 3.4), which is due to the partition of ^{234}Th in particulate phase followed by subsequent settling, implies that this is the region with highest rates of particle formation and sinking. The ^{234}Th/^{238}U ratios in 2012 were

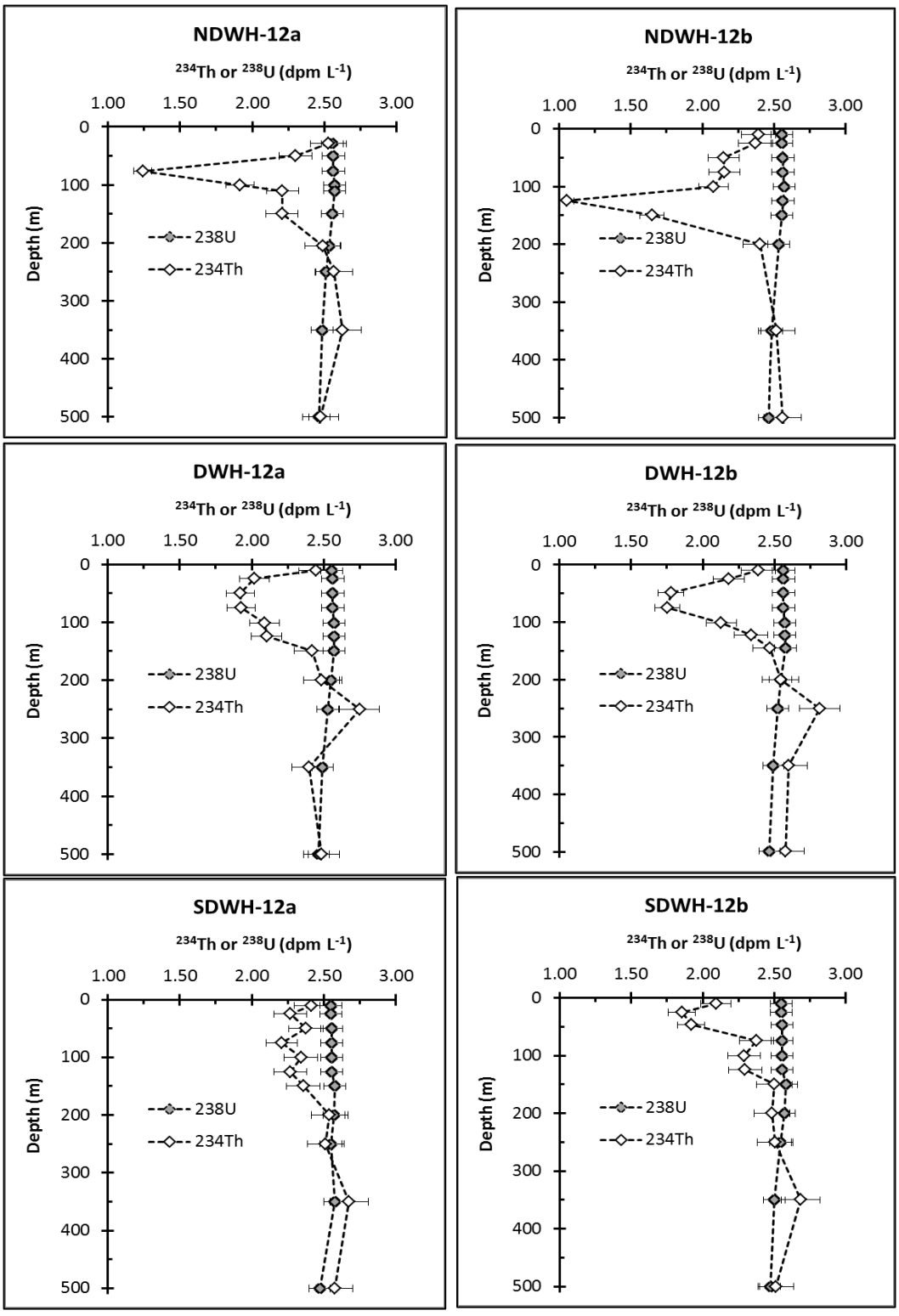

Figure 3.3. Total ^{238}U and ^{234}Th activities in upper 500 m of the northern Gulf of Mexico water column, in the samples collected during 2012. The letters 'a' and 'b' at the end of each station i.d. (e.g., NDWH-12a and NDWH-12b) represent the two sets of water samples collected from each station and analyzed for radioactivity. The error bars represent the propagated errors.

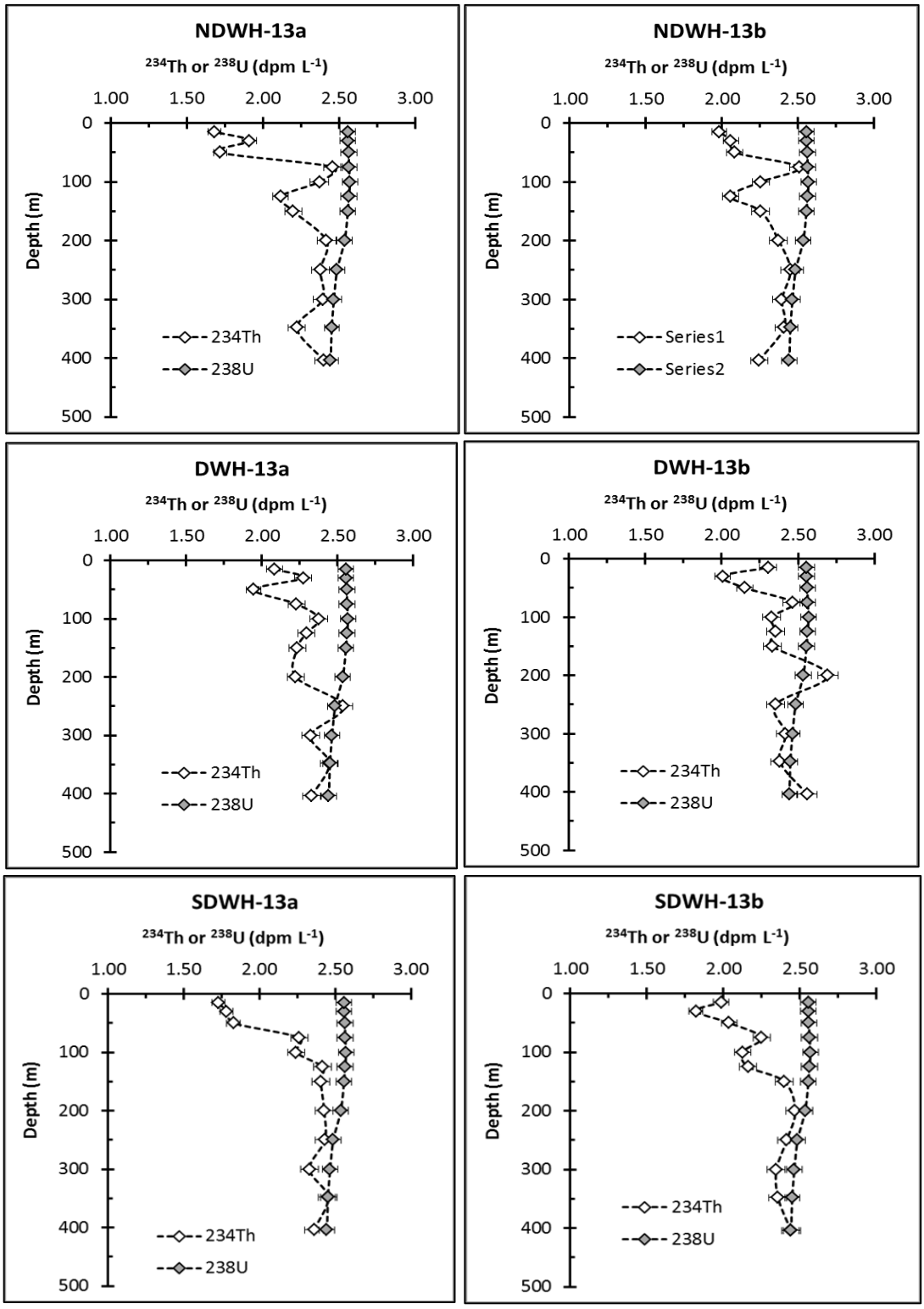

Figure 3.4. Total ^{238}U and ^{234}Th activities in upper 500 m of the northern Gulf of Mexico water column, in the samples collected during 2013. The letters 'a' and 'b' at the end of each station i.d. (e.g., NDWH-13a and NDWH-13b) represent the two sets of water samples collected from each station and analyzed for radioactivity. The error bars represent the propagated errors.

higher (~1) in surface, decreased at depth with a minima at ~150 m, and regained its equilibrium values at ~200 m of the water column (Figure 3.3). However, the $^{234}Th/^{238}U$ ratios showed a different pattern in 2013, minimum at upper 50 m of the water column and regained its equilibrium values at ~200 m (Figure 3.4). It suggests a temporal variability in particle dynamics, likely due to variation in particle formation stimulated by primary productivity, and/or change in additional sources of particles like atmospheric inputs in between 2012 and 2013. The particle flux of ^{234}Th, estimated using ^{238}U-^{234}Th disequilibria in the upper 350 m of the water column (Eq. 3), varied between 1001-3413 dpm m^{-2} d^{-1} (mean 1781 ± 625 dpm m^{-2} d^{-1}) and 151-1741 dpm m^{-2} d^{-1} (mean 907 ± 136 dpm m^{-2} d^{-1}), respectively in 2012 and 2013 (Table 3.3 and 3.4). The significantly higher ^{234}Th fluxes in 2012 ($P < 0.001$) than in 2013 was mainly attributed to the lower $^{234}Th/^{238}U$ ratios in 2012 than 2013 (Figure 3.3 and 3.4).

3.3.2. Particulate ^{234}Th activities and $\sum PAH_{43}/^{234}Th$ ratios

In order to use ^{238}U-^{234}Th disequilibria to estimate vertical fluxes of PAHs, the ratio of PAHs concentrations to ^{234}Th activities in suspended particles at the base of the depth interval of interest is needed (Buesseler et al., 2006; Maiti et al., 2012; Savoye et al., 2006). In this study, the particulate $\sum PAH_{43}/^{234}Th$ ratios and hence the export fluxes of particulate PAHs were estimated at depths 100, 150, 250 and 350 m of the water column. The activities of ^{234}Th in suspended particles varied between 0.04-0.45 dpm L^{-1} (mean 0.19 ± 0.10 dpm L^{-1}) and 0.05-0.25 dpm L^{-1} (mean 0.12 ± 0.05 dpm L^{-1}), respectively in 2012 and 2013. Particulate ΣPAH_{43} concentrations varied between 0.33-0.64 ng L^{-1} (average 0.44 ± 0.1 ng L^{-1}) in 2012, and 0.30-0.92 ng L^{-1} (average 0.54 ± 0.2 ng L^{-1}) in 2013 (Table 3.1 and 3.2). The $\sum PAH_{43}/^{234}Th$ ratios in suspended particles varied between 0.7-8.4 ng dpm^{-1} (3.2 ± 2.1 ng dpm^{-1}) in 2012, and

Table 3.1. The concentrations of particulate PAHs, ^{234}Th fluxes, PAHs/^{234}Th ratios in suspended particles collected by *in situ* pumps and the sinking particles captured in sediment traps, and ^{234}Th-derived and sediment trap-based particulate PAHs fluxes observed in 2012, in upper 350 m of the northern Gulf of Mexico water column. The ± represent the standard deviation.

Station ID	Depths (m)	$\sum PAH_{43}$ Conc. (ng L^{-1})	^{234}Th flux (dpm m^{-2} d^{-1})	PAH/^{234}Th ratio in suspended particles (ng dpm^{-1})	PAH/^{234}Th ratio in sinking particles (ng dpm^{-1})	^{234}Th-derived PAHs Fluxes (ng m^{-2} d^{-1})	Trap-derived PAHs Fluxes (ng m^{-2} d^{-1})
NDWH-12a							
	100	0.30	1347±202	8.4±1.2	-	11.3±1.7	-
	150	0.40	2185±327	6.9±1.03	-	15.1±1.5	-
	250	0.30	1886±283	2.9±0.4	-	5.6±0.8	-
	350	0.32	1915±287	0.9±0.1	-	1.7±0.2	-
NDWH-12b							
	100	0.57	1000±150	7.0±0.7	-	7.0±0.7	-
	150	0.42	2605±390	2.3±0.2	-	6.0±0.6	-
	250	0.37	3392±508	0.9±0.1	-	3.2±0.5	-
	350	0.34	3413±511	1.0±0.1	-	3.5±0.5	-
DWH-12a							
	100	0.65	1416±212	3.0±0.6	-	4.3±0.9	-
	150	0.46	1956±293	2.2±0.4	5.4±0.8	4.4±0.8	5.2±0.8
	250	0.39	1999±299	1.9±0.4	5.3±0.8	3.9±0.7	7.1±1.1
	350	0.36	1824±273	1.5±0.3	9.0±1.4	2.7±0.5	6.8±1.0
DWH-12b							
	100	0.63	1688±253	6.9±1.4	-	11.6±2.3	-
	150	0.38	2074±311	2.4±0.5	-	4.9±1.0	-
	250	0.29	1906±285	1.6±0.3	-	3.1±0.6	-
	350	0.33	1360±204	0.7±0.1	-	1.0±0.2	-
SDWH-12a							
	100	0.72	1250±187	4.8±0.7	-	6.0±0.9	-
	150	0.60	1242±186	4.2±0.6	5.8±0.9	5.2±0.8	6.2±0.9
	250	0.54	1021±153	2.7±0.4	5.9±0.88	2.9±0.4	6.3±0.9
	350	0.49	1152±172	2.4±0.4	11.9±1.8	2.8±0.4	7.8±1.2
SDWH-12b							
	100	0.54	1249±187	3.2±0.5	-	4.0±0.6	-
	150	0.52	1552±232	2.7±0.4	-	4.2±0.6	-
	250	0.38	1754±263	2.0±0.3	-	3.5±0.5	-
	350	0.37	1544±231	3.4±0.5	-	5.3±0.8	-

Table 3.2. The concentrations of particulate PAHs, ^{234}Th fluxes, PAHs/^{234}Th ratios in suspended particles collected by *in situ* pumps and the sinking particles captured in sediment traps, and ^{234}Th-derived and sediment trap-based particulate PAHs fluxes observed in 2013, in upper 350 m of the northern Gulf of Mexico water column. The ± represent the standard deviation.

Station ID	Depths (m)	$\sum PAH_{43}$ Conc. (ng L^{-1})	^{234}Th flux (dpm m^{-2} d^{-1})	PAH/^{234}Th ratio in suspended particles (ng dpm^{-1})	PAH/^{234}Th ratio in sinking particles (ng dpm^{-1})	^{234}Th-derived PAHs Fluxes (ng m^{-2} d^{-1})	Trap-derived PAHs Fluxes (ng m^{-2} d^{-1})
NDWH-13a							
	100	0.53	1586±237	7.8±1.2	-	12.3±1.8	-
	150	0.41	1614±242	8.2±1.2	-	13.3±2.0	-
	250	0.61	802±120	4.3±0.6	-	3.4±0.51	-
	350	0.82	585±87	3.3±0.5	-	1.9±0.3	-
NDWH-13b							
	100	1.31	1083±162	17.2±1.7	-	18.6±1.9	-
	150	1.15	1435±215	11.7±1.2	-	16.8±1.7	-
	250	1.21	1448±217	9.0±1.3	-	13.0±1.9	-
	350	0.92	455±68	8.0±1.2	-	3.7±0.5	-
DWH-13a							
	100	0.47	1141±171	9.9±2.0	-	11.3±2.2	-
	150	0.40	1350±202	3.6±0.7	2.0±0.3	4.8±0.9	2.0±0.3
	250	0.60	150±22	5.3±1.0	2.4±0.4	0.8±0.1	2.1±0.3
	350	0.65	241±36	5.6±1.1	-	1.3±0.3	-
DWH-13b							
	100	0.44	858±128	6.8±1.3	-	5.8±1.2	-
	150	0.33	959±143	3.0±0.6	-	2.9±0.6	-
	250	0.17	659±98	2.3±0.5	-	1.5±0.3	-
	350	0.22	526±78	1.3±0.3	-	0.7±0.1	-
SDWH-13a							
	100	0.34	1741±261	1.7±0.3	-	3.0±0.6	-
	150	0.35	658±98	2.2±0.4	2.6±0.5	1.4±0.3	2.4±0.5
	250	0.36	481±72	1.8±0.3	3.7±0.7	0.9±0.2	2.5±0.5
	350	0.31	192±28	1.6±0.3	2.8±0.5	0.3±0.1	1.9±0.4
SDWH-13b							
	100	0.41	1460±219	4.3±0.9	-	6.3±1.3	-
	150	0.30	855±128	2.2±0.4	-	1.8±0.4	-
	250	0.32	975±146	2.4±0.5	-	2.3±0.5	-
	350	0.29	502±75	1.9±0.4	-	0.9±0.2	-

1.3-17.2 ng dpm^{-1} (5.2 ± 3.9 ng dpm^{-1}) in 2013 (Table 3.1 and 3.2). In general, $\sum PAH_{43}/^{234}Th$ ratios decreased with depths during both sampling years, with a maxima at 100 m followed by a substantial decrease at 150 m (Figure 3.5a and 3.5b). The upper 150 m of the water column showed higher interstation variability in $PAHs/^{234}Th$ ratios, especially in 2013, than at the deeper depths (Figure 3.5a and 3.5b). Below 150 m, $PAHs/^{234}Th$ ratios remained similar both between the sampling years and sampling stations except at station NDWH-13a (Figure 3.5a and 3.5b). At station NDWH-13a, the $PAH_{43}/^{234}Th$ ratios were considerably higher than other stations as well as higher than the ratios at same station in 2012 (Figure 3.5a and 3.5b), which is mainly attributed to higher particulate PAHs concentrations in that station (Table 3.2).

There are no published studies reporting PAHs to ^{234}Th ratios to directly compare with the results from this study however, the decreasing trends in $\sum PAH_{43}/^{234}Th$ ratios with depths are similar to the reported variation of $C/^{234}Th$ ratios in the water column (Buesseler et al., 2006; Weinstein and Moran, 2005). A number of processes like composition and binding capacity of sinking particles, aggregation-disaggregation processes, zooplankton grazing can be attributed to the change in $PAHs/^{234}Th$ ratio with depth (Buesseler et al., 2006; Lepore et al., 2009). However, the primary factors that probably affect the particulate $PAH/^{234}Th$ ratios are preferential remineralization of select PAHs as particles sink and remineralization of organic matter (primarily POC) to which PAHs tend to bind. The molecular profiles of the particulate PAHs in the northern GOM is dominated by lower molecular weight PAHs (<4 rings) and their alkyl homologues (Appendix 3), which have lower partition coefficients and are likely to remineralize faster than higher molecular weight PAHs (Chen et al., 2004). Such a preferential remineralization of lower molecular weight PAHs decreases ΣPAH_{43} concentrations and hence the $\sum PAH_{43}/^{234}Th$ ratios as particles sink. The $\sum PAH_{43}/^{234}Th$ ratios in sinking particles captured

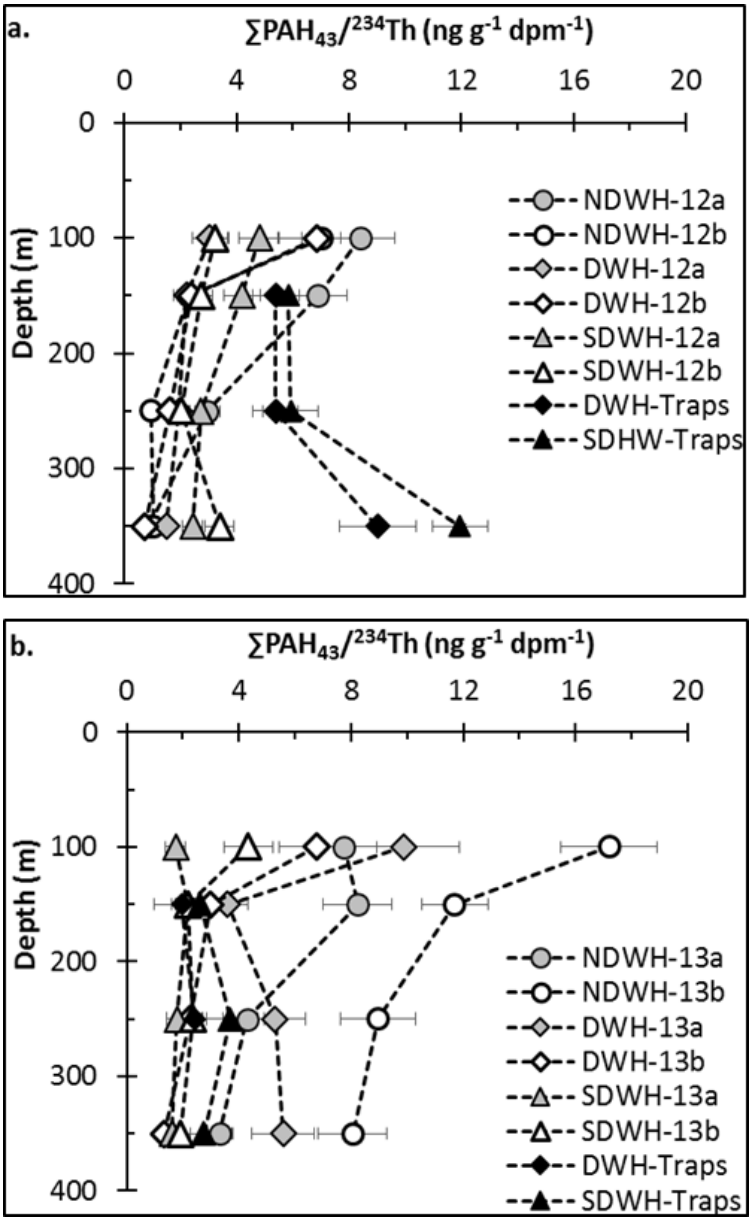

Figure 3.5. The ratios of the concentrations of $\sum PAH_{43}$ to ^{234}Th activities in the suspended and sinking particles in upper 350 m of the northern Gulf of Mexico water column, (a) in 2012 and (b) in 2013. Suspended particles were collected by using large volume *in situ* pumps while the sinking particles were capture in surface-tethered drifting sediment traps. The error bars represent the standard deviation.

by the drifting sediment traps deployed at depths 150, 250 and 350 m of the northern GOM water column varied between 5.4-12.0 ng dpm^{-1} and 2.0-3.7 ng dpm^{-1}, respectively in 2012 and 2013 (Table 3.1 and 3.2). The $\sum PAH_{43}/^{234}Th$ ratios in settling particles were higher than in suspended

particles, however they were within a factor of two, except at 350 m of the water column in 2012 (Table 3.1, Figure 3.5a). In general, this finding supports the previous results that the suspended particles collected using large volume *in situ* pumps represent the sinking particles in the upper ocean (Buesseler et al., 2006; Lepore et al., 2009). The $\sum PAH_{43}/^{234}Th$ ratios in sinking particles at 350 m in 2012 were ~5 times higher than the ratios in suspended particles at corresponding depths (Figure 3.5a). Exact reason of such discrepancies in PAHs/^{234}Th ratios at that particulate depth is unknown, however it could probably be due to the differential association of PAHs and ^{234}Th in suspended and sinking particles at greater depths, particle size fractions, preferential remineralization of ^{234}Th in sinking particles, or horizontal transport (Gustaffson et al., 1998).

3.3.3. ^{234}Th-derived particulate PAHs fluxes

The ^{234}Th-derived $\sum PAH_{43}$ fluxes in upper 350 m of the northern GOM water column varied between 1.0-15.1 μg m^{-2} d^{-1} (mean = 5.1 ± 3.2 μg m^{-2} d^{-1}) in 2012, and 0.3-18.6 μg m^{-2} d^{-1} (mean = 5.4 ± 5.5 μg m^{-2} d^{-1}) in 2013 (Table 3.1 and 3.2). The PAHs fluxes remained statistically similar between the sampling years ($P < 0.05$). All the sampling stations in both years, except NDWH-12a and NDWH-13a, show a near surface (at 100 m) maxima in $\sum PAH_{43}$ fluxes (Figure 3.6a and 3.6b). The PAHs fluxes at stations NDWH-12a and NDWH-13a were higher at 150 m than at 100 m. The chlorophyll-fluorescence maxima were observed at ~70 m which was at the base of the mixed layer (40-70 m), while the ^{238}U-^{234}Th disequilibria extended down to 150 m (Figure 3.3 and 3.4). Abundance of biology derived particulate matter and their subsequent sinking from the euphotic zone is the primary reason of higher PAHs fluxes from upper 100-150 m of the water column. The pelagic region of the northern GOM is oligotrophic (Wawrik and Paul, 2004) where the biologically derived particulate organic matters, primarily POC, in the upper ocean contribute to the major pool of the sinking particles. PAHs show higher affinity

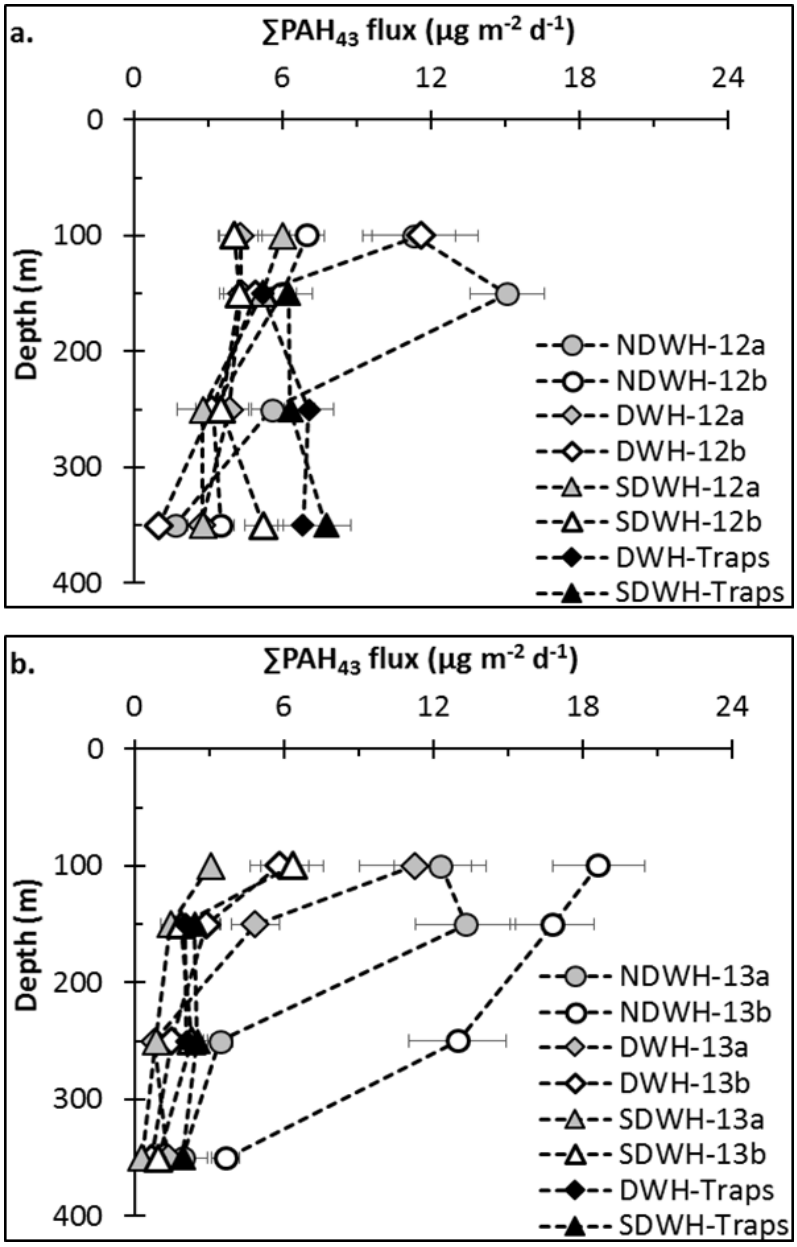

Figure 3.6. ^{234}Th-derived and sediment trap-based PAHs fluxes from the upper 350 m of the northern Gulf of Mexico water column during (a) 2012, and (b) 2013. The error bars represent the standard deviation.

towards POC (Means et al., 1980; Wang et al., 2001). The attenuation of PAHs fluxes at depths below 150 m could be attributed to the preferential remineralization of POC to which PAH are sorbed, as approximately, 45-70% of the POC sinking below 150 m is preferentially remineralized by 350 m (Adhikari et al., 2015). The variability in PAHs fluxes among the

sampling stations was maximum at upper 100-150 m of the water column (Figure 3.6a and 3.6b) which was mainly driven by the variation in PAHs/^{234}Th ratios (Figure 3.5). Below 150 m, $\sum PAH_{43}$ fluxes followed a consistent pattern of decrease in fluxes with depth and remained similar among the sampling stations in both years, except NDWH-13b (Figure 3.6a and 3.6b). The station NDWH-13b had higher PAHs fluxes than other stations.

The present study is the first to utilize ^{238}U-^{234}Th disequilibria to estimate vertical flux of particulate PAHs in the northern GOM which provides a unique opportunity to compare PAHs fluxes estimated using this method with surface-tethered drifting sediment trap-based measurements. Sediment trap-derived PAHs fluxes, at stations DWH and SDWH (for depths 150, 250 and 350 m), varied between 5.2-7.8 μg m^{-2} d^{-1} in 2012 and 2.0-2.5 μg m^{-2} d^{-1} in 2013 (Table 3.1, Figure 3.6a and 3.6b). In general, trap-based PAHs fluxes are found to be higher than the ^{234}Th-derived fluxes however, they are within the factor of three (except for SDWH-13 at 350 m). The difference between traps and ^{234}Th-based fluxes increases with depths and the trap-based fluxes were much higher (up to a factor of 6 at 350 m, at station SDWH in 2013). This is not surprising given the negligible disequilibria between ^{238}U-^{234}Th at depths below 250 m, which results in higher uncertainty in the ^{234}Th fluxes. It is important to point out that the ^{234}Th-based fluxes are integrated over past 3-4 weeks while trap-based fluxes are integrated over 2-3 days, which could be the reason of some of the observed differences in fluxes estimated via these two techniques. Considering the variability in oceanographic settings, uncertainties in PAHs and ^{234}Th analysis, PAHs/^{234}Th ratios, and assumptions on ^{234}Th flux estimation (steady-state conditions, negligible advection), the PAHs fluxes estimated using ^{234}Th and sediment traps in the upper 250 m of the water column are ideal, generally within the factor of three (Moran et al., 2003). There are no comparable studies using both of these methods to estimate particulate

PAHs fluxes in upper ocean however, similar variability of a factor of 2-4 between the traps and ^{238}U-^{234}Th-derived fluxes have been reported for PAHs (Palm et al., 2004 in Fjords), metals (Weinstein and Moran, 2005) and POC fluxes (Lepore et al., 2009; Maiti et al., 2009) by number of previous studies. The agreement between these two approaches validates the technique of coupling ^{238}U-^{234}Th disequilibria to estimate PAHs transport fluxes from the upper ocean in the northern GOM.

The traps and ^{234}Th-based PAHs flux estimations have their own characteristic strengths and weaknesses. The ^{234}Th-derived estimates are completely trap independent therefore, using both approaches together cross validates the flux data to give a more robust estimation of upper ocean PAHs fluxes (Buesseler, 1991; Gustaffson et al., 1997a). In contrast to the surface-tethered drifting sediment traps which usually provide fluxes integrated over 2-3 days, the ^{234}Th-derived fluxes are generally integrated over 3-4 weeks, which is the typical time scale of particle dynamics in the upper ocean (Buesseler et al., 1998, 2007; Maiti et al., 2012). The ^{234}Th-based method thus averages the PAHs fluxes over a longer time scale that smooth out any episodic flux events recorded by the traps. The ^{238}U-^{234}Th disequilibria has been mostly used to estimate particle transports at 100-150 m depth, at the base of the euphotic zone (Buesseler et al., 1998, 2006; Gustafsson et al., 1998). The results from this study show that this techniques can reasonably predict PAHs fluxes in upper mesopelagic zone up to 250 m and if disequilibria persists below 250 m it may be used to determine PAHs fluxes even at 350 m. The possibilities of utilizing ^{234}Th to provide insights into particle dynamics in the lower mesopelagic twilight zone (up to 1000 m depth) has been discussed (Waples et al., 2006). However, the results from this study show that due to the lack of ^{238}U-^{234}Th disequilibria (Figure 3.3 and 3.4) and the

resulting higher uncertainties associated with the difference in activities between ^{238}U and ^{234}Th , this method may not accurately estimate PAHs fluxes below 250 m of the water column.

Surface-tethered drifting sediment traps can provide a direct instantaneous measurements of particulate PAHs fluxes from the surface oceans however, they are difficult to deploy/retrieve especially in bad weather and high traffic areas like the northern GOM and are very time consuming (Buesseler et al., 2007). This study itself attests to the difficulties with trap deployment when no trap could be deployed in 2012 at NWH due to bad weather and trap array being damaged by seismic survey boats in 2013 at DWH. The logistics of deploying traps at higher spatial resolution coupled with expensive ship time often results in limited spatial coverage of vertical fluxes of PAHs or any other elements of interest. In contrast, ^{234}Th-based approach, as shown in the results of the present study, can provide indirect estimate of PAHs fluxes from the upper ocean with higher spatial and vertical resolution and may complement the trap-based PAHs fluxes (Maiti et al., 2012; Waples et al., 2006). This method is relatively easier, faster, and less prone to failure therefore, the future use of this technique can provide an opportunity to produce consistent upper ocean PAHs flux estimates, where such data are rare. This is a necessary first step to make progress towards the development of regional and a global PAHs mass balance.

3.4. Conclusion

This study, for the first time, utilizes a trap independent technique of coupling ^{238}U-^{234}Th disequilibria with PAHs/^{234}Th ratios in suspended particles, to estimate vertical transport fluxes of particulate PAHs from upper mesopelagic zone of the northern GOM. The ^{234}Th-derived vertical fluxes of particle-bound $\sum PAH_{43}$ in upper 350 m of the northern GOM water column varied between 1.0-15.1 μg m^{-2} d^{-1} and 0.3-18.6 μg m^{-2} d^{-1}, respectively in 2012 and 2013. Given

the variability in oceanographic settings, analytical uncertainties and the model assumptions (steady-state and negligible advective/diffusive processes), the ^{234}Th-derived and sediment trap-based PAHs fluxes at 150 and 250 m are found to be similar, within the factor of three. The results demonstrate that the upper ocean ^{238}U-^{234}Th disequilibria can be an effective tracer for vertical transport fluxes of particulate PAHs in the upper mesopelagic zone of this region. Unlike surface-tethered drifting sediment traps, this method is relatively easier, faster and less prone to failure, and can provide a relatively large number of consistent PAHs flux estimates with large spatial coverage in relatively short time. Therefore, this technique can be more appropriate for upper ocean vertical flux and residence time estimation of particle-reactive persistent organic pollutants (POPs) such as PAHs, especially in high traffic areas like the northern GOM, where drifting sediment traps are difficult to deploy. It can provide an opportunity to fill the considerable gap of reliable upper ocean PAHs flux estimates in the global ocean, and particularly in the northern GOM. It is an essential first step towards the development of a mass balance of PAHs as well as other hydrophobic organic compounds (HOCs) in marine ecosystems.

CHAPTER 4: DISTRIBUTIONS AND ACCUMULATION RATES OF POLYCYCLIC AROMATIC HYDROCARBONS IN THE NORTHERN GULF OF MEXICO SEDIMENTS

4.1. Introduction

The northern Gulf of Mexico (GOM) is an area with major ecosystem health concerns in terms of polycyclic aromatic hydrocarbons (PAHs) pollution and is one of the most extensively studied area of the world, both before and especially after Deepwater Horizon (DWH) oil spill in 2010. Mississippi River (MR) discharge, coastal erosion, atmospheric deposition of combustion products, natural oil seeps, gas hydrates and accidental oil leaks related to petroleum exploration/transportation release a large amount of PAHs into the GOM waters (Mitra and Bianchi, 2003; Overton et al., 2004; Park et al., 2001, 2002; Wade et al., 1989; Wang et al., 2011). In addition to these background sources, the DWH oil spill released ~2.1 x 10^{10} g of PAHs into the northern GOM waters (Reddy et al., 2012). PAHs with relatively low aqueous solubility get readily sorbed onto soil and sediments, and eventually deposited to the seafloor (Berrojalbiz et al., 2011; May et al., 1978; Karickhoff et al., 1979; Dachs et al., 2002; Lipiatou et al., 1997). Thus the seafloors are considered the repository of PAHs and the deep-sea sediments are therefore major global sinks for PAHs entering into ocean waters (Marini and Frapiccini, 2013; Gustafsson et al., 1997a; NRC, 2003). It has been estimated that 4-31% of the oil, and probably the same proportion of PAHs, released during DWH oil spill may have been deposited in 3200 km^2 of the northern GOM seafloor (Valentine et al. 2014). Another independent study (Chanton et al., 2015) estimated 3.0-4.9% of spilled oil settled in 2400 km^2 area around the DWH oil spill site. Deposition of such an unprecedented amount PAHs in a single event can substantially increase their concentrations in sediments and impair the benthic communities.

The toxic, carcinogenic, mutagenic and persistent nature of the PAHs (Albers et al., 2003; Neff 1979; Samanta et al., 2002; Yan et al., 2004) coupled with the large fishing industry in the Gulf make them critical group of organic contaminants that need to be monitored thoroughly. There are few pre-DWH spill studies on sediment PAHs in the shallow coastal regions of the GOM (Brooks et al., 1986; Overton et al., 2004; Wade et al., 1988) and such pre-spill studies in the deep-sea of the northern GOM are rare (Wade et al., 2008). Immediately after the DWH accident in 2010, a large number of sediment samples were collected from this region of the GOM by the Natural Resource Damage Assessment (NRDA) program, and analyzed for PAHs. These data are made publicly available by NOAA (http://www.gulfspillrestoration.noaa.gov/oil-spill/gulf-spill-data). In spite of persistent nature of PAHs, various diagenetic processes acting on deposited PAHs can alter their initial concentrations (Albers et al., 2003; Berrojalbiz et al., 2011; Cornelissen et al., 1998; Gutierrez, 2011; Head et al., 2006). Therefore, it is important to regularly monitor sediment PAHs in order to determine their long term fates and possible harmful impacts on benthic communities however, such studies in the GOM are limited (Turner et al., 2014; Wang et al., 2014). The focus of this study is to quantify PAHs concentrations and compositions 1-3 years after the DWH oil spill in selected northern GOM shelf, slope and ocean sediment, and to determine PAHs accumulation rates in this region in order to establish PAHs pollution trends.

4.2. Materials and methods

4.2.1. Sample collection

Sediment cores were collected from 17 sampling stations (Figure 4.1) on board three different opportunistic cruises in 2011 and 2013, in the northern GOM. Sediment samples from sites C1-C8 were collected aboard *R/V Endeavor* in August 2011, cores C9-C11 were collected

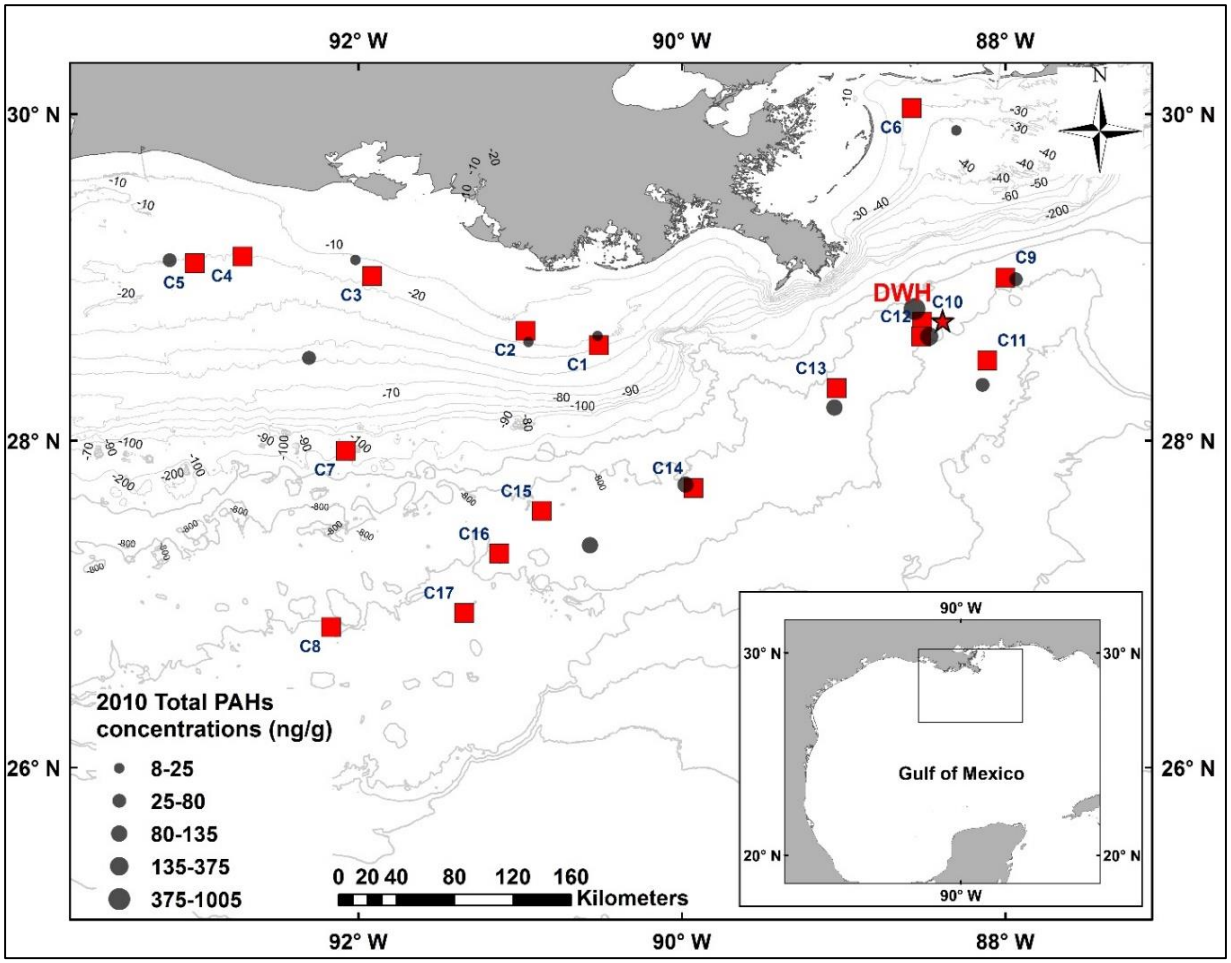

Figure 4.1. Sampling locations in the northern Gulf of Mexico (red squares), stations C1 to C8 were samples in August 2011 while the stations C9-C17 were sampled in April and June 2013. The gray circles represent ∑PAHs concentrations in the sediment samples collected by Natural Resource Damage Assessment (NRDA) in 2010 (publicly reported by NOAA).

aboard the *R/V Walton Smith* in April 2013, while the rest (C12-C17) were collected from the *R/V Pelican* in June 2013. The sampling stations C1-C7 represent coastal stations, C9-C13 as deep-sea stations east of Mississippi River (MR) delta in the vicinity of DWH spill sites, and rest (C8, and C14-C17) represent deep-sea stations west of the MR delta (Figure 4.1).

Sediment cores were collected using multi-corer with eight collection tubes. Two undisturbed cores from each cast were chosen for PAHs and ^{210}Pb-dating for this study. Only the top 6 cm of the first core from each station was used for PAHs analysis while the entire second

core was used for ^{210}Pb-dating. Sediment cores for PAHs analysis, collected in 2011 were sectioned into 2 cm intervals while the cores collected in 2013 were sectioned at 1 cm intervals up to 2 cm and at 2 cm intervals thereafter, except two cores in the vicinity of DWH (C9 and C10). The cores from stations C9 and C10 were sliced into 0.5 cm intervals up to 2 cm, at 1 cm intervals for next 2 slices and into 2 cm thereafter. The sediment subsamples for PAHs analysis were then frozen at -20 $^{\circ}$C until further lab processing. Sediment cores collected for ^{210}Pb-dating were sliced at similar intervals and directly collected in graduated glass vials and stored until analysis. Subsamples were also collected from each core section in glass vials of known volume to determine porosity.

4.2.2. PAHs extraction and analysis by GC/MS

The PAHs were extracted using EPA SW-846 method 3540C (US EPA, 2000). Prior to extraction, the frozen samples were transferred to refrigerator until defrosted and then homogenized by vigorous stirring. Subsamples of ~30 g of sediments were taken into a pre-cleaned 500-ml beaker, spiked with surrogate recovery standard (Phenanthrene-d10) and mixed with pre-cleaned anhydrous sodium sulfate until a dry sand-like matrix is created and transferred into a Soxhlet extraction thimble. Then the samples were Soxhlet extracted for 24 h with dichloromethane (DCM). The solvent extracts were then concentrated by rotary evaporation and nitrogen blowdown to 1 ml. Just prior to the instrumental analysis, a mixture of internal standards composed of Napthalene-d_8, Acenaphthene-d_{10}, Chrysene-d_{12}, and Perylene-d_{12} was added into the final sample extracts and analyzed using GC/MS.

The details on sample analysis using GC/MS and quality assurance/quality control (QA/QC) are explained elsewhere (Adhikati et al., 2015). Briefly, the sample extracts were analyzed using an Agilent 7890A GC interfaced with an Agilent 5975C inert XL mass selective

detector (MSD) operated in the selective ion monitoring (SIM) mode targeting for 43 PAHs; 18 parent PAHs with 2-6 aromatic rings [naphthalene to benzo(g,h,i)perylene] and 25 C1-C3 or C4 alkyl-substituted homologues of the parent PAHs. One procedural blanks for 15 samples was processed and analyzed in the same manner as the real samples. Most of the target analytes were not detected in the blanks, even the detected analytes were found to be below 2% of their concentrations in real samples. The recoveries of the surrogate standard (Phenanthrene-d_{10}) varied between 53% and 125%, with an average recovery of 67.0 ± 10.0%. Reported concentrations of target analytes are recovery corrected. The concentrations were normalized to dry weights of the sediments, and the sum of all 43 individual PAHs identified and quantified are presented as $\sum PAH_{43}$. The lists of the 43 PAHs compounds with their corresponding abbreviations used in this study are presented in Appendix 2.

4.2.3. ^{210}Pb analysis using gamma spectroscopy

Aliquots of finely ground dry sediments (8–30 g) were placed into counting vials of known geometry, sealed and measured for ^{210}Pb and ^{226}Ra (via ^{214}Pb) by direct gamma counting using two high purity germanium well detectors (Lubis, 2006; Maiti et al., 2010; Yeager et al., 2006). The detector efficiencies were determined using EPA standard-sand spiked with a National Institute of Standards and Technology (NIST) traceable mixed gamma liquid standard from Analytics™, Inc. No correction for self-absorption of the low energy gamma peaks ^{210}Pb was needed since the sample sediment was, within error, close to the density of the spiked sand used to calibrate the detectors. The gamma-ray spectra were then analyzed for peak area and position using the Genie 2000 Gamma Analysis Software (Genie 200 Software Family, Canberra Industries Inc. CT, USA). All activities were corrected for decay to the midpoint of sample collection. The ^{210}Pb was measured by its emission at 46.5 keV and ^{226}Ra by the 351 keV

emission of its daughter isotope ^{214}Pb. Unsupported ^{210}Pb ($^{210}Pb_{ex}$) was calculated as the difference between the measured total ^{210}Pb at 46.5 keV and the estimate of the supported ^{210}Pb activity given by its parent nuclide at 351 keV [$^{210}Pb_{ex} = {}^{210}Pb_{tot} - {}^{214}$Pb]. Both supported and total ^{210}Pb measurements were conducted at least 25 days after initial sample collection. The $^{210}Pb_{ex}$ profiles were used to calculate sedimentation rates from the surface layer to the deepest sampling interval where excess activities were detected. Below these layers the $^{210}Pb_{ex}$ activities were ≤ 0, within the propagated error. Errors represent counting statistics.

4.2.4. ^{210}Pb modeling approach

The liner sedimentation rates (cm yr^{-1}) and sediment accumulation rates (g cm^{-2} yr^{-1}) were calculated using both the CF:CS (constant flux-constant sedimentation) model (Appleby and Oldfield, 1978; Maiti et al., 2010; Yeager et al., 2004) and CRS (constant rate of supply) model (Appleby and Oldfield, 1978; de Souza et al., 2012; Lubis, 2006). The CF:CS models assumes steady state conditions with relatively constant porosity (Appleby and Oldfield, 1978; Yeager et al., 2004). The sedimentation rates based on this model can be calculated using following equations;

$$[^{210}\mathrm{Pb}_{\mathrm{ex}}(z)] = [^{210}\mathrm{Pb}_{\mathrm{ex}}(0)]\exp^{-\alpha z} \qquad (4.1)$$

$$\alpha = \lambda/S$$

Where $^{210}Pb_{ex}(z)$ and $^{210}Pb_{ex}(0)$ are the excess ^{210}Pb activities at depth z and on the surface of the sediment, respectively; α is the slope of the regression line for $^{210}Pb_{ex}$ plotted against mid depth of each core segment; λ is the ^{210}Pb radioactive decay constant (0.0311 y^{-1}); and S is the linear sedimentation rates (cm y^{-1}). The sediment mass accumulation rates were calculated as follows;

$$\text{Sediment accumulation rates (gm cm}^{-2}\ \text{y}^{-1}) = \rho \times S$$

Where ρ is sediment dry density (gm cm^{-3}), which was calculated as;

$$\text{Dry sediment density} = \text{Dry sediment weight} / \text{Dry sediment volume}$$

The CRS model assumes a constant atmospheric fallout of ^{210}Pb and a constant flux of unsupported ^{210}Pb to the sediments, however permits a variable sediment supply (Appleby and Oldfield, 1978; de Souza et al., 2012; Krichnaswami et al., 1971; Lubis, 2006). It can be briefly summarized as;

$$A_x = A_0 e^{-\lambda t} \qquad (4.2)$$

Where A_x is the excess ^{210}Pb inventory from depth x to the bottom of the core, A_0 is the excess ^{210}Pb inventory for the entire core, λ is the ^{210}Pb radioactive decay constant, and t is the age of the sediment at depth x. The A_x and A_0 were calculated by numerical integration of excess ^{210}Pb. Then the age of the sediment was estimated as;

$$t = \frac{1}{\lambda} \ln \frac{A_0}{A_x} \qquad (4.3)$$

After dating each segment of the sediment cores, the sediment accumulation rates were calculated as follows,

$$\text{Sediment accumulation rates (gm cm}^{-2}\text{y}^{-1}) = \frac{\text{Mass flux (g cm}^{-2}\text{)}}{\text{t (y)}} \qquad (4.4)$$

Where, the mass fluxes were calculated multiplying sediment dry density by the depth of each core.

Similarly, the sedimentation rates were calculated as;

$$\text{Sedimentation rates (cm y}^{-1}) = \frac{\text{Sediment accumulation rates (gm cm}^{-2}\text{y}^{-1})}{\text{Sediment dry density (gm cm}^{-3})} \qquad (4.5)$$

The estimates from both the methods were comparable (Table 4.1). However, the accumulation rates from CRS model was used in this study to estimate PAHs accumulation rates, which allows sedimentation rates to vary over time thus can be more representative for the

northern GOM with large anthropogenic activities, possibly altering the sediment loads (Lubis, 2006).

The PAHs accumulation rates (ng cm^{-2} y^{-1}) were calculated using following equation:

$$\sum PAH_{43} \text{ accumulation rates } = C_i \times A_i \qquad (4.6)$$

Where C_i (ng/g) and A_i (g cm^{-2} y^{-1}) represent $\sum PAH_{43}$ concentrations and sediment accumulation rates of each segment, respectively.

4.2.5. Elemental analysis

For the analysis of total organic carbon (TOC), dry sediment samples were weighed into silver capsules and placed in a desiccator with concentrated fuming hydrochloric acid for 36 h to remove inorganic carbon (Hedges and Stern, 1984). After acid fumigation the samples were dried at 50 °C and then analyzed for TOC using Elemental Analyzer (PerkinElmer, 2400 Series II CHNS/O Analyzer). Approximately 20% of the samples were run in duplicate and duplicates agreed to < 5% of each other. The analytical error associated with total carbon analysis was less than 3%.

4.3. Results and discussions

4.3.1. Sediment PAHs concentrations

The concentrations of $\sum PAH_{43}$ in sediments varied between 68.5 to160 (102 ± 29.0) ng g^{-1}, 35.3 to 158 (78.4 ± 38.6) ng g^{-1}, and 26.2 to 131 (63.5 ± 30.5) ng g^{-1}, respectively in the coastal stations, deep-sea stations east of MR delta and deep-sea stations west of MR delta (Table 4.1, Figure 4.2). The $\sum PAH_{43}$ in surficial sediments varied between 68.5 to 160 ng g^{-1}, 83.6 to 158 ng g^{-1}, and 44.3 to 131 ng g^{-1}, respectively in the coastal stations, deep-sea stations east of MR delta and deep-sea stations west of MR delta (Table 4.1, Figure 4.3).

Table 4.1. $\sum PAH_{43}$ concentrations and accumulation rates in the northern Gulf of Mexico sediments. $\sum PAH_{43}$ accumulation rates were estimated from ^{210}Pb based CRS sediment accumulation model.

Stations	Depths (m)	CF:CS sedimentation rate (cmy^{-1})	CRS sedimentation rates (cmy^{-1})	CRS sediment accumulation rate ($gcm^{-2}y^{-1}$)	$\sum PAH_{43}$ concentration (ngg^{-1})	$\sum PAH_{43}$ accumulation rate ($ngcm^{-2}y^{-1}$)
C1	0-2	0.09±0.02	0.07±0.005	0.09±0.005	78.3	7.41
	2-4		0.09±0.034	0.12±0.045	72.4	8.71
	4-6		0.11±0.054	0.16±0.075	69.4	11.52
C2	0-2	0.15±0.03	0.24±0.008	0.29±0.011	159.6	47.30
	2-4		0.24±0.010	0.31±0.013	142.3	45.35
	4-6		0.18±0.006	0.22±0.008	130.1	29.81
C3	0-2	NA	0.40±0.182	0.58±0.259	68.5	39.73
	2-4		0.21±0.052	0.32±0.080	74.6	24.24
	4-6		0.12±0.027	0.18±0.042	68.6	12.90
C4	0-2	0.61±0.12	0.35±0.017	0.30±0.015	150.7	45.73
	2-4		0.18±0.007	0.22±0.008	105.7	23.54
	4-6		0.16±0.006	0.19±0.007	106.4	21.01
C5	0-2	0.38±0.10	0.40±0.017	0.49±0.021	95.4	47.68
	2-4		0.43±0.017	0.54±0.021	88.4	48.26
	4-6		0.44±0.019	0.56±0.024	112.2	63.05
C6	0-2	0.15±0.02	0.29±0.008	0.32±0.009	148.6	48.19
	2-4		0.21±0.005	0.26±0.006	111.4	29.39
	4-6		0.19±0.004	0.26±0.006	106.9	27.93
C7	0-2	0.10±0.01	0.12±0.002	0.11±0.002	102.4	12.04
	2-4		0.10±0.001	0.11±0.001	82.4	9.37
	4-6		0.08±0.001	0.09±0.001	71.3	6.79
C8	0-2	0.09±0.01	0.05±0.001	0.05±0.001	114.3	5.72
	2-4		0.07±0.001	0.07±0.001	98.2	7.34
	4-6		0.20±0.013	0.2±0.013	89.5	18.49
C9	0-0.5	0.26±0.03	0.23±0.002	0.34±0.003	83.6	28.93
	0.5-1		0.11±0.001	0.15±0.001	48.5	7.55
	1-1.5		0.06±0.001	0.15±0.001	62.0	9.35
	1.5-2		0.04±0.001	0.09±0.002	60.8	5.81
	2-3		0.03±0.001	0.08±0.001	43.7	3.72
	3-4		0.02±0.001	0.06±0.001	42.5	2.71
	4-6		0.03±0.001	0.08±0.001	41.9	3.70

Table 4.1. Contd.

Stations	Depths (m)	CF:CS sedimentation rate (cmy^{-1})	CRS sedimentation rates (cmy^{-1})	CRS sediment accumulation rate ($gcm^{-2}y^{-1}$)	$\sum PAH_{43}$ concentration (ngg^{-1})	$\sum PAH_{43}$ accumulation rate ($ngcm^{-2}y^{-1}$)
C10	0-0.5	0.16±0.01	0.25±0.002	0.41±0.003	131.7	54.76
	0.5-1		0.09±0.001	0.16±0.001	145.3	23.86
	1-1.5		0.05±0.001	0.1±0.001	121.7	12.70
	1.5-2		0.04±0.001	0.08±0.001	107.1	8.60
	2-3		0.03±0.002	0.06±0.002	53.0	3.53
	3-4		0.02±0.001	0.05±0.001	52.8	3.04
	4-6		0.03±0.004	0.08±0.001	59.0	5.01
C11	0-1	0.07±0.01	0.30±0.001	0.32±0.001	157.7	51.14
	1-2		0.06±0.003	0.14±0.001	57.5	8.56
	2-4		0.04±0.001	0.08±0.001	51.2	4.45
	4-6		0.05±0.001	0.09±0.001	39.8	3.80
C12	0-1	0.06±0.02	0.09±0.001	0.15±0.001	125.6	19.34
	1-2		0.17±0.002	0.34±0.005	109.9	37.49
	2-4		0.12±0.002	0.29±0.004	95.2	27.68
	4-6		0.05±0.003	0.10±0.001	35.2	3.55
C13	0-1	0.50±0.18	0.13±0.002	0.31±0.005	44.3	13.74
	1-2		0.10±0.001	0.25±0.002	29.4	7.36
	2-4		0.07±0.001	0.17±0.002	26.2	4.61
	4-6		0.04±0.001	0.08±0.001	27.0	2.41
C14	0-1	0.05±0.02	0.06±0.001	0.12±0.001	49.9	6.19
	1-2		0.05±0.002	0.15±0.002	39.2	6.21
	2-4		0.07±0.001	0.18±0.004	33.9	6.26
C15	4-6		0.03±0.001	0.06±0.001	30.4	1.83
	0-1	0.05±0.01	0.04±0.001	0.09±0.002	83.1	7.69
	1-2		0.05±0.001	0.10±0.001	106.3	11.37
	2-4		0.04±0.002	0.10±0.001	73.1	7.37
	4-6		0.03±0.002	0.06±0.001	31.4	2.11
C16	0-1	0.04±0.002	0.04±0.002	0.08±0.001	130.9	11.00
	1-2		0.03±0.001	0.07±0.003	68.2	5.23
	2-4		0.03±0.001	0.07±0.001	56.4	4.15
	4-6		0.03±0.001	0.05±0.002	29.7	1.72
C17	0-1	0.05±0.003	0.05±0.003	0.11±0.003	66.68	7.77
	1-2		0.04±0.001	0.09±0.001	66.75	6.04
	2-4		0.03±0.001	0.06±0.002	77.61	5.39
	4-6		0.02±0.001	0.04±0.001	87.80	3.66

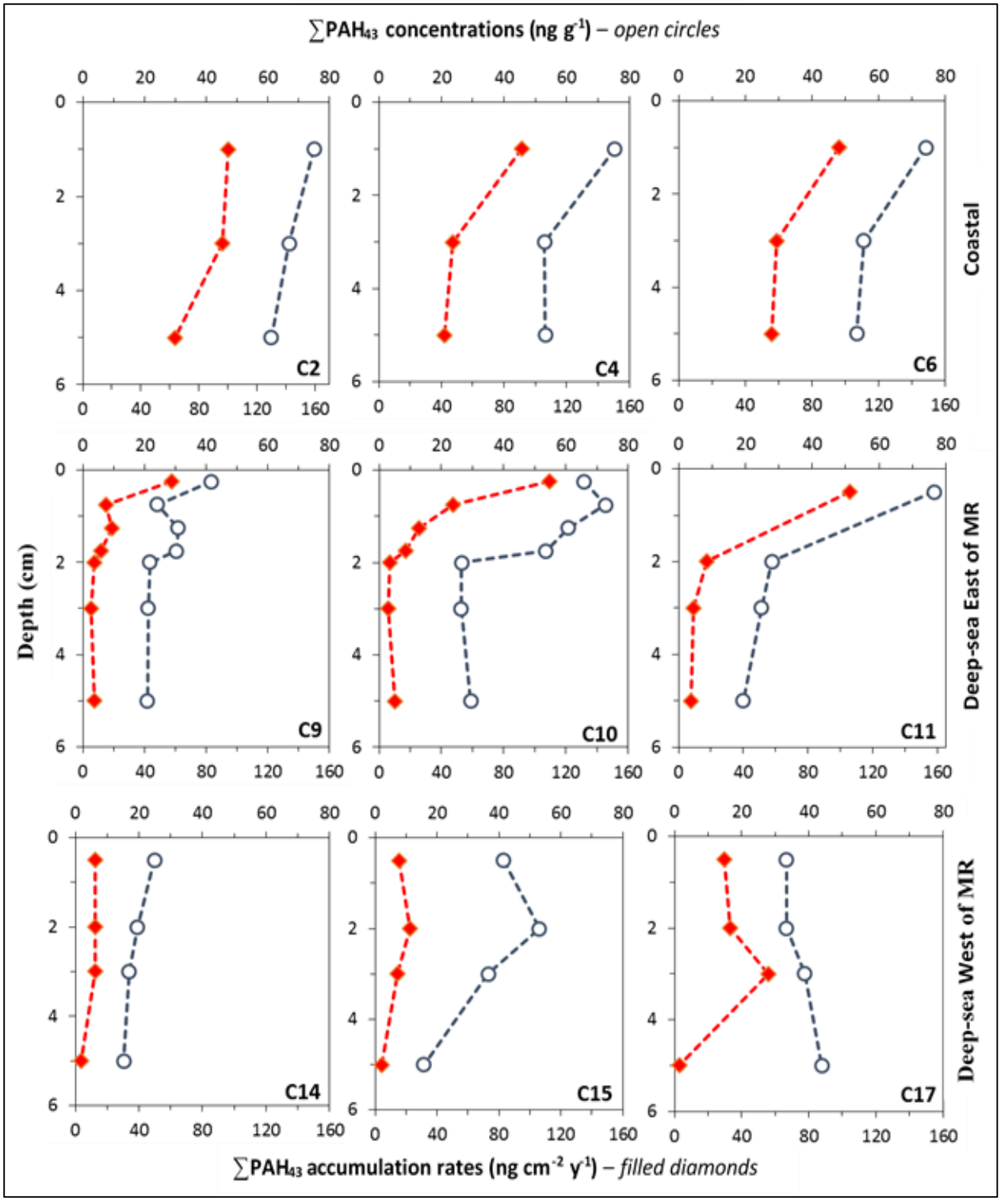

Figure 4.2. Depth profiles for the concentrations (open circles) and accumulation rates (filled diamonds) of ∑PAH$_{43}$ in recent sediments from the selected sampling locations; coastal, deep-sea stations east of Mississippi River delta in the vicinity of the Macondo Well head, and deep-sea stations east of Mississippi River delta in the northern Gulf of Mexico.

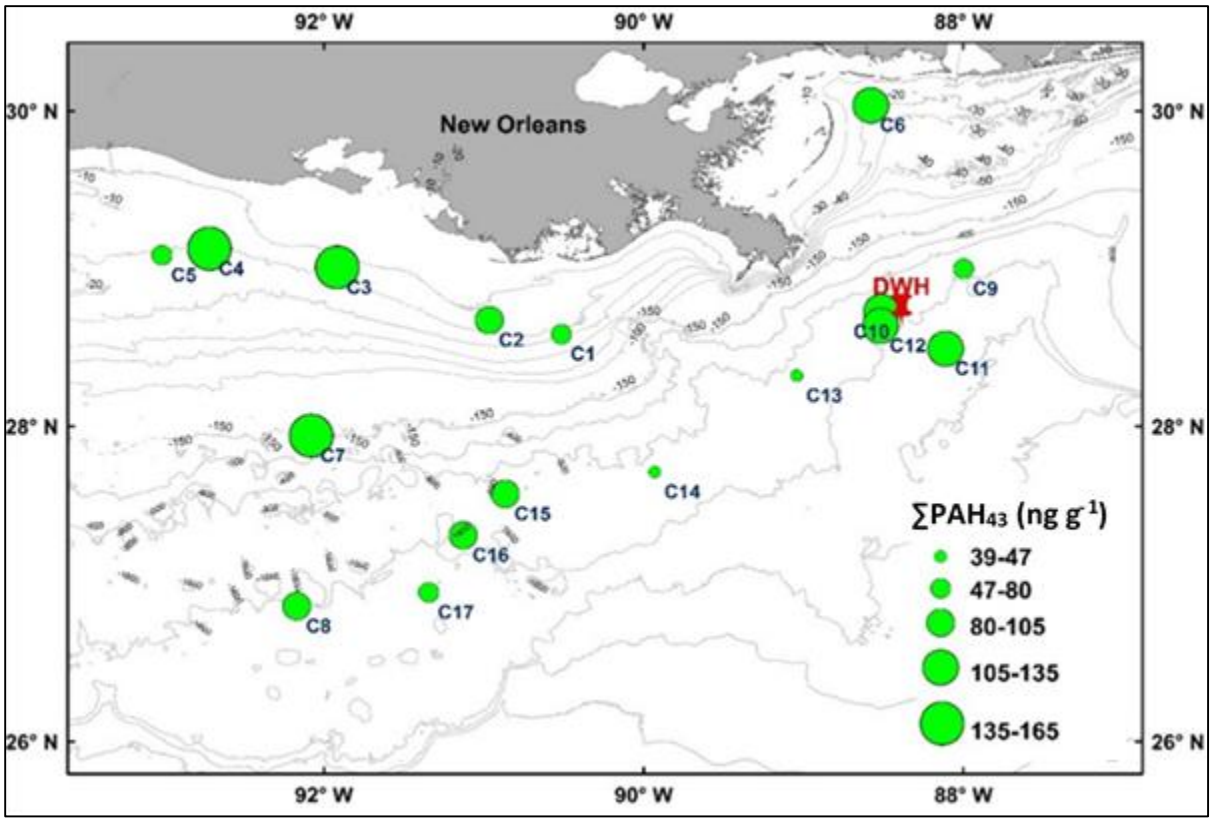

Figure 4.3. The distribution of surface $\sum PAH_{43}$ concentrations in the northern Gulf of Mexico sediments.

For statistical comparison, weighted average of $\sum PAH_{43}$ concentrations were calculated from each station and grouped into three depth intervals; 0-2 cm, 2-4 cm and 4-6 cm. A general linear mixed model, with interaction term depths*locations, was used in order to compare any possible variation in sediment PAHs along the sampling locations (three levels; coastal, deep-sea east of Mississippi River Delta, and deep-sea west of Mississippi River Delta) and the depth of the sediment cores (three levels; 0-2 cm, 2-4 cm and 4-6 cm. The depths of the sediment cores and the sampling locations were the fixed effect in the model while the sample ID was the random effect nested in locations. There were nine multiple tests to compare the concentrations of total PAHs at three different sediment core depths from three different sampling locations (locations at each slice of depths), therefore the Bonferroni correction was applied on the level of

significance (α-values) to account for the multiple tests, three within each slice (α/m= 0.05/9 = 0.005) (Holm, 1979). The differences in PAHs concentrations were considered to be significant at p-values <0.005 (refer Appendix 4 for details). The interaction effects of the depths and sampling locations was statistically significant which implies that the change in PAHs concentration with depths of the sediment cores was not consistent among the sampling locations (Figure 4.4). The down-core variability in PAHs concentrations were significantly different at the deep-sea stations east of MR delta (C9-C12) in the vicinity of Macondo well head ($p < 0.005$) while remain similar at other stations (Figure 4.2 and 4.4). At these stations, the surficial sediments (0-2 cm) had significantly higher ($p < 0.005$) concentrations of $\sum PAH_{43}$ (109 ± 13.4 ng g^{-1}) than the sediments below, 53.9 ± 13.4 ng g^{-1} at 2-4 cm, and 40.6 ± 13.4 ng g^{-1} at 4-6 cm (Figure 4.4), which is likely due to the impacts of DWH oil inputs.

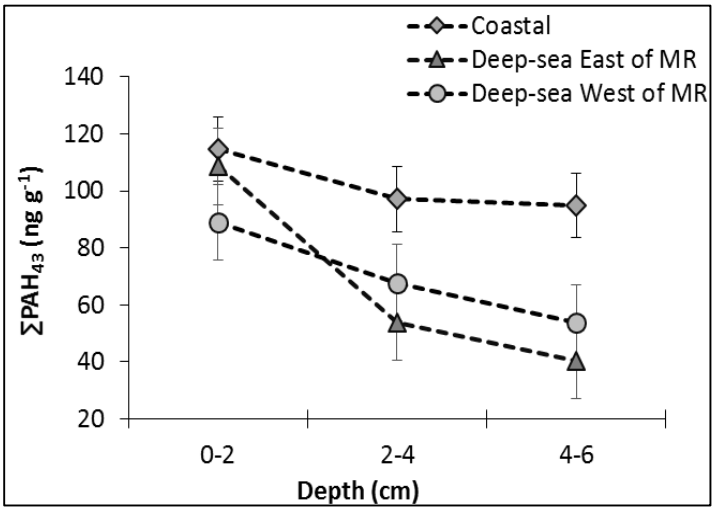

Figure 4.4. The vertical profiles of the average concentrations of $\sum PAH_{43}$ in three different sampling locations; coastal, deep-sea stations east of Mississippi River delta in the vicinity of the Macondo Well head, and deep-sea stations east of Mississippi River delta in the northern Gulf of Mexico.

The statistically similar down-core PAHs concentrations at the coastal stations is possibility attributed to the higher sediment accumulation rates, while at deep-sea stations west of MR delta could be due minimal effects of the both, the DWH oil inputs and accumulation

rates. The surficial (0-2 cm) PAHs concentrations were similar among the sampling stations, however at lower depths (4-6 cm), the coastal stations had significantly higher ($p < 0.005$) PAHs concentrations than the deep-sea stations (Table 4.1, Figure 4.4). At 2-4 cm depth interval, coastal sediments had significantly higher PAHs than the sediments at east of MR delta ($p < 0.005$), while it was statistically similar to the concentrations at west of MR delta (Figure 4.4). Similar concentrations in surficial sediments among all sampling stations could be due to the DWH oil inputs, altering the historic variation in PAHs distribution in the northern GOM, probably with higher degree of enrichment at deep-sea sediments around DWH well head than the other study locations.

The sediment PAHs concentrations were also compared by combining the top 6 cm depths together, which is often considered the zone of maximum biological interaction for benthic organisms (Kristensen, 2000; Rhoads and Young, 1970). The results of this comparison show that the sediments from costal-shallow stations had significantly higher concentrations of $\sum PAH_{43}$ (102 ± 29.0 ng g^{-1}) than the deep-sea sediments east (78.4 ± 38.6 ng g^{-1}) and west (63.5 ± 30.5 ng g^{-1}) of MR delta ($p < 0.05$). River run-off can be an important source of PAHs in coastal environment which could be the reason of historically higher PAHs in the coastal GOM than the deep-sea sediments (Mai et al., 2003; Overton et al., 2004; Soclo et al., 2000; Wade et al., 2008; Yunker et al., 2002). Baumard et al. (1998) categorized the PAHs pollutions into four levels; low (0-100 ng g^{-1}), moderate (100-1000 ng g^{-1}), high (1000-5000 ng g^{-1}) and very high (>5000 ng g^{-1}). Based on this classification, the northern GOM sediment can be considered as low to moderately polluted in terms of PAHs (26-160 ng g^{-1}). The sediment PAHs concentrations observed in this study are an order of magnitude lower than the ERL (effects range-low) values proposed for causing harmful effects in biota (Long et al., 1995) therefore, they are unlikely to

cause toxic threats to the organisms in the sediments. In general, the observed PAHs concentrations in surficial sediments were within the lower ranges of pre-spill values reported from the same area (below detection to 1033 ng g^{-1} with a mean of 140 ng/g; Wade et al., 2008), and the post-spill values from the Louisiana coast (100-856 ng g^{-1}; Wang et al., 2014). The NOAA (NRDA) reported a wide range of total PAHs concentrations ranging from 0 to 1.49 × 10^7 ng g^{-1} from various locations in the northern GOM (http://www.gulfspillrestoration.noaa.gov/oil-spill/gulf-spill-data). In order to make more precise spatial comparison on PAHs concentrations and distributions, I selected NRDA stations closest to my sampling stations (Figure 4.1), all of these samples were collected in 2010, within few months of the DWH oil spill. Then their sampling stations were grouped into three groups similar to my sampling stations; coastal, deep-sea east of MR and deep-sea west of MR. The general linear model as mentioned above was utilized to test the interaction effects of sampling locations (three levels) and the sampling years (two levels) on the variability of surficial PAHs concentrations (Appendix 4). There were three multiple tests to compare the concentrations of total PAHs in between two sampling periods for each sampling location therefore, the Bonferroni corrected level of significance (0.05/3 ~0.017) was utilized to test the statistical differences. The results show significant interaction effects of locations and sampling years on ∑PAHs concentrations, which implies that the change in PAHs concentrations between sampling years was inconsistent among the sampling locations (Figure 4.5). The surficial sediment ∑PAHs concentrations in the NOAA sediment samples (8 to 1006 ng g^{-1}) were similar to the surface $\sum PAH_{43}$ concentrations observed in this study, except for stations closest to the DWH spill sites. The NOAA reported surficial PAHs concentrations in 2010 at deep-sea stations east of MR were significantly higher than the observed concentrations in that location during this study in 2013 ($p < 0.017$) (Figure

4.5). The disagreement in PAHs concentrations in 2010 and three years after the spill at those stations could be either due to loss of DWH oil signatures via various biogeochemical processes acting on it or this study was unable to capture the patches of oil-rich sediments.

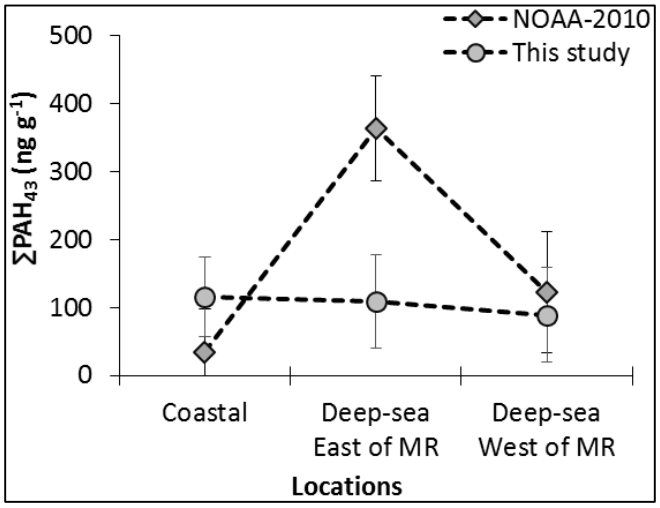

Figure 4.5. The concentrations of total PAHs in the northern Gulf of Mexico observed in this study and in the selected sediment samples collected by NRDA process in 2010, reported by NOAA.

4.3.2. PAHs accumulation rates in sediments

The ^{210}Pb-based sedimentation and accumulation rates for the northern GOM sediments estimated using CRS and CF:CS methods are as shown in Table 4.1. Sedimentation rates (CRS) varied between 0.03 to 0.45 cm y^{-1}, therefore depending upon the sampling locations the top 6 cm of the sediments analyzed for PAHs represent ~13 to 200 years of sediment accumulation.

Estimated $\sum PAH_{43}$ accumulation rates in all sediments varied between 1.4 to 63.1 (17.1 ± 16.1 ng cm^{-2} y^{-1}) (Table 4.1, Figure 4.2). Unlike PAHs concentrations and as expected, the coastal stations had significantly higher PAHs accumulation rates (29.1 ± 16.7 ng cm^{-2} y^{-1}) than both the deep-sea stations east (13.8 ± 14.6 ng cm^{-2} y^{-1}) and west (8.6 ± 6.6 ng cm^{-2} y^{-1}) of MR delta for all depths ($P < 0.005$). However, the accumulation rates remain similar on deep-sea stations. The PAHs accumulation rates gradually decreased from the upper surficial to lower

segments of the sediments (eg., Figure 4.2) however, like PAHs concentrations, the decreasing trends in accumulation rates were not statistically significant, except for the deep-sea stations in the vicinity of DHW well head. Statistically, similar down-core PAHs concentrations as well as accumulation rates for majority of the sediment samples (Table 4.1, Figure 4.2 and 4.4), suggest the persistent nature of the PAHs (Marini and Frapiccini, 2013; Tansel et al., 2011) and chronic PAHs loading in the northern GOM (Mitra and Bianchi, 2003; Overton et al., 2004).

The ^{210}Pb-based reconstruction of historic PAHs loadings using PAHs preserved in sediment column (Santschi et al., 2001) provides an opportunity to see if the DWH inputs significantly altered the trends and also to determine long term fates of the sediment PAHs. To the best of my knowledge, this is the first study to quantify historic PAHs accumulation rates in northern GOM deep-sea sediments and there are no comparable studies for that region. However, surficial PAHs accumulation rates in this study can be contrasted to the only available data on vertical fluxes of PAHs from the upper euphotic zone in this region (Adhikari et al., 2015). They have reported the vertical fluxes of $\sum PAH_{43}$ from upper 350 m of the water column in the vicinity of DWH oil spill sites to be 73-292 ng cm^{-2} y^{-1} (2-8 µg m^{-2} d^{-1}). The $\sum PAH_{43}$ accumulation rates in surficial sediments for stations C9-C12 in this study (water column depths 1200-2000 m), that were near their sampling stations, varied between 12.7 to 55.0 ng cm^{-2} y^{-1} (Table 4.1, Figure 4.2). If we assume vertical fluxes of particulate PAHs as a single source of PAHs to the bottom sediments, the results indicate that only ~20% of what sinks below 350 m gets deposited in the bottom sediments. The percent deposition of particulate PAHs is significantly higher than other organic particulate matter such as POC, only ~1-3% of POC sinking from the euphotic zone reaches the sea floor (Buesseler, 1998; De La Rocha and Passow, 2007; Martin et al., 1987; Suess, 1980). Nevertheless, ~80% of the PAHs sinking below 350 m

of the water column was lost via various physical, chemical and biological processes acting on them either during vertical transport or after deposition in the bottom sediments.

The overall results show a background level of PAHs concentrations and accumulation rates in the northern Gulf. It implies that the DWH oil input did not have significant impact on sediment PAHs in the study area, except for surficial sediments around DWH well head. Similar results have been reported by Wang et al. (2014) for the marsh and shelf sediments in the Louisiana coasts. The sediments were collected 1-3 years after DWH oil spills and a high degree of PAHs contamination in surficial sediment can be expected however, the observed PAHs levels were similar to the pre-spill concentrations (Wade et al., 2008). A number of studies have been conducted to estimate how much oil was released during DWH oil spill, what fractions of it was removed from the sea via various remediation efforts and natural processes, what fraction of the spilled oil remained in the sea, and what fractions of oil trapped in the sea actually got deposited in the bottom sediments (Chanton et al., 2015; McNaulty et al., 2012, Reddy et al., 2012; Valentine et al., 2014). If we take the estimated percentages of DWH oil deposition in the GOM seafloor (Valentine et al., 2014) and assume similar fractions (4-31%) of the total PAHs (2.1×10^{10} g; Reddy et al., 2012) released from Macondo well uniformly deposited in 3200 km^2 area; every square centimeter of the seafloor in that region of the northern GOM received 26-203 µg of total PAHs. This estimate is orders of magnitude higher than the accumulation rates estimated in my study. The possible explanation could primarily be the patchiness of DWH oil deposition. The total PAHs concentration reported by NOAA shows that high concentration patches were more in coastal/marsh areas. About 28% of their 512 samples (mainly from the coastline with few stations around Macondo well) had sediment PAHs concentrations more than 1000 ng g^{-1} with an average of $4.7 \pm 15\times10^{5}$ ng g^{-1}, while the average sediment PAHs

concentrations in rest of the samples was 160 ± 200 ng g^{-1}. Similarly, Turner et al. (2014) detected PAHs from Macondo oil only in 36% of their 405 wetlands sediment samples collected from Louisiana coasts in 2010 and 2011, where they found a large difference in PAHs concentrations for oiled (2.9 ± 1.1×10^4 ng g^{-1}) and un-oiled (161 ± 84 ng g^{-1}) sites. I did not collect samples from marshes, and my shelf, slope and deep-sea samples likely did not capture any patches with high oil deposition. Therefore, the observed concentrations are low, similar to the background sediment PAHs values. Comparatively lower concentrations of PAHs, reported by Wang et al. (2014), in shelf and marsh sediments collected during 2010 and 2012 also shows that the patches of high oil deposition can be easily overlooked. In addition, various biogeochemical processes acting on deposited PAHs can also lower their concentrations in surface sediments (Albers, 2003; Bauer and Capone, 1985; Cornelissen et al., 1998; Gutierrez, 2011).

4.3.3. Perylene concentrations

Perylene has both the biological (biogenetic) and anthropogenic sources and has been reported as one of the major PAHs even in relatively pristine sediments (Barakat et al., 2011; Baumard et al., 1998; Wade et al., 2008). The concentrations of perylene in all sediment samples varied between 0.77 to 20.0 ng g^{-1} while it was 1.1 to 14.4 ng g^{-1} in in surficial sediments (Figure 4.6). Observed perylene concentrations in this study are in the lower range of the values reported by Wade et al. (2008) from the same area of the GOM. Perylene comprised of 0.8 to 20% (5.8 ± 4.0%) of total PAHs, which is comparatively lower than the previous reported values in the GOM (Wade et al., 2008). The natural source of perylene is indicated by the higher abundance of perylene over other PAHs. The concentrations of perylene greater than 10% of the ∑penta-aromatic ring PAHs indicates diagenitic origin while less than 10% indicates pyrogenic sources

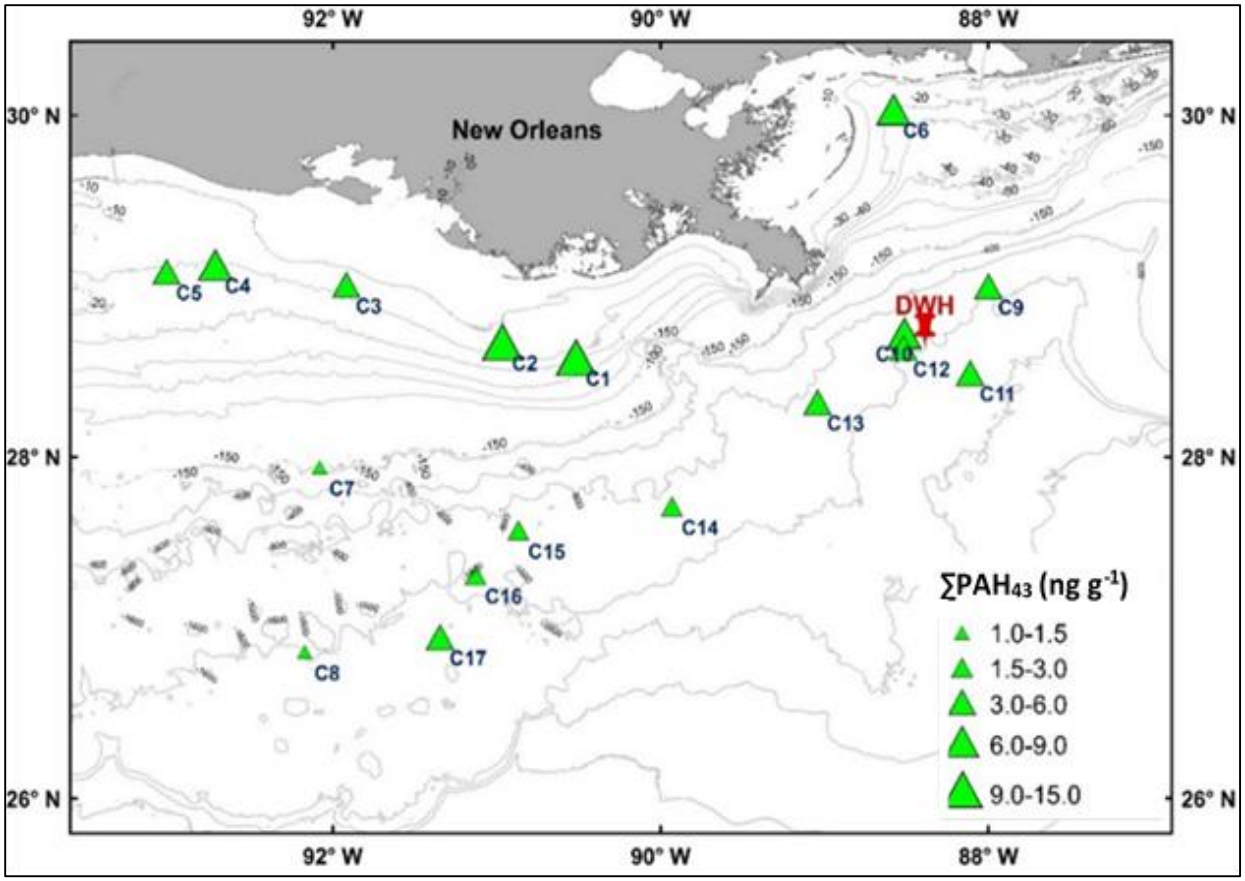

Figure 4.6. The distribution of surface perylene concentrations in the Gulf of Mexico sediments.

(Baumard et al., 1998; Laflamme and Hites, 1978). In this study, the percentage of perylene to ∑penta-aromatic ring PAHs was always more than 10% (21 to 88%) which indicates the dominancy of diagenetic source of perylene in the sediments (Barakat et al., 2011; Baumard et al., 1998). The shallow water stations (C1-C7) had significantly higher concentrations of perylene (8.2 ± 5.0 ng g^{-1}) than the deep-sea (C8-C17) sediments (3.0 ± 2.1 ng g^{-1}) ($P < 0.001$) however, it did not vary with depths. Shallow stations near the mouth of the MR delta (C1, C2) had highest surficial perylene concentrations probably due to terrestrial input associated with rivers (Baumard et al., 1998) while the deep stations (C8, C7) had lowest surface perylene concentrations (Figure 4.6).

4.3.4. Total organic carbon (TOC) and correlation with PAHs concentrations

The composition of the sediments generally determines the concentrations of PAHs (Mostafa et al., 2009). Organic matter such as TOC has higher PAHs sorption capacity (Means et al., 1980; Wang et al., 2001) and helps in accumulation of PAHs in sediments therefore the sediments with higher organic matter tend to have higher PAHs (Evans et al., 1990; Witt, 1995; Neff, 1979). However, PAHs in this study were not significantly correlated with TOC content in sediments ($p > 0.05$). Similar, poor correlation between PAHs and TOC in sediments have been demonstrated by previous studies (Mostafa et al., 2003, 2009; Wade et al., 2008; Wang et al., 2014). These results indicate that the sediment PAHs concentrations is determined more by the direct input rather than the chemical composition such as TOC contents of the bottom sediments. Adhikari et al. (2014) demonstrated a positive correlation between particulate organic carbon (POC) and PAHs in sinking particles in upper euphotic zones in the GOM water column. The observed poor correlation in this study indicates that such association is possibly altered during the course of particle sinking and after deposition as POC is preferentially remineralized while PAHs remain persistent (Buesseler, et al., 2006; Marini and Frapiccini, 2013; Tansel et al., 2011).

4.3.5. Molecular profiles, principal component analysis and sources of PAHs

For the classification purpose, PAHs with 2-3 benzene rings were categorized as lower molecular weight PAHs (LMW-PAHs), with 4 rings as middle molecular weight (MMW-PAHs) and the PAHs with >4 rings as higher molecular weight (HMW-PAHs). Abundance of LMW-PAHs (62.8 ± 18.4% of the total PAHs without perylene) dominated the PAHs profiles in all samples followed by MMW-PAHs (31.7 ± 17.4%) and HMW-PAHs (5.5 ± 3.0%). The coastal sediments had significantly higher percentages of LMW-PAHs (83.1 ± 3.7%) than the deep-sea

sediments (53.2 ± 15.3%), while the percentages of MMW-PAHs in deep-sea sediments (40.7 ± 13.6%) were significantly higher than the coastal sediments (12.5 ± 3.1%) ($p < 0.001$). The composition of HMW-PAHs remained similar among both coastal and deep-sea sediments. The alkyl homologues were more abundant than the parent PAHs contributing 57.1 to 88.4% (mean 78.2 ± 6.0%) of the total PAHs, which remains statistically similar ($p > 0.05$) throughout the study areas. The molecular profiles of individual PAH analytes in surficial sediments from selected sampling locations are presented in Appendix 3.

Principal component analysis (PCA) was used to evaluate the composition of PAHs profiles in the GOM sediments. The first two principal components (PC) explained 76.7% (PC1 ~61.3% and PC2 ~16.4%) of the total variance in PAHs composition (Figure 4.7). The overall composition of all the PAHs analytes was clearly separated along both PC1 and PC2; coastal and deep-sea stations, except station C8 which was grouped with coastal stations despite its location (Figure 4.7a). PC1 was positively loaded with perylene and alkyl homologues of LMW-PAHs, characterizing the coastal sediment PAHs, while the PC2 was loaded with MMW-PAHs characterizing the deep-sea sediments in the loading plot (Figure 4.7b). The coastal sediments characterized by perylene and alkyl homologues of LMW-PAHs indicate that the un-combusted petroleum primarily contributed to the coastal PAHs (Bence et al., 2007; Laflamme and Hites, 1978; Sporstol et al., 1983). Four representative PAH analytes with higher loadings on each PC; C-1 fluorene, C-2 fluorene, C-1 phenanthrene and perylene with higher PC1 loading, and C-3 napthobenzothiophene (C-3 NBT), C2- crysene, C-3 crysene, and C-4 pyrene with higher PC2 loadings were selected to compare their depth profiles among different sampling regimes. The general linear mixed model used for total PAHs (Section 4.3.1) was also utilized to test the effects of sampling locations and depths on the variability of selected individual PAHs

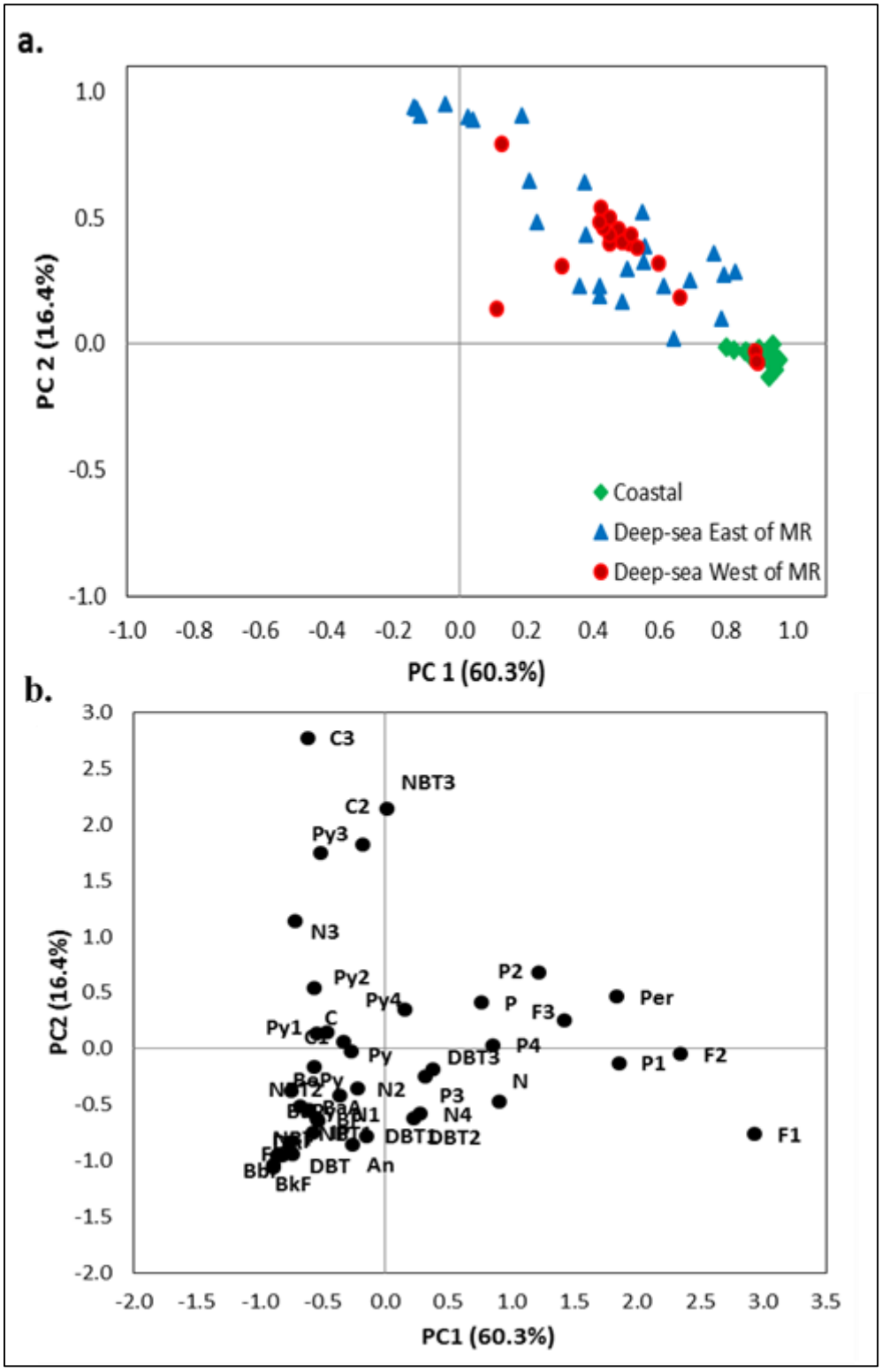

Figure 4.7. Principal component analysis (a) score plots and (b) loading plots for individual PAHs in the northern Gulf of Mexico sediments. The name of the PAHs analytes abbreviated in the figure are presented in Appendix 2.

concentrations (Appendix 4). There was significant interaction effect of core depths and sampling locations on individual PAHs concentrations which indicate that the individual PAH analytes follow similar trend of change in concentrations among the sampling locations and the sediment core depths (Figure 4.8). The C-1 fluorene and C-2 fluorene at coastal stations were significantly higher than the deep-sea stations at all depths ($p < 0.005$). The C-1 phenanthrene in surficial sediments and perylene at lower depths were significantly higher ($p < 0.005$) at coastal stations than the deep-sea sites (Figure 4.8). None of these PAHs with higher PC1 loadings significantly varied between the coastal stations east and west of the MR delta (Figure 4.8). The C-3 NBT, C2- crysene, C-3 crysene, and C-4 pyrene were higher in surface sediments from deep-sea stations east of the MR delta ($p <0.005$), while remain similar among sampling stations at depths (Figure 4.8). These results indicate that the coastal stations were historically loaded with LMW-PAHs and the recent deep-sea sediments had some additional sources of MMW-PAHs. In order to compare any differences in PAHs compositions between samples collected in 2010 (NRDA/NOAA reported) and the samples for the present study, PCA was performed on NOAA samples collected closest to the sampling stations for this study (Figure 4.9). Similar to this study, PAHs composition in the NOAA samples were clearly separated between coastal and deep-sea stations (Figure 4.9a) in both PC1 (89.8%) and PC2 (7.3%) however, the loading plot shows a shift in PAHs compositions between 2010 and 1-3 years after (Figure 4.9b). The coastal sediment PAHs in 2010 were characterized by both LWM and HMW-PAHs, while they were predominately due to LWM-PAHs in the samples analyzed in this study (Figure 4.7 and 4.9). The deep-sea sediments had higher positive loadings for both PC1 and PC2 which was mainly characterized by the alkyl homologues of MMW-PAHs including some parent PAHs benzo(a)anthracene, and Napthobenzothiophene (Figure 4.9a and 4.9b).

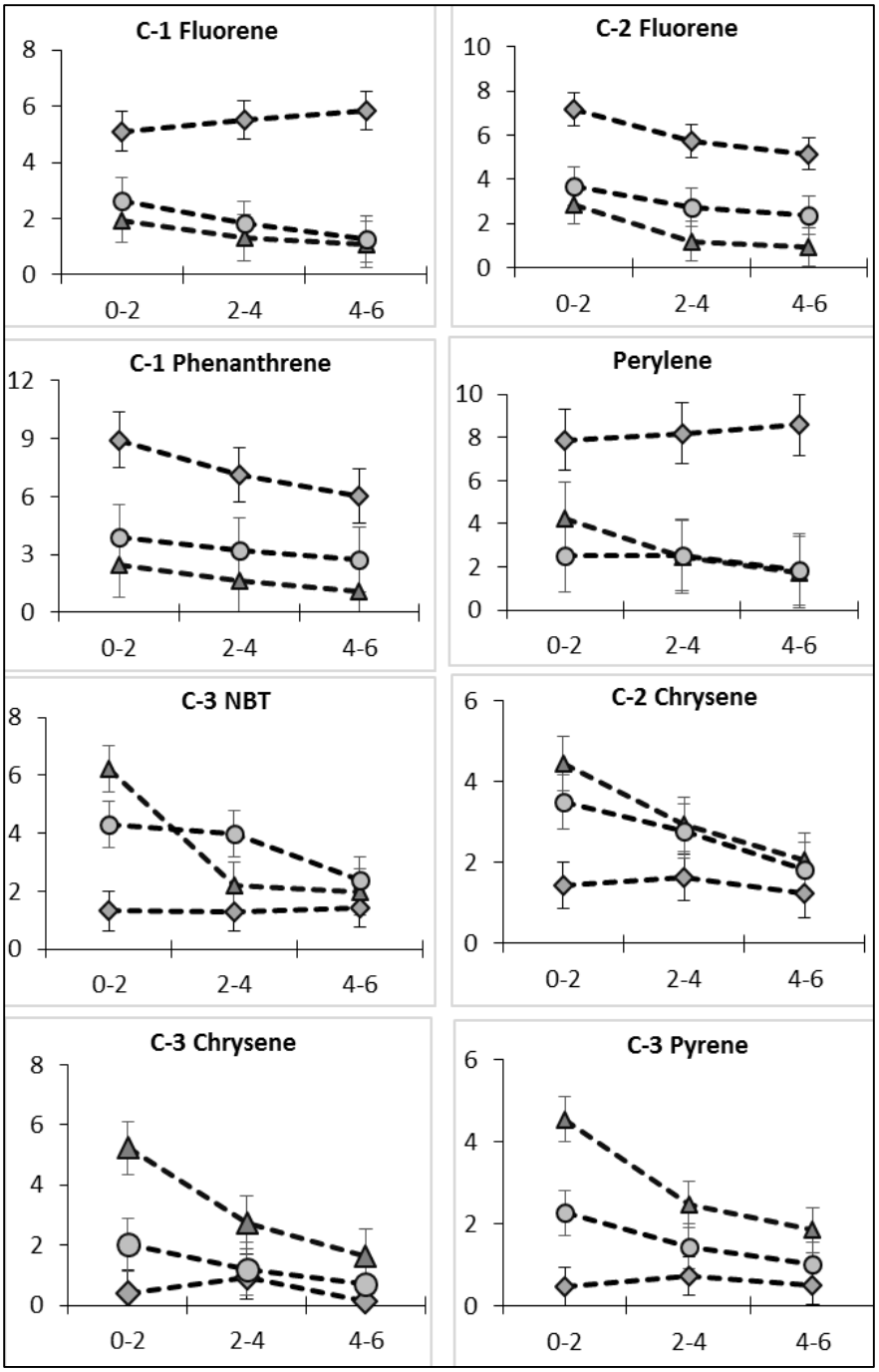

Figure 4.8. Concentrations of selected PAHs analytes with higher PC loading for coastal (diamonds), deep-sea stations east of Mississippi delta (triangles), and deep-sea stations east of Mississippi delta (circles). C-1 Fluorene, C-2 Fluorene, C-1 Phenenthrene and Perylene had higher loading on PC1, and represented coastal stations. While, C-3 NBT (Napthobenzothiophene), C-2 Crysene, C-3 Chrysene, and C-3 Pyrene had higher loading on PC2, representative of deep-sea stations.

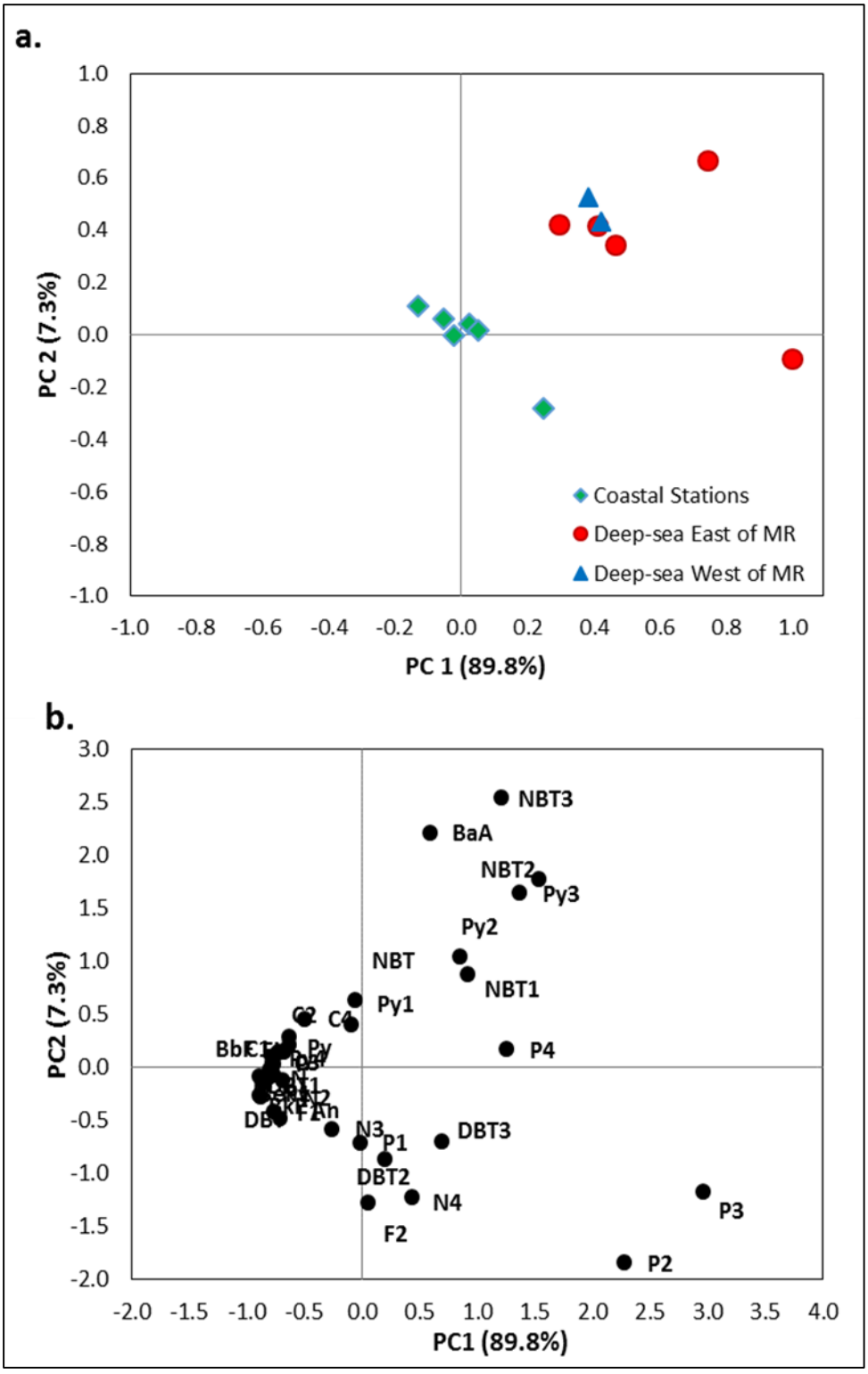

Figure 4.9. Principal component analysis (a) score plots and (b) loading plots for sediment PAHs in the northern Gulf of Mexico, in the selected sediment samples collected by NRDA process in 2010.

In order to differentiate PAHs from petrogenic and pyrogenic sources, I utilized four different isomeric ratios; anthracene to anthracene plus phenanthrene [An/(An+P)], fluoranthene to fluoranthene plus pyrene [Fl/(Fl+Py)], benzo(a)anthracene to benzo(a)anthracene plus chrysene [BaA/(BaA+C)] and indeno(1,2,3-cd)pyrene to indeno(1,2,3-cd)pyrene plus benzo(g,h,i)perylene [IP/(IP+BP)]. The [An/(An+P)], [Fl/(Fl+Py)], [BaA/(BaA+C)] and [IP/(IP+BP)] ratios less than 0.1, 0.4, 0.2, and 0.2 respectively, indicate petroleum sources whereas values higher than these generally indicate combustion sources (Budzinski et al., 1997; Yunker et al., 2002). It must be noted here that these source recognition ratios come with various caveats and their interpretation can be complicated (Yunker et al., 2002). Calculated source recognition ratios showed mixed results and were unable to precisely characterize the origin of PAHs in the northern GOM sediments. The [An/(An+P)], [BaA/(BaA+C)] and IP/(IP+BP) ratios indicated mixed and combustion as the major sources of PAHs, while the [FL/(FL+Py)] ratio indicated petroleum origin of PAHs (Figure 4.10a-c).

The ΣMethylphenanthrenes to phenanthrene (ΣMP/P) ratios were found to be greater than 2 in 94% of the sediment samples, characterizing the PAHs of petroleum origin (Sporstol et al., 1983). Similarly, the ratio of alkylated PAHs to parent PAHs without perylene (A-PAHs/P-PAHs) was 3.6 ± 1.3 suggesting the dominancy of alkyl homologous over un-substituted PAHs (Prahl and Carpenter, 1983). The abundance of LMW-PAHs and the dominance of alkylated homologues over parent compounds reflects a major contribution of unburned fossil sources (Bence et al., 2007; Budzinski et al., 1997; Laflamme and Hites, 1978; Mostafa et al., 2009; Sporstol et al., 1983). The sources recognition parameters were not found to be conclusive but the general view indicate a petrogenic origin for PAHs in the northern GOM sediments. Furthermore, persistent petroleum biomarkers, Hopens and Steranes were analyzed in the

sediments samples for crude oil fingerprinting. The concentration of biomarkers were below detection limits in most of the samples except for stations C6, C10 and C16 (Wang et al., 2006). The presence of biomarkers in those sediment samples could be due to the DWH oil input.

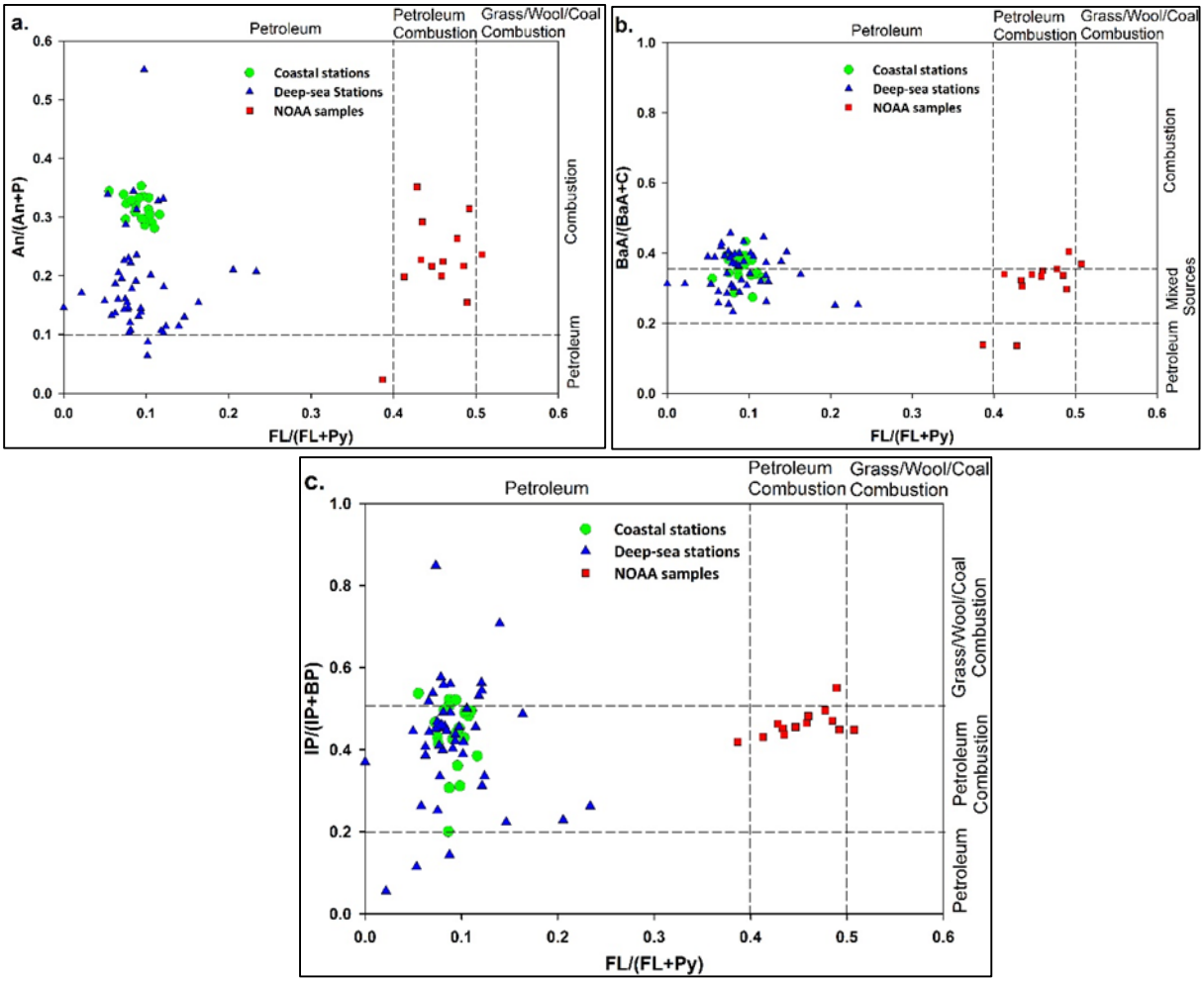

Figure 4.10. Anthracene to anthracene plus phenanthrene [An/(An+P)], fluoranthene to fluoranthene plus pyrene [FL/(FL+Py)], benzo(a)anthracene to benzo(a)anthracene plus chrysene [BaA/(BaA+C)], and indeno(1,2,3-cd)pyrene to indeno(1,2,3-cd)pyrene plus benzo(g,h,i)perylene [IP/(IP+BP)] ratios for the source recognition of the northern Gulf of Mexico Sediments PAHs (Yunker et al. 2002). The green circles and blue triangles represent coastal and deep water sediment samples collected in this study (in 2011 and 2013), while the red squares represent the samples collected by NRDA process in 2010 and publicly reported by NOAA.

Unlike in the samples for this study, all four source recognition ratios calculated for NOAA samples indicated combustion as a primary source of sediment PAHs in the GOM

(Figure 4.10a-c). The ∑MP/P and A-PAHs/P-PAHs remained similar to my samples however, the alkyl homologues contributed 56.7 ± 20% of the total PAHs, which is lower than what I observed in 2011 and 2013 (78.2 ± 6.0%) from same area. These source diagnostic ratios indicate gasoline and diesel combustion as general source of sediment PAHs in 2010. In the NOAA samples LMW contributes 41.8 ± 10.4 % of the total PAHs (without perylene), MMW contributed 39.4 ± 9.7% while HMW comprised 18.8 ± 9.4% of the total PAHs which is a noticeable difference in PAHs composition in terms of their molecular weight when compared to my samples. It shows that relative concentrations of alkyl homologues and LMW-PAHs has been increased in past 3 years after the DWH oil spill. In contrast, the proportions of un-alkylated parents as well as HWM-PAHs has been decreased, while the MMW-PAHs remained similar. This results are consistent with the PCA outputs (Figure 4.7, and 4. 9). The preferential deposition of parents and HWM-PAHs, the byproducts of the large scaled controlled combustion of DWH oil (Allen et al., 2011), could have resulted in proportionally higher concentrations of those compounds in 2010. The PAHs composition with abundance of alkyl homologues and LMW followed by MMW observed in this study likely represents the background distributions of PAHs in this region. Each source has characteristics PAH pattern therefore a correlation analysis of all individual PAHs can be used to identify if they were originated from same source or not (Baumard et al., 1998). The correlation analysis between individual PAHs observed in this study and the NOAA reported PAHs in 2010 showed a poor correlation ($p > 0.05$) indicating difference in origin of PAHs. The correlation analysis, comparison of PAHs ratios and PCA results (Figure 4.7, and 4.9) all indicate a noticeable change in PAHs composition in the northern GOM sediments in past 3-years, probably due to the change in PAHs inputs in this region.

4.4. Conclusion

This study reports PAHs distributions in the northern GOM sediments 1-3 years after the DWH oil spill, one of the largest marine spills in the world. The concentrations of $\sum PAH_{43}$ in the northern GOM sediments varied between 26.2 to 160 ng g^{-1} suggesting low to moderate levels of PAHs pollution in this region which are unlikely to cause toxic threats to the organisms in the sediments. The pre-post DWH spill comparison on PAHs concentrations suggest a little impacts of the DWH oil input to the GOM sediments in terms of PAHs accumulation. The PCA analysis and source diagnostic parameters carried out between samples collected in 2010 right after the oil spill (NOAA samples) and the samples collected 1-3 years later (this study), suggested a shift in PAHs compositions/distributions in this region, switching towards LMW dominancy in the PAHs profiles. Results indicate PAHs concentrations in surface sediments have returned to values similar to pre-DWH spill and this study can serve as post-spill baseline concentrations and accumulation rates of PAHs in the northern GOM sediments. Extrapolating the average PAHs accumulation rates from deep-sea stations (11.6 ng cm^{-2} y^{-1}) to entire deep-sea region (~5.3 × 10^5 km^2) in the northern GOM (>150 m deep and from Florida tip to Texas tip), I estimate ~6.1 × 10^7 g of PAHs are being deposited annually in this region. Similarly, if we assume a constant PAHs accumulation rate (28.0 ng cm^{-2} y^{-1}, average of all the shallow water stations west of the MR delta) and apply it for the entire area (~1.4 × 10^5 km^2) of the Louisiana-Texas coasts (<150 m) west of the MR delta, about 3.8 × 10^7 g of PAHs are being annually deposited in this region.

CHAPTER 5: CONCLUSIONS

Polycyclic aromatic hydrocarbons (PAHs) are introduced into the northern Gulf of Mexico (GOM) via river discharge, coastal erosion, atmospheric deposition, gas hydrates, oil seeps and oil spills related to petroleum exploration and transportation. An estimated 2.1 x 10^{10}g of PAHs also entered into the northern GOM during Deepwater Horizon (DWH) oil spill in 2010 (Reddy et al., 2012). Release of such an unprecedented amount of PAHs can substantially impair the health of marine ecosystems, both the pelagic and benthic communities. It became evident following the DWH oil spill that an accurate quantification of the ultimate fate of the spilled oil is extremely challenging. The baseline data on concentrations and transport fluxes of PAHs are missing for this region, primarily due to lack of feasible method to quantify this mechanism. Toxic, persistent, mutagenic and carcinogenic nature of PAHs make them a critical group of organic contaminants that need to be monitored thoroughly however, very little is known about how PAHs behave in the marine systems and what drives their fate and distribution in the open ocean.

The primary focus of this research was to provide scientific understanding on removal of PAHs from upper ocean via vertical sinking and their accumulation rates in bottom sediments in the northern GOM. Little to no such data exists for northern GOM. This study, for the first time, quantifies PAHs in four different phases (dissolved, suspended particles, settling particles and seafloor sediments) to estimate vertical flux, residence time and accumulation rate of PAHs in this region. This is the first instance not only to use surface-tethered drifting sediment traps, but also to utilize ^{234}Th as a tracer to estimate particulate PAHs fluxes from the upper mesopelagic zone of the northern GOM. This study thus provides a rare opportunity to compare the PAHs fluxes measured simultaneously using two different approaches (sediment traps and ^{238}U-^{234}Th

disequilibria). These water column flux estimates were also compared with the ^{210}Pb-based PAHs accumulation rates in the bottom sediments to provide a more compressive understanding of their fate in marine systems.

The concentrations of dissolved and particulate ΣPAH_{43} in the water column varied between 24.2-58.0 ng L^{-1} and 0.17-1.31 ng L^{-1}, respectively during this study period. The observed concentrations of dissolved PAHs were found to be orders of magnitude lower than the values reported during DWH oil spill (Diercks et al., 2010), indicating significant attenuation in PAHs concentrations probably to the background levels in the 2-3 years after the spill. The surface-tethered drifting sediment trap-based vertical sinking fluxes of particulate ΣPAH_{43} at 150 m (at the base of the euphotic zone) varied between 5.2-6.3 µg m^{-2} d^{-1} in 2012 and 2.0-2.4 µg m^{-2} d^{-1} in 2013. This demonstrate that the vertical flux is an important mechanism of PAHs loss from the upper ocean, with 3-7% of total particulate PAHs inventory in the euphotic zone being lost daily via this pathway. The estimated rate of loss implies that the entire particulate PAHs inventory in the euphotic zone can be lost within 15-32 days, which can be regarded as the residence time of particulate PAHs in upper 150 m of the water column. In spite of similar dissolved and particulate PAHs concentrations in the water column, the vertical fluxes were 2-4 times higher in 2012 than in 2013. The reported variability in PAHs fluxes was likely primarily mediated by the change in concentration of carbon rich marine particles driven by biological production and zooplankton grazing however, other processes like atmospheric input cannot be ruled out (Adhikari et al., 2015; Buesseler et al., 2007; Gustafsson et al., 1997a, 1997b). The surface-tethered drifting sediment traps provide direct instantaneous upper ocean flux measurements however, the short deployment length of drifting sediment traps (2-3 days) posed the challenge as to whether enough particles can be collected to quantify PAH fluxes. The results

from this study show that these traps are sufficient to collect and characterize upper ocean PAHs fluxes which will open doors to future research on further understanding the role of various biogeochemical processes in controlling PAHs fluxes in the mesopelagic zone.

The trap independent particulate $\sum PAH_{43}$ fluxes in upper 350 m of the northern GOM water column, estimated via ^{238}U-^{234}Th disequilibria, varied between 1.0-15.1 μg m^{-2} d^{-1} and 0.3-18.6 μg m^{-2} d^{-1}, respectively in 2012 and 2013. Considering the variability in oceanographic settings, analytical uncertainties and model assumptions, the ^{234}Th-derived and sediment trap-based PAHs fluxes at 150 and 250 m are found to be similar, within the factor of three. This agreement between the two methods demonstrate that the ^{238}U-^{234}Th disequilibria can be an effective tracer of particulate PAHs fluxes from upper mesopelagic zone of the northern GOM. The ^{234}Th-based method provides reliable data with large spatial coverage in relatively shorter time and can be more appropriate for upper ocean PAHs flux estimation especially in high traffic areas like the northern GOM, where drifting sediment traps are difficult to deploy. The potential use of this technique can have a wide range of application for vertical flux and residence time estimation of particle-reactive persistent organic pollutants (POPs) such as PAHs in the upper ocean. It can provide an opportunity to fill the considerable gap of reliable PAHs flux estimates in global ocean.

The concentrations and ^{210}Pb-based accumulation rates of sediment ΣPAH_{43} varied between 26.2-160 ng g^{-1} and 1.4-63.1 ng cm^{-2} y^{-1}, respectively. Observed ΣPAH_{43} concentrations are similar to the background pre-spill values, indicating long term impacts of the spill on sediment PAHs to be minimal. The ΣPAH_{43} concentrations are an order of magnitude lower than the ERL (effects range-low) values and are unlikely to cause toxicity to benthic communities (Long et al., 1995). Source diagnostic analysis suggest a noticeable change in sedimentary PAHs

composition in the last few years, towards lower molecular weight dominancy in PAHs profiles, attributed to the deposition of higher molecular PAHs byproducts by control combustion during the DWH oil spill.

In summary, the most important findings of this research are: i) vertical flux of particulate PAHs is a significant PAHs loss term in the upper mesopelagic zone of northern GOM, ii) the ^{238}U-^{234}Th disequilibria can be an effective tracer of particulate PAHs fluxes from upper mesopelagic zone of the northern GOM, iii) the concentrations of PAHs in water and seafloor sediments have been greatly reduced in 1-3 years after the DWH oil spill, possibly to the pre-spill levels, iv) 1-3 years after the DWH oil spill, the distributions of PAHs profiles in the seafloor sediments have been significantly shifted towards the dominancy of lower molecular weight PAHs. The findings of this study can serve as post-spill baseline information on PAHs in this region which will be invaluable for understanding the long term fate of PAHs and the environmental impacts of any possible future oil spill. It is an essential first step towards the development of a mass balance of PAHs as well as other hydrophobic organic compounds (HOCs) in marine ecosystems.

The vertical transport is not the only loss term of PAHs in the marine environment. Several other factors like evaporation, biodegradation, photo-chemical oxidation, dispersion and lateral transport can affect PAHs dynamics in the upper oceans and their accumulation in seafloor. All these processes essentially reduce the residence time of particulate PAHs in the water column to varying degrees. This present work assumed one dimensional steady-state conditions and ignored all the above mentioned PAHs loss terms thus, the estimated residence time can only be regarded as an upper limit. The vertical flux, residence time and sedimentary PAHs accumulation is also expected be sensitive to any processes that change the particle size

distributions in the water column such as biological production, atmospheric deposition and/or riverine input. Little to no information exist about how the above mentioned processes modulate PAH fluxes in the open ocean. Therefore, there is a need for extensive studies in future to quantify, how all these factors potentially affecting biogeochemical cycling of PAHs in the northern GOM.

REFERENCES

Adhikari, P.L., Maiti, K., Overton, E.B., 2015. Vertical fluxes of polycyclic aromatic hydrocarbons in the northern Gulf of Mexico. Marine Chemistry 168, 60-68.

Albers, P.H., 2003. Petroleum and Individual Polycyclic Aromatic Hydrocarbons. In Handbook of Ecotoxicology, 2nd ed.; Hoffman, D.J., Rattner, B.A., Burton, A.G., Cairns, J., Eds.; CRC Press LLC: Boca Raton, FL, pp. 342-360.

Allan, S.E., Smith, B.W., Anderson, K.A., 2012. Impact of the Deepwater Horizon oil spill on bioavailable polycyclic aromatic hydrocarbons in Gulf of Mexico coastal waters. Environmental Science & Technology 46, 2033-2039.

Anderson, R.F., 1982. Concentration, vertical flux, and remineralization of particulate uranium in seawater. Geochimica et Cosmochimica Acta 46, 1293-1299.

Appleby, P. G., and F. Oldfield, Application of Lead-210 to sedimentation studies, in Uranium-Series Disequilibrium, Applications to Earth, Marine, and Environmental Sciences, edited by I. Ivanovich, and R. S. Harmon, pp. 732–778, Clarendon, Oxford, UK, 1992.

Bacon, M.P., Cochran, J.K., Hirschberg, D., Hammar, T.R., Fleer, A.P., 1996. Export flux of carbon at the equator during the EqPac time-series cruises estimated from ^{234}Th measurements. Deep Sea Research Part II: Topical Studies in Oceanography 434, 1133-1153.

Barakat, A.O., Mostafa, A., Wade, T.L., Sweet, S.T., El Sayed, N.B., 2011. Distribution and characteristics of PAHs in sediments from the Mediterranean coastal environment of Egypt. Marine Pollution Bulletin 62, 1969-1978.

Baskaran, M., Santschi, P.H., Guo, L., Bianchi, T.S., Lambert, C., 1996. ^{234}Th:^{238}U disequilibria in the Gulf of Mexico: the importance of organic matter and particle concentration. Continental Shelf Research 16, 353-380.

Baskaran, M., Swarzenski, P.W., 2007. Seasonal variations on the residence times and partitioning of short-lived radionuclides (^{234}Th, ^{7}Be and ^{210}Pb) and depositional fluxes of ^{7}Be and ^{210}Pb in Tampa Bay, Florida. Marine Chemistry 104, 27-42.

Bauer, J.E., Capone, D.G., 1985. Degradation and mineralization of the polycyclic aromatic hydrocarbons anthracene and naphthalene in intertidal marine sediments. Applied and Environmental Microbiology 50, 81-90.

Baumard, P., Budzinski, H., Garrigues, P., 1998. Polycyclic aromatic hydrocarbons in sediments and mussels of the western Mediterranean Sea. Environmental Toxicology and Chemistry 17, 765-776.

Bechtold, T., Mussak, R., 2009. Natural colorants-quinoid, naphthoquinoid and anthraquinoid dyes. Handbook of Natural Colorants, 151-182.

Bence, A.E., Page, D.S., Boehm, P.D., 2007. Advances in Forensic techniques for petroleum Hydrocarbons: The Exxon Valdez Experience. In Oil Spill environmental Forensics, Fingerprinting and Source Identification, Wang, Z., Stout, S.A; Elsevier Inc. pp. 449-487.

Benner, R., 2000. Missing pieces of the ocean cycle puzzle. Ocean Carbon Transport, Exchanges and Transformations (OCTET) Workshop Report, March 7-10, Warrenton, VA.

Berrojalbiz, N., Dachs, J., Ojeda, M.J., Valle, M.C., Castro-Jimenez, J., Wollgast, J., Ghiani, M., Hanke, G., Zaldivar, J.M., 2011. Biogeochemical and physical controls on concentrations of polycyclic aromatic hydrocarbons in water and plankton of the Mediterranean and Black Seas. Global Biogeochemical Cycles 25, GB4003.

Bhat, S.G., Krishnaswamy, S.K., Lal, D., Rama, D., Moore, W.S., 1969. $^{234}Th/^{238}U$ ratios in the ocean. Earth and Planetary Science Letters 5, 483-491.

Boffetta, P., Jourenkova, N., Gustavsson, P., 1997. Cancer risk from occupational and environmental exposure to polycyclic aromatic hydrocarbons. Cancer Causes Control 8, 444-72.

Bolker, B.M., Brooks, M.E., Clark, C.J., Geange, S.W., Poulsen, J.R., Stevens, M.H.H., White, J.S.S., 2009. Generalized linear mixed models: a practical guide for ecology and evolution. Trends in ecology & evolution, 24, 127-135.

Bossert, I., Kachel, W.M., Bartha, R., 1984. Fate of hydrocarbons during oily sludge disposal in oil. Applied & Environmental Microbiology 47, 763-767.

Bosu, S., 2014. Temporal variability of particulate organic carbon fluxes in the northern Gulf of Mexico. M.S. Thesis, Department of Oceanography and Coastal Science, Louisiana State University, Baton Rouge, Louisiana.

Bouloubassi, I., Mejanelle, L., Pete, R., Fillaux, J., Lorre, A., Point, V., 2006. PAH transport by sinking particles in the open Mediterranean Sea: a 1 year sediment trap study. Marine Pollution Bulletin 52, 560-571.

Bouloubassi, I., Saliot, A., 1993. Dissolved, particulate and sedimentary naturally derived polycyclic aromatic hydrocarbons in a coastal environment: geochemical significance. Marine Chemistry 42, 127-143.

Brooks, J.M., Cox H.B., Bryant, W.R., Kennicutt, M.C., Mann, R.G., Mcdonald, T.J., 1986. Association of Gas Hydrates and Oil Seepage in the Gulf of Mexico. Organic Geochemistry 10, 221–234.

Bruzzoniti, M.C., Fungi, M., Sarzanini, C., 2010. Determination of EPA's priority pollutant polycyclic aromatic hydrocarbons in drinking waters by solid phase extraction-HPLC. Analytical Methods, 2, 739-745.

Budzinski, H., Jones, I., Bellocq, J., Pierard, C., Garrigues, P., 1997. Evaluation of sediment contamination by polycyclic aromatic hydrocarbons in the Gironde estuary. Marine Chemestry 58, 85-97.

Buesseler, K.O., 1991. Do upper-ocean sediment traps provide an accurate record of particle flux?. Nature 353, 420-423.

Buesseler, K.O., Anita, A.N., Chen, M., Fowler, S.W., Gardner, W.D., Gustafsson, O., Harada, K., Mishaels, A.F., van der Loeff, M.R., Sarin, M., Steinberg, D.K., Trull, T., 2007. An assessment of the use of sediment traps for estimating upper ocean particle fluxes. Journal of Marine Research 65, 345-416.

Buesseler, K.O., Bacon, M.P., Cochran, J.K., Livingston, H.D., 1992. Carbon and nitrogen export during the JGOFS North Atlantic Bloom Experiment estimated from ^{234}Th:^{238}U disequilibria. Deep-Sea Research 39, 1115-1137.

Buesseler, K.O., Ball, L., Andrews, J., Benitez-Nelson, C., Belastock, R., Chai, F., Chao, Y., 1998. Upper ocean export of particulate organic carbon in the Arabian Sea derived from thorium-234. Deep-Sea Res. II, Arabian Sea 45, 2461-2487.

Buesseler, K.O., Ball, L., Andrews, J., Cochran, J.K., Hirschberg, D.J., Bacon, M.P., Fleer, A., Brzezinski, M., 2001. Upper ocean export of particulate organic carbon and biogenic silica in the Southern Ocean along 1708W. Deep-Sea Research. Part 2. Topical Studies In Oceanography 48, 4275-4297.

Buesseler, K.O., Benitez-Nelson, C.R., Moran, S.B., Burd, A., Charette, M., Cochran, J.K., Coppola, L., Fisher, N.S., Fowler, S.W.,Gardner,W.D., Guo, L.D., Gustafsson, O., Lamborg,C., Masque, P., Miquel, J.C., Passow, U., Santschi, P.H., Savoye, N., Stewart, G., Trull, T., 2006. An assessment of particulate organic carbon to thorium-234 ratios in the ocean and their impact on the application of ^{234}Th as a POC flux proxy. Marine Chemistry 100, 213-233.

Chanton, J., Zhao, T., Rosenheim, B.E., Joye, S. B., Bosman, S., Brunner, C.A., Yeagear, K.M., Diercks, A.R., Hollander, D., 2015. Using Natural Abundance Radiocarbon to trace the Flux of Petrocarbon to the Seafloor following the Deepwater Horizon Oil Spill. Environmental Science & Technology 49, 847-854.

Chen, B., Xuan, X., Zhu, L., Wang, J., Gao, Y., Yang, K., Shen, X., Lou, B., 2004. Distributions of polycyclic aromatic hydrocarbons in surface waters, sediments and soils of Hangzhou City, China. Water Research 38, 3558-3568.

Chen, J.H., Edwards, R.L., Wasserburg, G.J., 1986. ^{238}U, ^{234}U and ^{232}Th in seawater. Earth and Planetary Science Letters 80, 241-251.

Colombo, J.C., Cappelletti, N., Lasci, J., Migoya, M.C., Speranza, E., Skorupka, N., 2006. Sources, vertical fluxes, and equivalent toxicity of aromatic hydrocarbons in coastal sediments of the Rio de la Plata estuary, Argentina. Environmental Science & Technology 40, 734-740.

Cornelissen, G., Rigterink, H., Ferdinandy, M.M., van Noort, P.C., 1998. Rapidly desorbing fractions of PAHs in contaminated sediments as a predictor of the extent of bioremediation. Environmental Science & Technology 32, 966-970.

Dachs, J., Bayona, J.M., Fowler, S.W., Miquel, J.C., Albaiges, J., 1996. Vertical fluxes of polycyclic aromatic hydrocarbons and organochlorine compounds in the western Alboran Sea (Southwestern Mediterranean). Marine Chemistry 52, 75-86.

Dachs, J., Bayona, J.M., Raoux, C., Albaiges, J., 1997. Spatial, vertical distribution and budget of polycyclic aromatic hydrocarbons in the western Mediterranean seawater. Environmental Science & Technology 31, 682-688.

Dachs, J., Lohmann, R., Ockenden, W.A., Mejanelle, L., Eisenreich, S.J., Jones, K.C., 2002. Oceanic biogeochemical controls on global dynamics of persistent organic pollutants. Environmental Science & Technology 36, 4229-4237.

De La Rocha, C.L., Passow, U., 2007. Factors influencing the sinking of POC and the efficiency of the biological carbon pump. Deep Sea Research Part II: Topical Studies in Oceanography 54, 639-658.

de Souza, V.L., Rodrigues, K.R., Pedroza, E.H., Melo, R.T.D., Lima, V.L.D., Hazin, C.A., de Almeida, M.G.O, Nascimento, R.K.D., 2012. Sedimentation Rate and ^{210}Pb Sediment Dating at Apipucos Reservoir, Recife, Brazil. Sustainability, 4, 2419-2429.

Deyme, R., Bouloubassi, I., Taphanel-Valt, M.H., Miquel, J.C., Lorre, A., Marty, J.C., Mejanelle, L., 2011. Vertical fluxes of aromatic and aliphatic hydrocarbons in the Northwestern Mediterranean Sea. Environmental Pollution 159, 3681-3691.

Diercks, A.R., Highsmith, R.C., Asper, V.L., Joung, D., Zhou, Z., Guo, L., Shiller, A.M., Joye, S.B., Teske, A.P., Guinasso Jr., N.L., Wade, T.L., Lohrenz, S.E., 2010. Characterization of Subsurface Polycyclic Aromatic Hydrocarbons at the Deepwater Horizon Site. Geophys. Res. Lett. 37, L20602. DOI 10.1029/2010GL045046.

Eisler, R., 1987. Polycyclic aromatic hydrocarbon hazards to fish, wildlife, and invertebrates: a synoptic review. U.S. Fish and Wildlife Service Biological Report 85 (1.11).

Eisler, R., 2000. Polycyclic aromatic hydrocarbons, in Handbook of Chemical Risk Assessment. Lewis Publishers, Boca Raton, Florida.

Elder, D.L., Fowler, S.W., 1977. Polychlorinated biphenyls: penetration into the deep ocean by zooplankton fecal pellet transport. Science 197, 459-461.

Evans, K.M., Gill, R.A., Robotham, P.W.J., 1990. The PAH and organic content of sediment particle size fractions. Water, Air, and Soil Pollution 51, 13-31.

Gardner, W.D., 1985. The effect of tilt on sediment trap efficiency. Deep-Sea Research 32, 349-361.

Grimmer, G. (Ed.), 1983. Environmental Carcinogens: Polycyclic Aromatic Hydrocarbons. CRC Press, Boca Raton, Florida.

Gust, G., Bowles, W., Giordano, S., Huettel, M., 1996. Particle accumulation in a cylindrical sediment trap under laminar and turbulent steady flow: An experimental approach. Aquatic Science 58, 297-326.

Gustafsson, O., Buesseler, K.O., Geyer, W.R., Moran, S.B., Gschwend, P.M., 1998. An assessment of the relative importance of horizontal and vertical transport of particle-reactive chemicals in the coastal ocean. Continental Shelf Research 18, 805-829.

Gustafsson, O., Gschwend, P.M., Buesseler, K.O., 1997a. Using ^{234}Th disequilibria to estimate the vertical removal rates of polycyclic aromatic hydrocarbons from the surface ocean. Marine Chemistry 57, 11-23.

Gustafsson, O., Haghseat, F., Chan, C., MacFarlane, J., Gschwend, P.M., 1997b. Quantification of the dilute sedimentary ‘‘soot-phase: Implications for PAH speciation and bioavailability. Environmental Science & Technology 31, 203-209.

Gustafsson, O., Gschwend, P.M., Buesseler, K.O., 1997c. Settling removal rates of PCBs into the Northwestern Atlantic derived from ^{238}U-^{234}Th disequilibria. Environmental Science & Technology 31, 3544-3550.

Gustafsson, O., Nilsson, N., Bucheli, T.D., 2001. Dynamic colloid-water partitioning of pyrene through a coastal Baltic spring bloom. Environmental Science & Technology 35, 4001-4006.

Gutierrez, T., 2011. Identifying polycyclic aromatic hydrocarbon-degrading bacteria in oil-contaminated surface waters at Deepwater Horizon by cultivation, stable isotope probing and pyrosequencing. Reviews in Environmental Science and Bio/Technology 10, 301-305.

Harvey, R.G., 1991. Polycyclic aromatic hydrocarbons: chemistry and carcinogenicity. CUP Archive.

Haynes, W.M. (Ed.)., 2013. CRC handbook of chemistry and physics, 94th edition. CRC Press, Inc., Boca Raton, Florida.

Head, I.M., Martin, J.D., Roling, W.F.M., 2006. Marine microorganisms make a meal of oil. Nature Review Microbiology 4, 173-182.

Hedges, J.I., Stern, J.H., 1984. Carbon and nitrogen determinations of carbonate containing solids. Limnology Oceanography 49, 657-663.

Holm, S., 1979. A simple sequential rejective multiple test procedure. Scandinavian Journal of Statistics 6, 65-70.

Hung, C.C., Guo, L., Roberts, K.A., Santschi, P.H., 2004. Upper ocean carbon flux determined by the ^{234}Th approach and sediment traps using size-fractionated POC and ^{234}Th data from the Gulf of Mexico. Geochemical Journal 38, 601-611.

Irigoien, X., Klevjer, T.A., Rostard, A., Martinez, U., Boyra, G., Acuna, J.L., Bode, A., Echevarria, F., Gonzalez-Gordillo, J.I., Hernandez-Leon, S., Agusti, S., Aksnes, D.L., Duarte, C.M., Kaartvedt, S., 2014. Large mesopelagic fishes biomass and trophic efficiency in the open ocean. Nature Communications 5, 3271.

Kanaly, R.A., Harayama, S., 2000. Biodegradation of high-molecular-weight polycyclic aromatic hydrocarbons by bacteria. Journal of Bacteriology 182, 2059-2067.

Karickhoff, S.W., Brown, D.S., Scott, T.A., 1979. Sorption of hydrophobic pollutants on natural sediments. Water Resources 13, 241-248.

Kim, K.H., Jahan, S.A., Kabir, E., Brown, R.J., 2013. A review of airborne polycyclic aromatic hydrocarbons (PAHs) and their human health effects. Environment International 60, 71-80.

Kiss, G., Varga-Puchony, Z., Hlavay, J., 1996. Determination of polycyclic aromatic hydrocarbons in precipitation using solid-phase extraction and column liquid chromatography. Journal of Chromatography A 725, 261-272.

Ko, F.C., Baker, J.E., 1995. Partitioning of hydrophobic organic contaminants to resuspended sediments and plankton in the mesohaline Chesapeake Bay. Marine Chemistry 49, 171-188.

Ko, F.C., Sanford, L.P., Baker, J.E., 2003. Internal cycling of particle reactive organic chemicals in the Chesapeake Bay water column. Marine Chemistry 81, 163-176.

Kootstra, P.R., Straub, M.H.C., Stil, G.H., van der Velde, E.G., Hesselink, W., Land, C.C.J., 1995. Solid-phase extraction of polycyclic aromatic hydrocarbons from soil samples. Journal of Chromatography A 697, 123-129.

Krishnaswami, S., Lal, D., Martin, J.M., Meybeck, M., 1971. Geochronology of lake sediments. Earth and Planetary Science Letters 11, 407–414.

Kristensen, E., 2000. Organic matter diagenesis at the oxic/anoxic interface in coastal marine sediments, with emphasis on the role of burrowing animals. Hydrobiologia 426, 1-24.

Laflamme, R.E., Hites, R.A., 1978. The global distribution of polycyclic aromatic hydrocarbons in recent sediments. Geochimica et Cosmochimica Acta 42, 289-303.

Lamborg, C.H., Buesseler, K.O., Valdes, J., Bertrand, C.H., Bidigare, R., Manganini, S., Pike, S., Steinberg, D.K., Trull, T., Wilson, S., 2008. The flux of bio-and lithogenic material associated with sinking particles in the mesopelagic ‘‘twilight zone’’ of the northwest and north central Pacific Ocean. Deep-Sea Res. II 55, 1540-1563.

Lee, C., Hedges, J.I., Wakeham, S.G., Zhu, N., 1992. Effectiveness of various treatments in retarding microbial activity in sediment trap material and their effects on the collection of swimmers. Limnology and Oceanography 37, 117–130.

Lee, S.D., and L. Grant (eds.). 1981. Health and ecological assessment of polynuclear aromatic hydrocarbons. Pathotex Publ., Park Forest South, Illinois. 364 pp.

Lepore, K., Moran, S.B., Burd, A.B., Jackson, G.A., Smith, J.N., Kelly, R.P., Kabri, H., Stavrakakis, S., Assimakopoulou, G., 2009. Sediment trap and in-situ pump size-fractionated POC/^{234}Th ratios in the Mediterranean Sea and Northwest Atlantic: Implications for POC export. Deep Sea Research Part I: Oceanographic Research Papers 56, 599-613.

Lipiatou, E., Marty, J.C., Saliot, A., 1993. Sediment trap fluxes of polycyclic aromatic hydrocarbons in the Mediterranean Sea. Marine Chemistry 44, 43-54.

Lipiatou, E., Tolosa, I., Simo, R., Bouloubassi, I., Dachs, J., Marty, S., Sicre, M.A., Bayona, J.M., Grimalt, J.O., Saliot, A., Albaiges, J., 1997. Mass budget and dynamics of polycyclic aromatic hydrocarbons in the Mediterranean Sea. Deep-Sea Research II 44, 881-905.

Liu, Z., Liu, J., Gardner, W.S., Shank, G.C., Ostrom, N.E., 2014. The impact of Deepwater Horizon oil spill on petroleum hydrocarbons in surface waters of the northern Gulf of Mexico. Deep-Sea Res. II (http://dx.doi.org/10.1016/j.dsr2.2014.01.013i).

Long, E.R., MacDonald, D.D., Smith, S.L., Calder, F.D., 1995. Incidence of adverse biological effects within ranges of chemical concentrations in marine and estuarine sediments. Environmental Management 19, 81-97.

Lubis, A.A., 2013. Constant rate of supply (CRS) model for determining the sediment accumulation rates in the coastal area using 210Pb. Journal of Coastal Development 10, 9-18.

Mackay, D., Shiu, W.Y., 1977. Aqueous solubility of polynuclear aromatic hydrocarbons. Journal of Chemical & Engineering Data 22, 399-402.

Mai, B., Qi, S., Zeng, E.Y., Yang, Q., Zhang, G., Fu, J., Sheng, G., Peng, P., Wang, Z., 2003. Distribution of polycyclic aromatic hydrocarbons in the coastal region off Macao, China: assessment of input sources and transport pathways using compositional analysis. Environmental Science & Technology 37, 4855-4863.

Maiti, K., Buesseler, K. O., Pike, S. M., Benitez-Nelson, C., Cai, P., Chen, W., Cochran, K., Dai, M., Dehairs, F., Gasser, B., Kelly, R.P., Masque, P., Miller, L.A., Miquel, J.C, Moran, S.B., Morris, P.J., Peine, F., Planchon, F., Renfro, A.A., Rutgers van der Loeff, M, Santchi, P.H., Turnewitsch, R., Waples, J.T., Xu, C., 2012**.** Intercalibration studies of short-lived thorium^{-234} in the water column and marine particles. Limnology and Oceanography: Methods 10 631-644.

Maiti, K., Benitez-Nelson, C.R., Lomas, M.W., Krause, J.W., 2009. Biogeochemical responses to late-winter storms in the Sargasso Sea, III—Estimates of export production using ^{234}Th:^{238}U disequilibria and sediment traps. Deep Sea Research Part I: Oceanographic Research Papers 56, 875-891.

Maiti, K., Carroll, J., Benitez-Nelson, C.R., 2010. Sedimentation and particle dynamics in the seasonal ice zone of the Barents Sea. Journal of Marine Systems 79, 185-198.

Maiti, K., Charette, M.A., Buesseler, K.O., Kahru, M., 2013. An inverse relationship between production and export efficiency in the Southern Ocean. Geophysical Research Letters 40, 1557-1561.

Marce, R.M., Borrull, F., 2000. Solid-phase extraction of polycyclic aromatic compounds (review). Journal of Chromatography A 885, 273-290.

Marini, M., Frapiccini, E., 2013. Persistence of polycyclic aromatic hydrocarbons in sediments in the deeper area of the Northern Adriatic Sea (Mediterranean Sea). Chemosphere, 90, 1839-1846.

Martin, J.H., Knauer, G.A., Karl, D.M., Broenkow, W.W., 1987. VERTEX: carbon cycling in the northeast Pacific. Deep Sea Research Part A. Oceanographic Research Papers 34, 267-285.

Mastral, A.M., Callen, M.S., 2000. A review on polycyclic aromatic hydrocarbon (PAH) emissions from energy generation. Environmental Science & Technology 34, 3051-3057.

May, W.E., Wasik, S.P., Freeman, H.F., 1978. Determination of the solubility behavior of some polycyclic aromatic hydrocarbons in water. Analytical Chemistry 50, 997-1000.

McNutt, M.K., Camilli, R., Guthrie, G.D., Hsieh, P.A., Labson, V.F., Lehr, W.J., Maclay, D., Ratzel, A.C., Sogge, M.K., 2011. Assessment of flow rate estimates for the Deepwater Horizon/Macondo well oil spill. US Department of the Interior.

Meador, J.P., Stein, J.E., Reichert, W.L., Varanasi, U., 1995. Bioaccumulation of polycyclic aromatic hydrocarbons by marine organisms. In Reviews of environmental contamination and toxicology (pp. 79-165). Springer, New York.

Means, J.C., 1995. Influence of salinity upon sediment-water partitioning of aromatic hydrocarbons. Marine Chemistry 51, 3-16.

Means, J.C., Wood, S.G., Hasset, J.J., Banwart, W.L., 1980. Sorption of Polynuclear Aromatic Hydrocarbons by Sediments and Soils. Environmental Science & Technology 14, 1524-1528.

Mitra, S., Kimmel, D.G., Snyder, J., Scalise, K., McGlaughon, B.D., Roman, M.R., Jahn, G.L., Pierson, J.J., Brandt, S.B., Montoya, J.P., Rosenbauer, R.J., Lorenson, T.D., Wong, F.L., Campbell, P.L., 2012. Macondo-1 well oil-derived polycyclic aromatic hydrocarbons in mesozooplankton from the northern Gulf of Mexico. Geophysical Research Letters 39, 1.

Mitra, S.; Bianchi, T.S., 2003. A preliminary assessment of polycyclic aromatic hydrocarbon distributions in the lower Mississippi River and Gulf of Mexico. Marine Chemistry 82, 273-288.

Moran, S.B., Buesseler, K.O., 1993. Size-fractionated ^{234}Th in continental-shelf waters off New-England-implications for the role of colloids in oceanic trace-metal scavenging. Journal of Marine Research 51, 893-922.

Moran, S.B., Weinstein, S.E., Edmonds, H.N., Smith, J.N., Kelly, R.P., Pilson, M.E.Q., Harrison, W.G., 2003. Does ^{234}Th/^{238}U disequilibrium provide an accurate record of the export flux of particulate organic carbon from the upper ocean?. Limnology and Oceanography 48, 1018-1029.

Mostafa, A.R., Barakat, A.O., Qian, Y., Wade, T.L., 2003. Composition, distribution and sources of polycyclic aromatic hydrocarbons in sediments of the western harbor of Alexandria, Egypt. Journal of Soils & Sediments 3, 173-179.

Mostafa, A.R., Wade, T.L., Sweet, S. T., Al-Alimi, A.K.A., Barakat, A. O., 2009. Distribution and characteristics of polycyclic aromatic hydrocarbons (PAHs) in sediments of Hadhramout coastal area, Gulf of Aden, Yemen. Journal of Marine Systems 78, 1-8.

Mumtaz, M.M., George, J.D., Gold, K.W., Cibulas, W., Derosa, C.T., 1996. ATSDR evaluation of health effects of chemicals. IV. Polycyclic aromatic hydrocarbons (PAHs): understanding a complex problem. Toxicology and Industrial Health 12, 742-971.

Neff, J.M., 1979. Polycyclic aromatic hydrocarbons in the aquatic environment: sources, fates and biological effects. In Polycyclic aromatic hydrocarbons in the aquatic environment: sources, fates and biological effects. Applied Science, London.

Neff, J.M., 1985. Polycyclic aromatic hydrocarbons, in Fundamentals of Aquatic Toxicology: Methods and Applications. Hemisphere Publishing Corporation Washington, DC.

NOAA (National Oceanic and Atmospheric Administration), National Ocean Service, 2008. The Gulf of Mexico at a Glance. Washington, D.C.: U.S. Department of Commerce, NOAA.

NRC (National Research Council), 2003. Oil in the Sea III: Inputs, Fates, and Effects. The National Academies Press.

Olsson, A.C., Fevotte, J., Fletcher, T., Cassidy, A., Mannetje, A., Brennan P., 2010. Occupational exposure to polycyclic aromatic hydrocarbons and lung cancer risk: a multicenter study in Europe. Occupational & Environmental Medicine 67, 98-103.

Overton, E.B., Ashton, B.M., Miles, M.S., 2004. Historical polycyclic aromatic and petrogenic hydrocarbon loading in Northern Central Gulf of Mexico shelf sediments. Marine Pollution Bulletin 49, 557-563.

Owens, S.A., Buesseler, K.O., and Sims, K.W.W., 2011. Re-evaluating the ^{238}U-salinity relationship in seawater: Implications for the ^{238}U-^{234}Th disequilibrium method, Marine Chemistry 127, 31-39.

Palm, A., Cousins, I., Gustafsson, O., Axelman, J., Grunder, K., Broman, D., Brorstrom-Lunden, E., 2004. Evaluation of sequentially-coupled POP fluxes estimated from simultaneous measurements in multiple compartments of an air-water-sediment system. Environmental Pollution 128, 85-97.

Park, J.S., Wade, T.L., Sweet, S.T., 2001. Atmospheric distributions of polycyclic aromatic hydrocarbons (PAHs) and depositions to Galveston Bay, Texas. Atmospheric Environment 39, 3241-3249.

Park, J.S., Wade, T.L., Sweet, S.T., 2002. Atmospheric deposition of PAHs, PCBs, and organochlorine pesticides to Corpus Christi Bay, Texas. Atmospheric Environment 36, 1707-1720.

Pike, S., Buesseler, K., Andrews, J., Savoye, N., 2005. Quantification of ^{234}Th recovery in small volume sea water samples by inductively coupled plasma mass spectrometry. Journal of Radio analytical and Nuclear Chemistry 263, 355-360.

Prahl, F.G., Carpenter, R., 1983. Polycyclic aromatic hydrocarbon (PAH) phases associations in Washington coastal sediments. Geochimmica et Cosmochimica Acta 47, 1013-1023.

Raoux, C., Bayona, J.M., Miquel, J.C., Teyssie, J.L., Fowler, S.W., Albaiges, J., 1999. Particulate fluxes of aliphatic and aromatic hydrocarbons in near-shore waters to the Northwestern Mediterranean Sea, and the effect of continental runoff. Estuarine, Coastal and Shelf Science 48, 605-616.

Reddy, C.M., Arey, J.S., Seewald, J.S., Sylva, S.P., Lemkau, K.L., Nelson, R.K., Carmichael, C.A., McIntyre, C.P., Fenwick, J., Ventura, G.T., Van Mooy, B.A.S., Camilli, R., 2012. Composition and fate of gas and oil released to the water column during the Deepwater Horizon oil spill. Proceedings of National Academy of Sciences of the United States of America 109, 20229-20234.

Rhoads, D.C., Young, D. K., 1970. The influence of deposit-feeding organisms on sediment stability and community trophic structure. Journal of Marine Research 28, 150-178.

Rodriguez y Baena, A.M., Miquel, J.C., Masque, P., Povinec, P.P., La Rosa, J., 2006. A single vs. double spike approach to improve the accuracy of ^{234}Th measurements in small-volume seawater samples. Marine Chemistry 100, 269-281.

Rutgers van der Loeff, M., Sarin, M.M., Baskaran, M., Benitez-Nelson, C., Buesseler, K.O., Charette, M., Dai, M., Gustafsson, O¨ ., Masque, P., Morris, P.J., Orlandini, K., Rodriguez y Baena, A., Savoye, N., Schmidt, S., Turnewitsch, R., Vo¨ ge, I., Waples, J.T., 2006. A review of present techniques and methodological advances in analyzing ^{234}Th in aquatic systems. Marine Chemistry 100, 190-212.

Rutgers van der Loeff, M.M., Buesseler, K.O., Bathmann, U., Hense, I., Andrews, J., 2002. Comparison of carbon and opal export rates between summer and spring bloom periods in the region of the Antarctic Polar Front, SE Atlantic. Deep-Sea Research. Part 2. Topical Studies In Oceanography 49, 3849-3870.

Samanta, S.K., Singh, O.V., Jain, R.K., 2002. Polycyclic aromatic hydrocarbons: environmental pollution and bioremediation. Trends in Biotechnology 20, 243-248.

Sammarco, P.W., Kolian, S.R., Warby, R.A., Bouldin, J.L., Subra, W.A., Porter, S.A., 2013. Distribution and concentrations of petroleum hydrocarbons associated with the BP/Deepwater Horizon Oil Spill, Gulf of Mexico. Marine Pollution Bulletin 73(1), 129-143.

Santodonato, J., Howard, P., Basu, D., 1981. Health and ecological assessment of polynuclear aromatic hydrocarbons. Journal of Environmental Pathology and Toxicology 5, 1-364.

Santschi, P.H., Presley, B.J., Wade, T.L., Garcia-Romero, B., Baskaran, M., 2001. Historical contamination of PAHs, PCBs, DDTs, and heavy metals in Mississippi river Delta, Galveston bay and Tampa bay sediment cores. Marine Environmental Research 52, 51-79.

Savoye, N., Benitez-Nelson, C., Burd, A.B., Cochran, J.K., Charette, M., Buesseler, K.O., Jackson, G.A., Roy-Barman, M., Schmidt, S., Elskens, M., 2006. Th-234 sorption and export models in the water column: a review. Marine Chemistry 100, 234-249.

Schabenberger, O., 2005. Introducing the GLIMMIX procedure for generalized linear mixed models. SUGI 30 Proceedings, 196-30.

Soclo, H.H., Garrigues, P. H., Ewald, M., 2000. Origin of polycyclic aromatic hydrocarbons (PAHs) in coastal marine sediments: case studies in Cotonou (Benin) and Aquitaine (France) areas. Marine Pollution Bulletin 40, 387-396.

Sporstol, S., Gjos, N., Lichtenthaler, R.G., 1983. Source identification of aromatic hydrocarbons in sediments using GC/MS. Environmental Science & Technology 17, 282-286.

Suess, E., 1980. Particulate organic carbon flux in the oceans—surface productivity and oxygen utilization. Nature 288, 261.

Sverdrup, L.E., Nielsen, T., Krogh, P.H., 2002. Soil ecotoxicity of polycyclic aromatic hydrocarbons in relation to soil sorption, lipophilicity, and water solubility. Environmental Science & Technology 36, 2429-2435.

Tansel, B., Fuentes, C., Sanchez, M., Predoi, K., Acevedo, M., 2011. Persistence profile of polyaromatic hydrocarbons in shallow and deep Gulf waters and sediments: effect of water temperature and sediment-water partitioning characteristics. Marine Pollution Bulletin 62, 2659-2665.

Tao, Y., Zhang, S., Zhu, Y.G., Christie, P., 2009. Uptake and acropetal translocation of polycyclic aromatic hydrocarbons by wheat (*Triticum aestivum L.*). Environmental Science & Technology 43, 3556-3560.

Tsapakis, M., Apostolakis, M., Eisenreich, S., Stephanou, E.G., 2006. Atmospheric deposition and marine sedimentation fluxes of polycyclic aromatic hydrocarbons in eastern Mediterranean basin. Environmental Science & Technology 40, 4922-4927.

Turner, R.E., Overton, E.B., Meyer, B.M., Miles, M.S., McClenachan, G., Hooper-Bui, L., Engel, A.S., Swenson, E.M., Lee, J.M., Milan, C.S., Gao, H., 2014. Distribution and recovery trajectory of Macondo (Mississippi Canyon 252) oil in Louisiana coastal wetlands. Marine Pollution Bulletin 87, 57-67.

Valentine, D.L., Fisher, G.B., Bagby, S.C., Nelson, R.K., Reddy, C.M., Sylva, S.P., Woo, M.A., 2014. Fallout plume of submerged oil from Deepwater Horizon. Proceedings of the National Academy of Sciences 111, 15906-15911.

Venables, W.N., Dichmont, C.M., 2004. GLMs, GAMs and GLMMs: an overview of theory for applications in fisheries research. Fisheries research, 70, 319-337.

Wade, T.L., Kennicutt II, M.C., Brooks, J.M., 1989. Gulf of Mexico Hydrocarbon Seep Communities: Part III. Aromatic Hydrocarbon Concentrations in Organisms, Sediments and Water. Marine Environmental Research 27, 19-30.

Wade, T.L., Soliman, Y., Sweet, S.T., Wolff, G.A., Presley, B.J., 2008. Trace elements and polycyclic aromatic hydrocarbons (PAHs) concentrations in deep Gulf of Mexico sediments. Deep Sea Research Part II: Topical Studies in Oceanography 55, 2585-2593.

Wang, C., Sun, H., Chang, Y., Song, Z., Qin, X., 2011. PAHs distribution in sediments associated with gas hydrate and oil seepage from the Gulf of Mexico. Marine Pollution Bulletin 62, 2714-2723.

Wang, X., Zhang, Y., Chen, R.F., 2001. Distribution and Partitioning of Polycyclic Aromatic Hydrocarbons (PAHs) in Different Size Fractions in Sediments from Boston Harbor, United States. Marine Pollution Bulletin 42, 1139-1149.

Wang, Z., Liu, Z., Xu, K., Mayer, L.M., Zhang, Z., Kolker, A.S., Wu, W., 2014. Concentrations and sources of polycyclic aromatic hydrocarbons in surface coastal sediments of the northern Gulf of Mexico. Geochemical Transactions 15, 2.

Wang, Z., Stout, S.A., Fingas, M., 2006. Forensic fingerprinting of biomarkers for oil spill characterization and source identification. Environmental Forensics 7, 105-146.

Waples, J.T., Benitez-Nelson, C., Savoye, N., van der Loeff, M.R., Baskaran, M., Gustafsson, O., 2006. An introduction to the application and future use of ^{234}Th in aquatic systems. Marine Chemistry 100, 166-189.

Wawrik, B., Paul, J.H., 2004. Phytoplankton community structure and productivity along the axis of the Mississippi River plume in oligotrophic Gulf of Mexico waters. Aquatic Microbial Ecology 35, 185-196.

Weinstein, S.E., Moran, S.B., 2005. Vertical flux of particulate Al, Fe, Pb, and Ba from the upper ocean estimated from ^{234}Th/^{238}U disequilibria. Deep Sea Research Part I: Oceanographic Research Papers 52, 1477-1488.

Wilcke, W., Amelung, W., Martius, C., Garcia, M.V., Zech, W., 2000. Biological sources of polycyclic aromatic hydrocarbons (PAHs) in the Amazonian rain forest. Journal of Plant Nutrition and Soil Science 163, 27-30.

Wild, S.R., Jones, K.C., 1995. Polynuclear aromatic hydrocarbons in the United Kingdom environment: a preliminary source inventory and budget. Environmental pollution, 88, 91-108.

Windsor, J.G., Hites, R.A., 1979. Polycyclic aromatic hydrocarbons in Gulf of Maine sediments and Novia Scotia soils. Geochimica et Cosmochimica Acta 43, 27-33.

Witt, G., 1995. Polycyclic aromatic hydrocarbons in water and sediment of the Baltic Sea. Marine Pollution Bulletin 31, 237-248.

Xia, K., Hagood, G., Childers, C., Atkins, J., Rogers, B., Ware, L., Armbrust, K., Jewell, J., Diaz, D., Gatian, N., Folmer, H., 2012. Polycyclic aromatic hydrocarbons (PAHs) in Mississippi seafood from areas affected by the Deepwater Horizon oil spill. Environmental Science & Technology 46, 5310-5318.

Yan, J., Wang, L., Fu P.P., Yu, H., 2004. Photomutagenicity of 16 polycyclic aromatic hydrocarbons from the U.S. EPA priority list. Mutation Ressearch 557, 99-108.

Yeager, K.M., Santschi, P.H., Rowe, G.T., 2004. Sediment accumulation and radionuclide inventories (^{239,240}Pu, ^{210}Pb and ^{234}Th) in the northern Gulf of Mexico, as influenced by organic matter and macrofaunal density. Marine Chemistry 91, 1-14.

Yunker, M.B., Macdonald, R.W., Vingarzan, R., Mitchell, H., Goyette, D., Sylvestre, S., 2002. PAHs in the Fraser River basin: a critical appraisal of PAH ratios as indicators of PAH source and composition. Organic Geochemistry 33, 489-515.

APPENDIX 1: PERMISSION REQUESTS TO REPRINT

Adhikari, P.L., Maiti, K., Overton, E.B., 2015. Vertical fluxes of polycyclic aromatic hydrocarbons in the northern Gulf of Mexico. Marine Chemistry 168, 60-68.

To whom it may concern,

I have a paper published in Marine Chemistry which is a part of my PhD dissertation. In order to use this article in my dissertation, my university 'Louisiana State University, Baton Rouge, USA' requires me to have a permission letter from the publisher. I was hoping you could either provide such a letter or guide me in the right direction where I can get it.

The citation is as mentioned below:
Adhikari, P.L., Maiti, K., Overton, E.B., 2015. Vertical fluxes of polycyclic aromatic hydrocarbons in the northern Gulf of Mexico. Marine Chemistry 168, 60-68.

Regards,
Puspa L. Adhikari
Department of Oceanography and Coastal Sciences
Louisiana State University, Baton Rouge, LA, 70803, USA

Dear Puspa:

As an Elsevier journal author, you retain various rights including Inclusion of the article in a thesis or dissertation whether in part or *in total*; seehttp://www.elsevier.com/about/policies/author-agreement/lightbox_scholarly-purposes for more information. As this is a retained right, no written permission is necessary provided that the original source is properly acknowledged.

If I may be of further assistance, please let me know. Best of luck with your PhD dissertation.

Regards,
Hop
Hop Wechsler
Permissions Helpdesk Manager
Elsevier
1600 John F. Kennedy Boulevard
Suite 1800
Philadelphia, PA 19103-2899
Tel: +1-215-239-3520
Mobile: +1-215-900-5674
Fax: +1-215-239-3805
E-mail: h.wechsler@elsevier.com
Contact the Permissions Helpdesk:
+1-800-523-4069 x 3808 permissionshelpdesk@elsevier.com

APPENDIX 2: NAME OF THE POLYCYCLIC AROMATIC HYDROCARBON (PAH) COMPOUNDS IDENTIFIED AND QUANTIFIED IN THIS STUDY WITH THEIR CORRESPONDING ABBREVIATIONS

Table A2.1: Name of the polycyclic aromatic hydrocarbon (PAH) compounds identified and quantified in this study with their corresponding abbreviations used in main text and appendices.

PAH Analytes	Abbreviation
Naphthalene	N
C-1 Naphthalene	N1
C-2 Naphthalene	N2
C-3 Naphthalene	N3
C-4 Naphthalene	N4
Fluorene	F
C-1 Fluorene	F1
C-2 Fluorene	F2
C-3 Fluorene	F3
Dibenzothiophene	DBT
C-1 Dibenzothiophene	DBT1
C-2 Dibenzothiophene	DBT2
C-3 Dibenzothiophene	DBT3
Phenanthrene	P
C-1 Phenanthrene	P1
C-2 Phenanthrene	P2
C-3 Phenanthrene	P3
C-4 Phenanthrene	P4
Anthracene	An
Fluoranthene	Fl
Pyrene	Py
C-1 Pyrene	Py1
C-2 Pyrene	Py2
C-3 Pyrene	Py3
C-4 Pyrene	Py3
Napthobenzothiophene	NBT
C-1 NBT	NBT1
C-2 NBT	NBT2
C-3 NBT	NBT3
Benzo(a)Anthracene	BaA
Chrysene	C
C-1 Chrysene	C1
C-2 Chrysene	C2
C-3 Chrysene	C3
C-4 Chrysene	C4
Benzo (b) Fluoranthene	BbF
Benzo (k) Fluoranthene	BKF
Benzo (e) Pyrene	BePy
Benzo (a) Pyrene	BaPy
Perylene	Per
Indeno (1,2,3 - cd) Pyrene	IP
Dibenzo (a,h) anthracene	Da
Benzo (g,h,i) perylene	BP

APPENDIX 3: TYPICAL MOLECULAR PROFILES OF INDIVIDUAL PAH CONCENTRATIONS AND THEIR VERTICAL FLUXES FROM SELECTED STATIONS IN THE NORTHERN GULF OF MEXICO

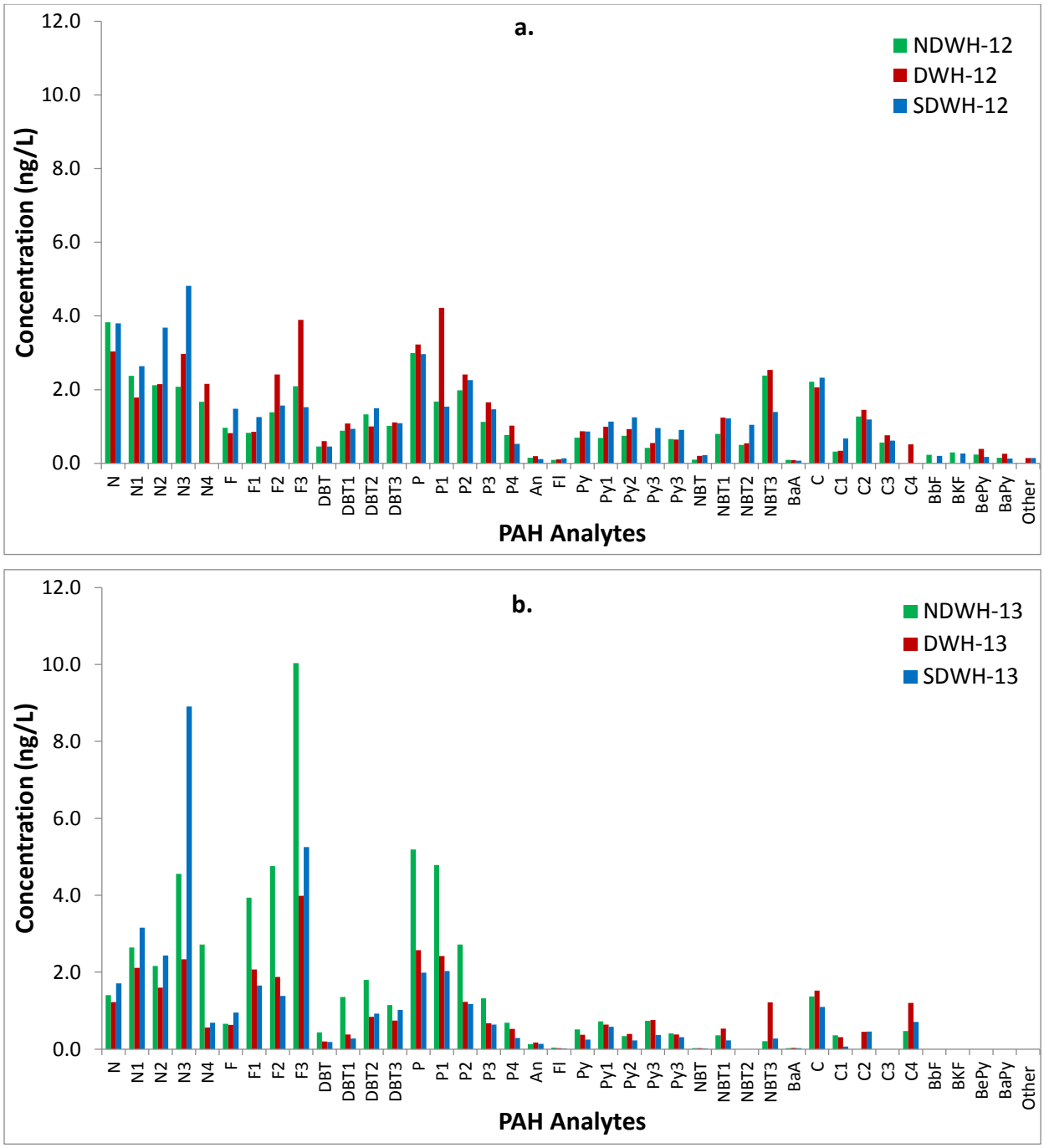

Figure A3.1. Typical molecular profiles of dissolved PAH concentrations at 150 m of water column in year 2012 (a) and 2013 (b), in the northern Gulf of Mexico, in the vicinity of Deepwater Horizon Oil Spill sites.

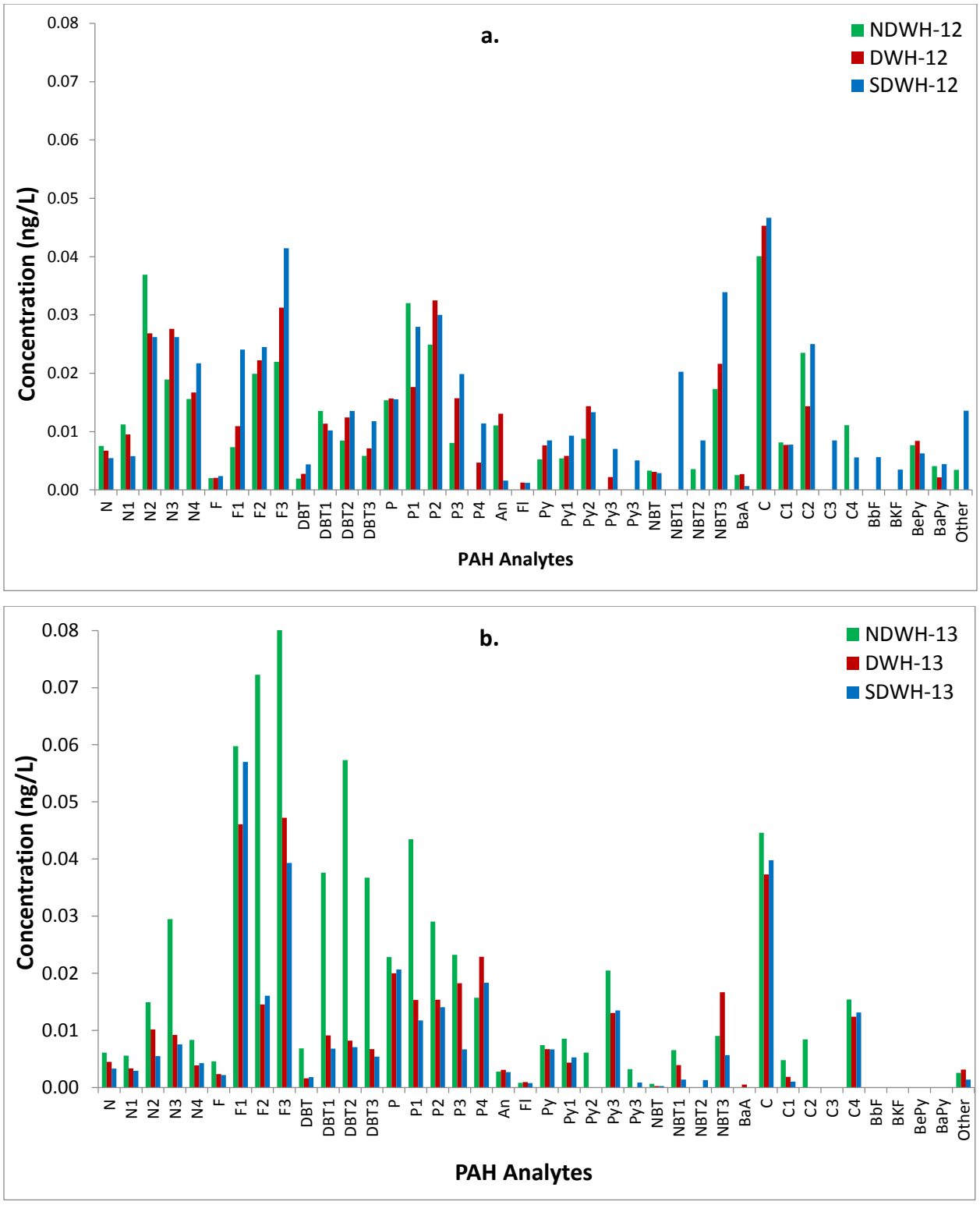

Figure A3.2. Typical molecular profiles of particulate PAH concentrations at 150 m of water column in year 2012 (a) and 2013 (b), in the northern Gulf of Mexico, in and around Deepwater Horizon Oil Spill sites.

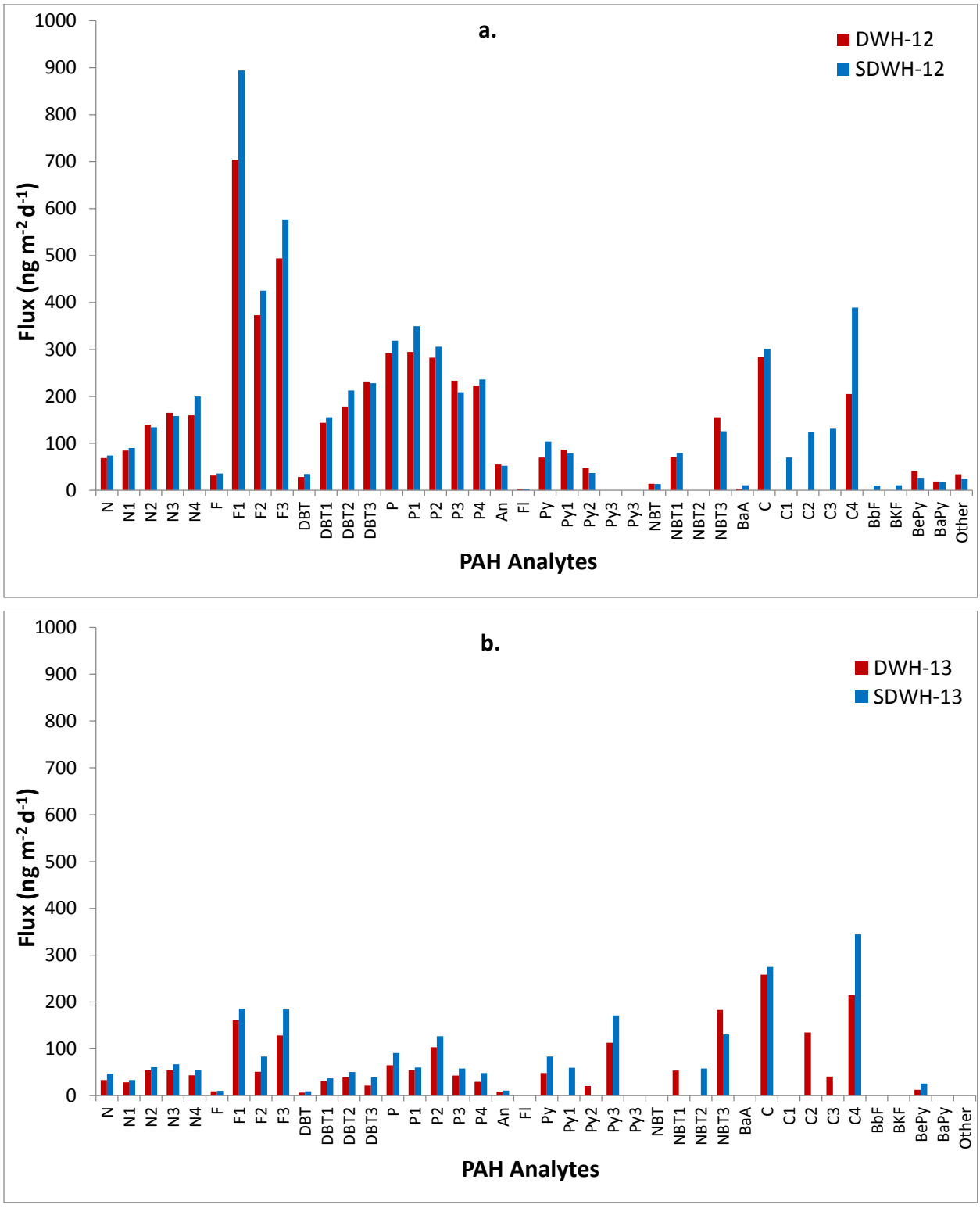

Figure A3.3. Typical molecular profiles of PAH fluxes at 150 m of water column in year 2012 (a) and 2013 (b), in the northern Gulf of Mexico, in and around Deepwater Horizon Oil Spill sites.

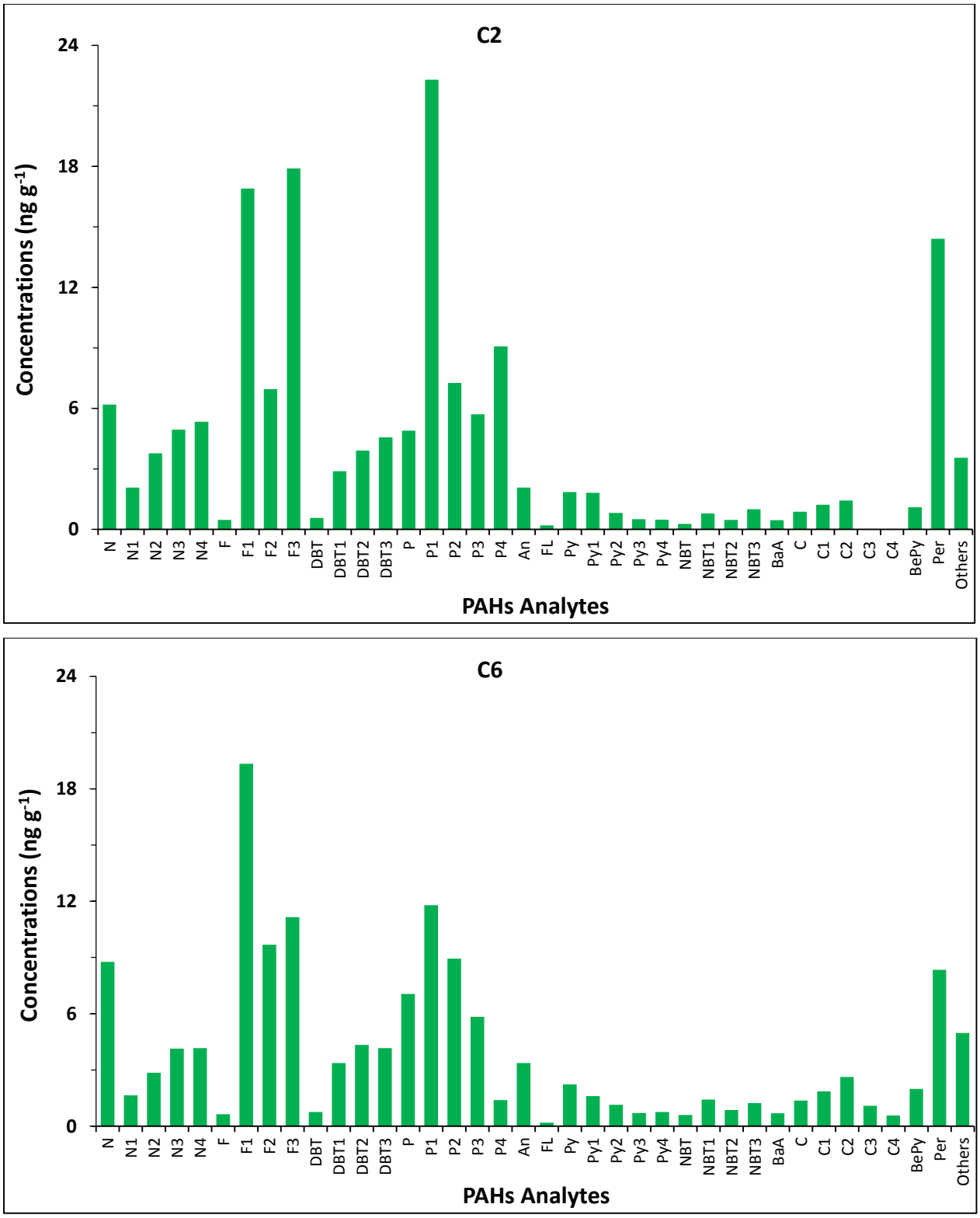

Figure A3.4. Typical molecular profiles of PAH concentrations in surficial sediments at selected coastal stations (C2 and C6) in the northern Gulf of Mexico.

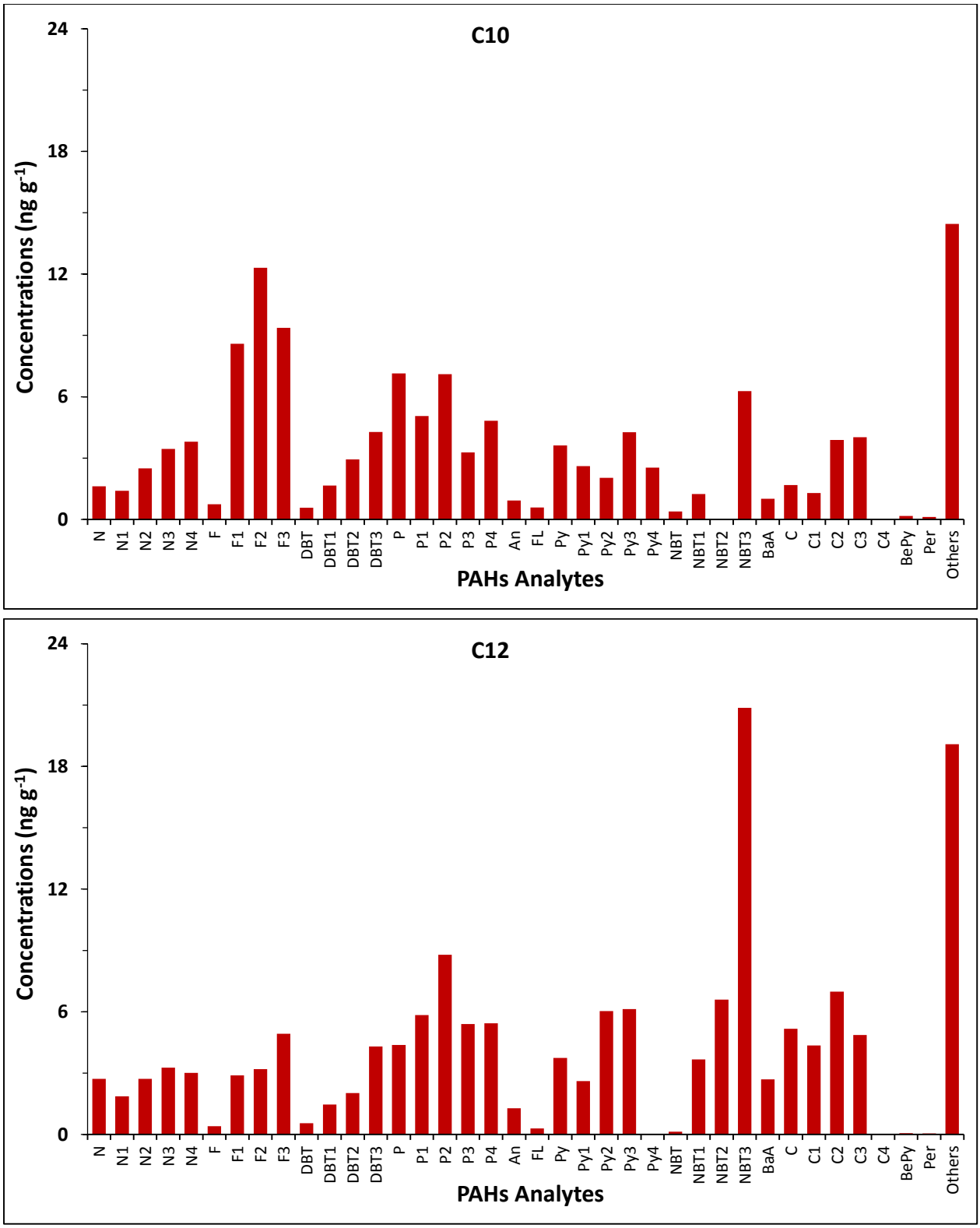

Figure A3.5. Typical molecular profiles of PAH concentrations in surficial sediments at selected deep-sea stations east of the Mississippi River Delta (C10 and C12) in the northern Gulf of Mexico.

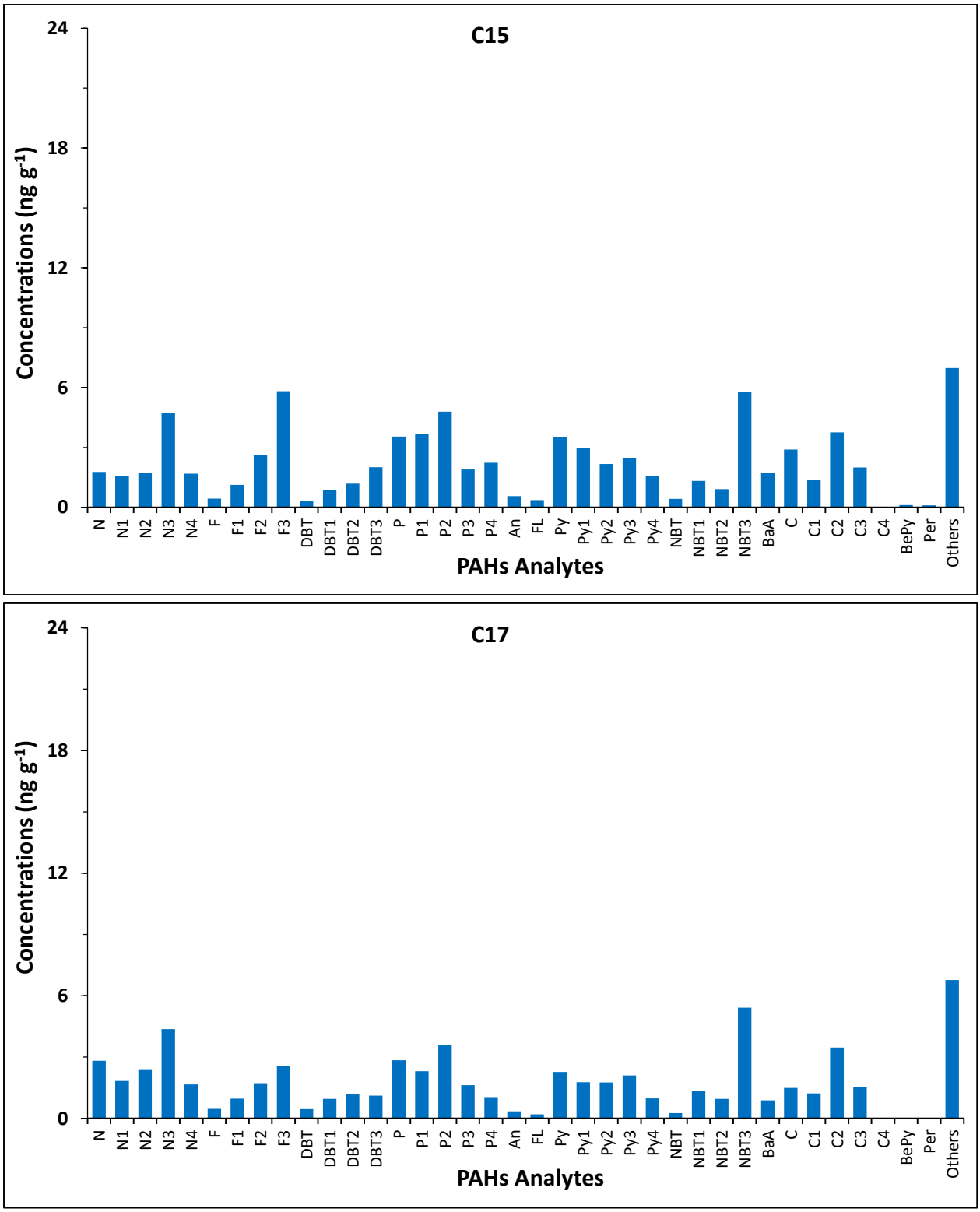

Figure A3.6. Typical molecular profiles of PAH concentrations in surficial sediments at selected deep-sea stations west of the Mississippi River Delta (C15 and C17) in the northern Gulf of Mexico.

APPENDIX 4: STATISTICAL ANALYSIS; GENERAL LINEAR MIXED MODEL

A4.1. Variability in PAHs concentrations - effects of sampling locations and depths of the sediment cores.

The weighted average concentrations of $\sum PAH_{43}$ in each core from each station were grouped into three depth intervals (0-2 cm, 2-4 cm and 4-6 cm) in order to compare any possible variation in sediment PAHs along the sampling locations (three levels; coastal, deep-sea east of Mississippi River Delta, and deep-sea west of Mississippi River Delta) and the depth of the sediment cores (three levels; 0-2 cm, 2-4 cm and 4-6 cm). A general linear mixed model, as shown in the equation below, was then utilized to test the interaction effects of depths and locations on sediment PAHs.

$$Y_{ijk} = \mu + D_i + L_j + S(L)_{k(j)} + D*L_{ij} + E_{ijk} \qquad (A4.1)$$

Where, Y_{ijk} is the response (PAHs concentrations), μ overall mean, D is the depth of the sediment cores, L is the sampling location, S is the sample ID within the sampling locations, and E is the residuals. Each sampling station (for each sample ID as shown in Figure 4.1) had three sediment core samples (for three depth intervals) therefore, the sample ID were random factors nested in the location effects in the mixed model. The Bonferroni correction was applied on the level of significance (α-values) in order to account for multiple tests (Holm, 1979). The concentrations of sediment PAHs were compared for each level of depths and locations which includes 3*3 = 9 multiple tests (m) therefore, the Bonferroni corrected level of significance (α/m= 0.05/9 = 0.005) was used to test the statistical differences. The general linear mixed model was run in SAS®9.4 (SAS Institute Inc., Cary, NC, USA) using following SAS codes. The *pdiff*

function in SAS *Proc Mixed* was used to identify the significant interaction effects on PAHs concentrations at the Bonferroni corrected level of significance ($p<0.005$) (Table A4.1).

```
Proc Mixed data = Model1;
Class Depth Location ID;
Model PAH = Depth Location Depth*Location;
Random ID(location);
Lsmeans Depth*Location/ pdiff;
Run; quit;
```

Table A4.1. The differences of least squares mean concentrations of polycyclic aromatic hydrocarbons (PAHs) in the northern Gulf of Mexico sediments. Only the significant interactions, with p-value <0.005 are selected.

Effect	Depth (cm)	Location	Depth (cm)	Location	Estimate	SE	DF	t-value	Pr > |t|
Depth*Location	0-2	Coastal	2-4	**EMR	60.9	17.6	28	3.47	0.0017
Depth*Location	0-2	Coastal	4-6	EMR	74.2	17.6	28	4.23	0.0002
Depth*Location	0-2	Coastal	4-6	**WMR	61.0	17.6	28	3.47	0.0017
Depth*Location	0-2	EMR	2-4	EMR	54.7	12.8	28	4.26	0.0002
Depth*Location	0-2	EMR	4-6	EMR	68.0	12.8	28	5.30	0.0001
Depth*Location	0-2	EMR	4-6	WMR	54.8	19.0	28	2.89	0.0043
Depth*Location	2-4	Coastal	4-6	EMR	56.5	17.6	28	3.22	0.0032
Depth*Location	4-6	Coastal	4-6	EMR	54.4	17.6	28	3.10	0.0044

*EMR and WMR represent the Deep-sea stations east of the Mississippi River Delta, and Deep-sea stations west of the Mississippi River Delta, respectively.

The least square means estimates (with standard errors) were plotted, which shows the significant interaction effects of the depths and locations on PAHs concentrations (Figure 4.4). The result shows that the change in PAHs concentrations with depths of the sediment cores was inconsistent among the sampling locations, indicating the significant interaction effects of depths and locations on PAHs concentrations (Figure 4.4).

The same statistical model explained above was also utilized for four individual PAHs analytes with higher loadings on each principal components, PC1 and PC2 (Figure 4.8), to compare their depth profiles among different sampling regimes. The results show significant interaction effects of sampling locations and sediment core depths on the concentrations of individual PAHs analytes (Figure 4.8). Similar to the tests above, the Bonferroni corrected level of significance ($\alpha/m = 0.05/9 = 0.005$) was used to test the significance of the statistical differences.

A4.2. Variation in PAHs concentrations among the sampling locations in between two sampling events; NOAA 2010 samples and samples collected in this study.

The surficial (0-2 cm) PAHs concentrations observed in this study were compared with the surficial sediment PAHs concentrations in 2010, reported by NOAA/NRDA, using the general linear model (Equation, A4.2).

$$Y_{ij} = \mu + S_i + L_j + S*L_{ij} + E_{ij} \qquad \text{(A4.2)}$$

$$ij = 1, 2, 3\ldots$$

Where, Y_{ij} is the response (PAH concentrations), μ overall mean, S is the sampling year (our vs NOAA), L is the sampling location and E is the residuals.

For this comparison the model has two main effects; samples with two levels (the sampling years; this study and NOAA) and locations with three levels (sampling locations; coastal, deep-sea east of Mississippi River Delta, and deep-sea west of Mississippi River Delta). The primary focus of this model was to test the variation of PAHs concentrations in between two sampling periods for each sampling location, therefore it has only three tests to be compared (PAHs concentrations between 2010 and this study in coastal, deep-sea east of MR and deep-sea west of MR). The Bonferroni corrected level of significance ($\alpha/m = 0.05/3 \sim 0.017$) was utilized to test the statistical differences in PAH concentrations. The following SAS codes was used to

perform the general linear model using SAS®9.4. Unlike previous model, each sampling locations for this comparison had a single sediment core samples (only the top 2 cm) therefore, the model does not have sample ID nested in the location in the mixed model.

```
Proc Mixed data = Model2;
Class Depth Samples Location;
Model PAHs = Samples Location Samples*Location;
Lsmeans Samples*Location/ pdiff;
Run; quit;
```

The result shows the significant interaction effects of the sampling years (samples) and sampling locations on PAHs concentrations (Figure 4.5). The significant interaction effect implies that the change in PAH concentrations between sampling years was inconsistent among the sampling locations (Figure 4.5 and Table A4.2).

Table A4.2. The differences of least squares mean concentrations of polycyclic aromatic hydrocarbons (PAHs) in the northern Gulf of Mexico sediments collected in 2010 (samples collected during and immediately after the Deepwater Horizon oil spill and publicly reported by NOAA) and the samples collected in this study.

Effect	Sample	Location	Sample	Location	Estimate	SE	DF	t-value	Pr> |t|
Samples*Location	NOAA	Coastal	Current	Coastal	-80.1	86.01	24	-0.93	0.361
Samples*Location	NOAA	**EMR	Current	EMR	273.2	103.7	24	2.63	0.014
Samples*Location	NOAA	**WMR	Current	WMR	38.3	112.9	24	0.34	0.737

**EMR and WMR represent the Deep-sea stations east of the Mississippi River delta, and Deep-sea stations west of the Mississippi River delta, respectively.

APPENDIX 5: PHOSPHORUS SPECIATION AND SEDIMENTARY PHOSPHORUS RELEASE FROM THE GULF OF MEXICO SEDIMENTS: IMPLICATION FOR HYPOXIA

A5.1. Introduction

Phosphorus (P) is an essential macronutrient which plays an important role in regulating biological community structure as well as biogeochemical cycling of other elements in aquatic environments (Benitez-Nelson, 2000; Filippelli, 2008). Phosphorus can limit primary production and excess loading of P to coastal waters can have detrimental effects on water quality including eutrophication, algal blooms and hypoxia (Jickells, 2005; Paytan and McLaughlin, 2007). This condition is particularly true for river-dominated coastal ocean margins like the northern Gulf of Mexico (GOM) (Brunner et al., 2006; Rabalais, et al., 2009; Bianchi et al., 2010). River discharge is a predominant source of P to the coastal waters with more than 90% of the riverine P fluxes into the oceans being carried by the suspended particulate material (Meybeck, 1982, 1993; Benitez-Nelson et al., 2000; Guo et al., 2004). A large portion of this particle-bound P is deposited within the nearshore coastal shelf environment (Gibbs, 1981; Meade, 1982; Benitz-Nelson, 2000). In addition to this loading, approximately 50% of water column primary production and associated P in coastal systems is deposited in bottom sediments (Suess, 1980; Ruttenberg and Benner, 1993). Therefore, the continental margins are key zones for deposition and regeneration of P (Lebo and Sharp, 1992; Conley et al., 1995; Zhang et al., 2004). Phosphorus in bottom sediments are efficiently buried under oxic conditions while anoxic sediment conditions enhance P regeneration or release (Ingall and Jahnke, 1994; Roy et al., 2012; Zhang et al., 2012). Organic matter decomposition and iron oxides reduction can remobilize P from sediment and the remobilized P may precipitate as carbonates or sorbed onto iron oxides (Ingall and Jahnke, 1994; Filippelli and Belaney, 1996; Paytan and McLaughlin,

2007). However, sediment resuspension in coastal areas, iron reduction due to low bottom water dissolved oxygen (DO) and reduced conditions in sediments can cause significant releases of reactive P into the overlying water column (Ingall and Jahnke, 1994; VanCappellen and Ingall, 1994). Sedimentary P exists in different forms/fractions and bioavailability varies with speciation (Benitez-Nelson, 2000; Wang et al., 2006; Paytan and McLaughlin, 2007). Phosphorus burial in sediments, ease of transformation of sedimentary P into other forms and fluxes of bioavailable-P into the overlying water column via various biogeochemical processes depends on the relative proportion of different pools of P (Ruttenberg and Berner, 1993; Delaney, 1998; Filippelli, 2008). Therefore, it is essential to quantify both the distributions of different P fractions and potential release rate of P from coastal marine sediments in order to determine the role of released sediment P on coastal ecosystems (Ruttenberg et al., 1992, 2009; Reddy et al., 1998; Anderson and Delaney, 2000).

The northern GOM along Louisiana and Texas shelf experiences one of the largest annually documented coastal hypoxia zones in the world due to eutrophication caused by excessive nutrients loading from the Mississippi and Atchafalaya Rivers, and the seasonal vertical stratification of the river water over the Gulf water (Rabalais et al., 2002a, 2002b; Scavia and Donnelly, 2007; Bianchi et al., 2010). Algal growth stimulated by high bioavailable nitrogen (N) loading, which has almost tripled since the middle of the last century, is considered to be the major driver behind hypoxia formation in the northern GOM (Goolsby et al., 2001; Rabalais et al., 2002b; Justic et al., 2003; Scavia et al., 2004). Therefore, the Action Plan for Reducing, Mitigating, and Controlling Hypoxia in the northern GOM (EPA, 2015) has been primarily focusing on N load reduction (Rabalais et al., 2002b; Justic et al., 2003; Scavia et al., 2003). External P loading via river discharge has been recognized as an additional factor for coastal

eutrophication in the northern GOM. However, sedimentary release of P can also maintain eutrophic condition even after external loads are reduced (Sylvan et al., 2006; Scavia and Donnelly, 2007).

The seasonal hypoxic region of the northern GOM, with high N loading from the Mississippi and Atchafalaya Rivers, is an ideal location to examine sedimentary P-fractionation, P-release rates under anoxic conditions and potential impacts to ecosystem function. Despite the potential role of internal P loadings in the GOM hypoxia formation, no previous studies have quantified sedimentary P-fractions coupled to rates of P-release from the GOM shelf, slope and deep-sea sediments. Therefore, the objectives of this study are to: 1) chemically separate different forms of P in the northern GOM sediments using a sequential extraction method and 2) determine the rate of potential sedimentary P release under anoxic conditions.

A5.2. Materials and methods

A5.2.1. Sample collection

Surface sediment were collected from 7 sampling locations from the *R/V Endeavor* in July-August, 2011 in the northern GOM along a shelf transect spanning the Mississippi birdfoot delta to the Atchafalaya River to include the coastal area annually affected by hypoxia (Figure A5.1). The stations west of the mouth of Mississippi River, in the direction of river plume, were labeled in numerical order by increasing distance from the river mouth (S1-S6) while station S7 on (eastern) leeward side of the river plume was assigned a negative distance. NOAA (2011) bottom water dissolved oxygen (DO) data revealed that the coastal stations west of the Mississippi River (S1, S2, S3, and S5) were primarily affected by a low DO regime at the time of sampling (Fig. 1). Sediment cores were collected using a multi-corer with eight collection tubes; collected cores were of 10 cm diameter and 40 cm long. Immediately after the recovery of the

multi-corer, top 5 cm of each core was sectioned at 1 cm intervals and the sediment slices were stored at 4 ºC until analysis.

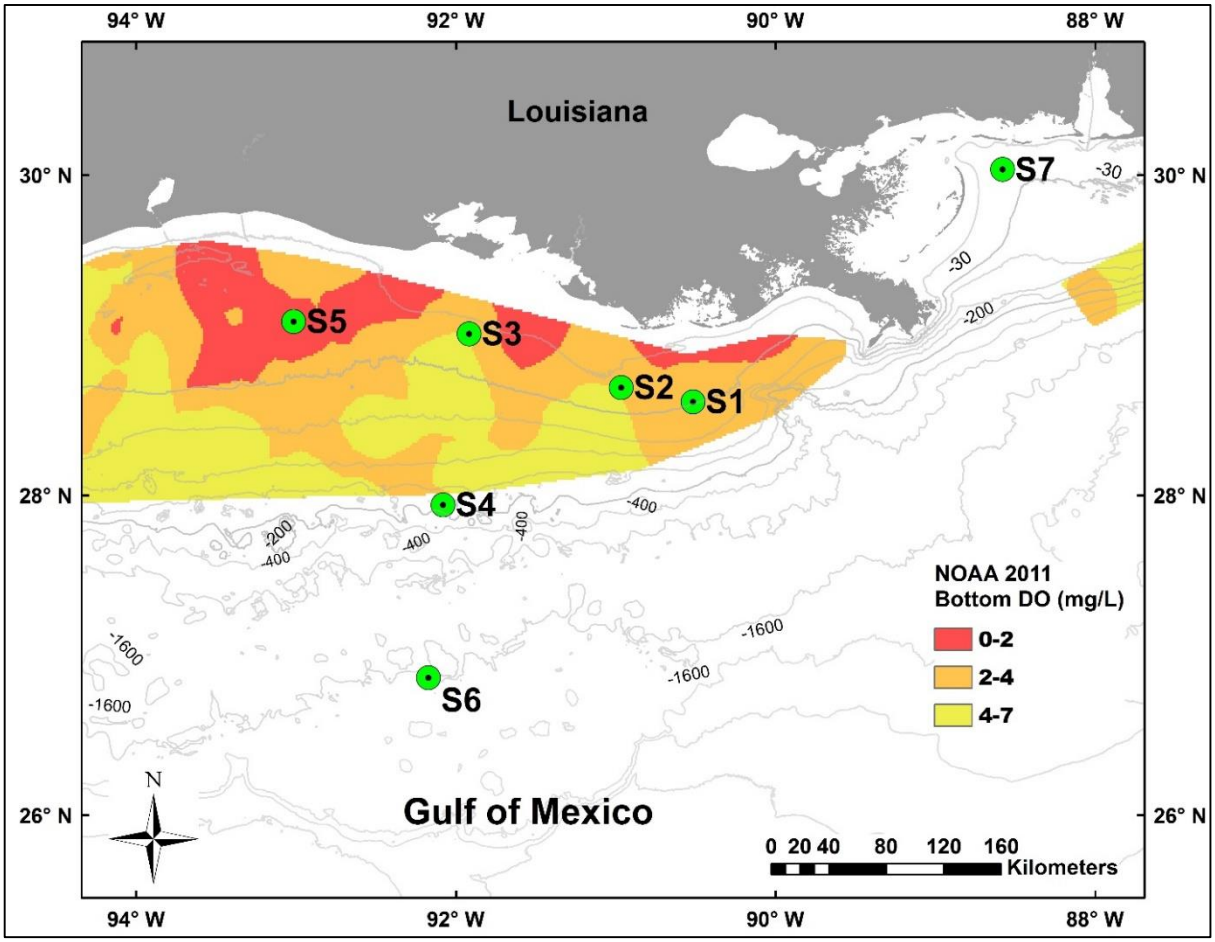

Figure A5.1. Sampling locations in the northern Gulf of Mexico. The stations west of the mouth of Mississippi River (MR), in the direction of the river plume (S1-S6), are labelled with increasing distance from the River mouth while the station S7 is on the leeward side of the river plume. The shaded areas were plotted for dissolved oxygen (DO) concentrations (mg/L) reported by NOAA, during June 25-July 17, 2011.

A5.2.2. Phosphorus fractionation

Sequential phosphorus extractions have been developed and utilized by a number of investigators to chemically separate different pools of P in soil and sediments (Ruttenberg, 1992, 2009; Reddy et al., 1998; Anderson and Delaney, 2000; Sutula et al., 2004; White et al., 2004; Zang et al., 2004, 2010). The fractionation scheme utilized in this study, (Figure A5.2) after

Reddy et al. (1998) and White et al. (2004), operationally separates five different pools of P in sediments; 1) readily available-P [*KCl Extraction*], 2) Fe/Al bound-P [*NaOH Extraction*], 3) alkali extractable organic-P (= *NaOH-TP – NaOH-Pi),* 4) Ca/Mg bound-P [*HCl-Extraction*], and 5) residual-P [*Residual-TP digestion*]. About 1-2 g field moist sediment samples (equivalent to ~0.5 g dry weight) underwent extraction for P-fractionation. For each station, five sediment samples (the top 5 cm of each sediment core, sliced at 1 cm intervals) underwent P-fractionation to discern any differences with depth on different P pools. After each extraction step, the supernatants were immediately filtered through 0.45 µm membrane filters and the filtrates analyzed for DIP (USEPA, Method 365.1, 1993) while the residual sediment was passed to the next extraction step. The centrifuge tubes used for extraction were weighed after each extraction step to correct for extracted P still present in the sample.

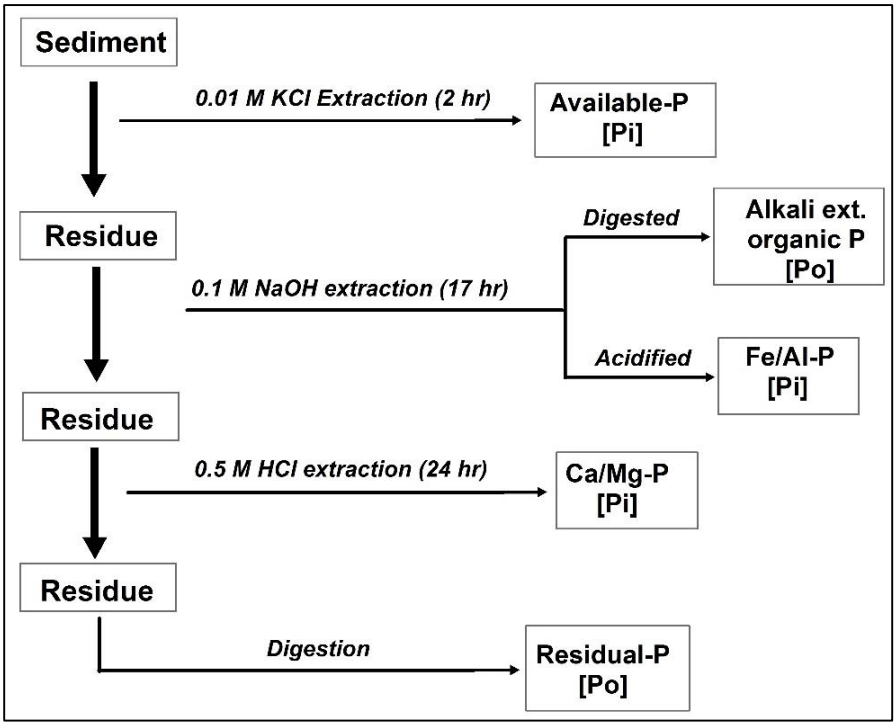

Figure A5.2. Procedure for sequentially extraction of phosphorus forms from northern Gulf of Mexico sediments.

The NaOH extraction removes both Fe/Al-P and P associated with humic and fulvic acids (Reddy et al., 1998). Therefore, after a subsample of the filtrate was first analyzed for DIP to get Fe/Al-P, a subsample was digested and analyzed for TP (NaOH -TP), in order to get an estimation of alkali ext. organic-P. For the NaOH-TP digestion, 5 ml of the aliquot, 1 ml of 11 M H_2SO_4, and ~0.35 g of $K_2S_2O_8$ were added to a digestion tube and heated for 4 h at 150 °C to remove water from the sample. The temperature was then increased to 380 °C, for 4 h for complete digestion. After the completion of digestion, samples were allowed to cool, diluted with 10 ml deionized water, filtered through 0.45 µm membrane filters and then analyzed for DIP (USEPA, Method 365.1, 1993). Subtracting Fe/Al-P (NaOH-Pi) from NaOH-TP gives us an estimation of alkali ext. organic-P. The operationally defined NaOH extraction step used to extract iron-bound P in this study potentially underestimates the Fe/Al-P as the Fe extracted in this step can re-precipitate and potentially remove phosphate from the solution (DeGroot and Golterman, 1990; Golterman, 1996). Therefore, the concentrations of Fe/Al-P extracted using this technique should be considered as a lower limit.

Total P of the entire sediment sample was determined using two different approaches, one direct and one indirect. Firstly, ~0.3 g dry weight equivalent of the original sediment samples was analyzed for TP using the ashing-digestion method (USEPA, Method 365.1, 1993) as a direct measure of TP. Our indirect accounting of TP was achieved by summing all five P-fractions to get the sum-TP of the sediment;

Sum-TP = [Available-P + Fe/Al-P + Alkali extr. organic-P + Ca/Mg-P + Residual-P]

The difference between the direct and indirect TP determination provides an estimation of the extraction efficiency of the fractionation scheme.

A5.2.3. Total organic carbon (TOC) analysis

For solid phase total organic carbon (TOC) analysis, dried and ground sediment samples in silver capsules were placed in a desiccator with fumes of concentrated hydrochloric acid for 36 h to remove inorganic carbon (Hedges and Stern, 1984; Harris et al., 2001). The samples were then dried at 50 °C and analyzed for TOC using an Elemental Analyzer (PerkinElmer, 2400 Series II CHNS/O Analyzer).

A5.2.4. Anaerobic sediment incubation

Sediment samples were incubated under anaerobic conditions for a month in order to determine potential sedimentary P-release rates for the northern GOM bottom sediments. Since the P fractions within the top 5 cm did not vary significantly with depth, sediment samples from top 5 cm were mixed together and treated as a single sample for the incubation study. Approximately, 5-10 gm sediments were placed in glass serum bottles, weighed and the bottles were filled with 90 ml of deoxygenated, artificial seawater. The artificial seawater (salinity: 35 psu) was prepared using instant ocean and then purged with 99.99 % O_2-free N_2 gas. The glass serum bottles were then capped and sealed with a rubber septa and aluminum crimps. The headspace was evacuated to -75 kPcal using a vacuum pump and filled with 99.99 % O_2-free N_2 gas. Sediment samples were then incubated in an incubation shaker (Jeio Tech Lab Companion Is-971R refrigerated and incubation shaker, Jeio Tech, Co, Ltd, Seoul, South Korea) at 30 °C with continuous orbital shaking. The sample bottles were taken out of the incubator at designated time intervals (2, 5, 8, 13, 19, 26, and 30 days) and left undisturbed for about 1 h to allow sediments in suspension to settle to the bottom. Five ml of the aqueous phase were sampled using a syringe, filtered through 0.45 µm membrane syringe filters and then analyzed for DIP. In order to maintain a constant water volume, 5 ml of O_2-free filtered seawater, was added back to

each serum bottle after sampling. Sampling events were repeated seven times during the 30 d incubation period. Concentrations of P at each sampling event were corrected for the change in P values due to the removal and addition of aqueous samples. The P-release from the sediment was determined by quantifying the changes in DIP over time (Fisher and Reddy, 2001; Roy et al., 2012; Zhang et al., 2012).

A5.3. Results and discussion

A5.3.1. Phosphorus fractionation

There was no significant difference in distribution of P fractions with depth in the top 5 cm, therefore results of the P fractionation for top 5 cm of each core are presented as average concentrations (Figure A5.3). The mean total P (TP) in the sediment samples from the northern GOM transect varied between 474 ± 41 and 1035 ± 631 mg kg^{-1} (Figure A5.3a). The station closest to the mouth of the Mississippi River (S1) had the highest TP however; there was no consistent pattern of decreasing TP concentrations with an increase in distance from the mouth of the river (Figure A5.3a). The TP presented in this study is the P directly determined by the ashing-digestion method. Comparison of TP to sum-TP showed a reasonable agreement as the sum-TP values ranged from 77-130% (mean; 99 ± 13%) of the original TP.

The TP values observed in this study are similar to those of Huanxin et al. (1994) who reported TP concentrations varying from 56 to 1422 mg kg^{-1} from estuarine sediments along the GOM coastline (Texas to Florida). Huanxin et al. (1994) found that the sediment TP along the Louisiana coast was higher than other coastal GOM estuaries, except for the phosphate deposit regions of the Florida coasts. The observed concentrations of TP in this study are also within the range of TP values reported by others; Ruttenberg and Goni (1997); 565-1043 mg kg^{-1} in GOM sediments from areas proximal to our sampling stations, Sutula et al. (2004); 434-1549 mg kg^{-1}

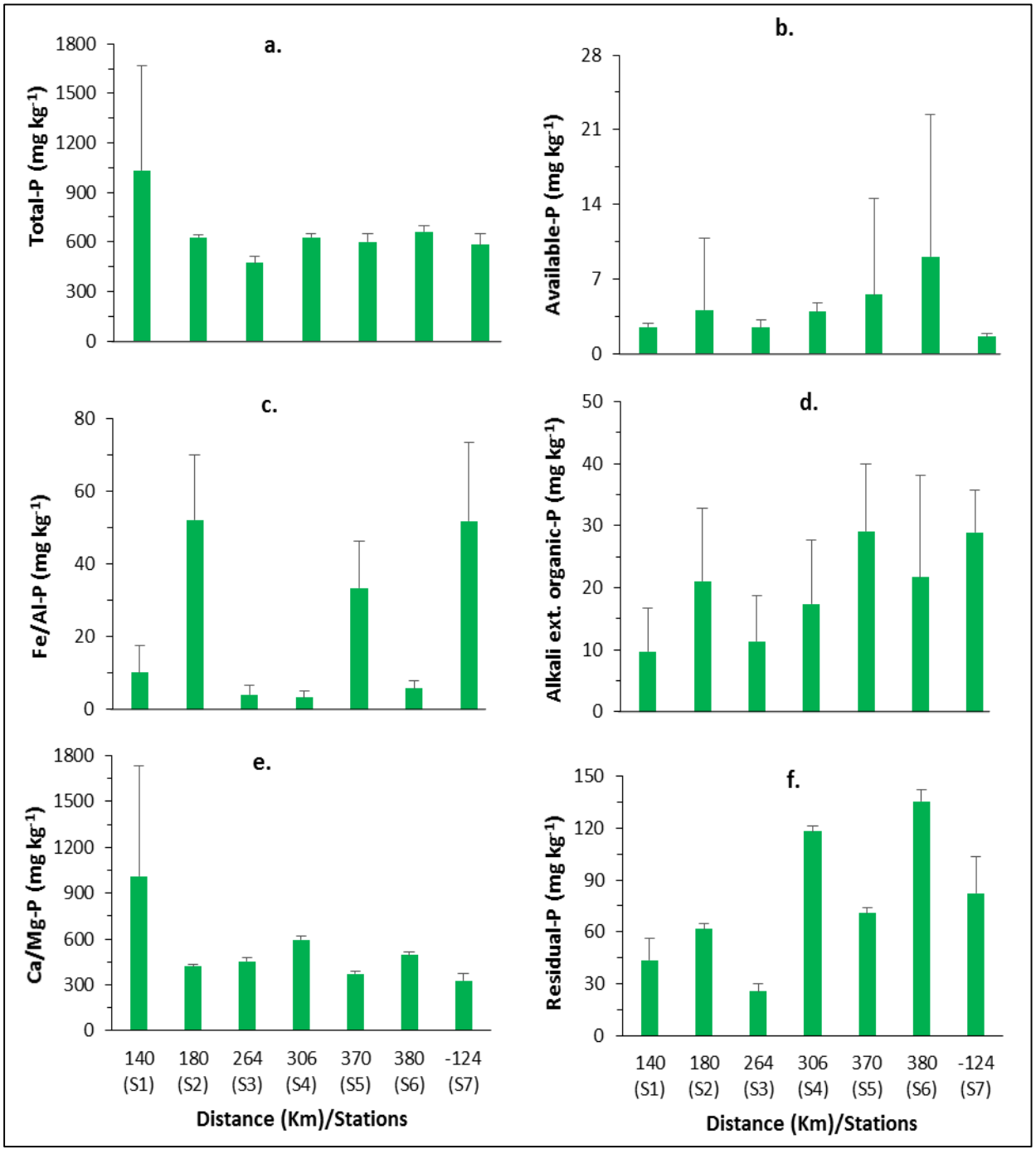

Figure A5.3. Concentrations of different fractions of phosphorus in the northern Gulf of Mexico sediments plotted against distance from the mouth of the Mississippi River along the river plume to the corresponding stations. Station S7 has negative distance because of its location at the leeward side of the normal river plume.

in the lower Mississippi River bed sediments and the coastal GOM sediments near the mouth of the Mississippi River, and Ruttenberg and Berner (1993); 546-605 mg kg^{-1} in the birdfoot delta.

The concentrations of available-P, Fe/Al-P, alkali ext. organic-P, Ca/Mg-P, and residual-P varied between 1.6 ± 0.3 to 9.1 ± 13.3 mg kg^{-1}, 3.3 ± 2.0 to 52.2 ± 18.0 mg kg^{-1}, 9.7 ± 6.9 to 29.1 ± 16.5 mg kg^{-1}, 329 ± 43 to 1010 ± 720 mg kg^{-1}, and 26.0 ± 4.3 to 135 ± 7 mg kg^{-1}, respectively (Figure A5.3b-3f). Stations S2, S5 and S7 had significantly higher Fe/Al-P ($P < 0.05$) than the other stations (Figure A5.3c). Phosphorous fractions were variable and did not show a consistent pattern with distance from the mouth of the Mississippi River. The Ca/Mg-P was highest at station S1 and similar in concentration at other stations, consistent with TP (Figure A5.3a and 3e). The correlation analysis suggests that the available-P was positively correlated to alkali extr. organic-P ($P=0.04$) and total-P was positively correlated to Ca/Mg-P ($P=<0.001$) (Table A5.1). Similarly, Fe/Al-P and alkali extr. organic-P were positively correlated with sediment TOC, P-values <0.001 and 0.01, respectively (Table A5.1). Potentially reactive-P pools (available-P, Fe/Al-P, alkali ext. organic-P and Ca/Mg-P), that can be solubilized over shorter timescales, accounted for 87.4 ± 5.6% of the TP in the GOM sediments (Paytan and McLaughlin, 2007). While the resistant refractory pool of P (residual-P) comprised of 12.6 ± 5.6% of the TP (Reddy et al., 1998; Paytan and McLaughlin, 2007).

The proportion of Ca/Mg-P was highest of all the P fractions (67-92% of TP) followed by residual-P (5-21% of TP) (Figure A5.4). To the best of our knowledge, this is the first study to utilize sequential extractions to quantify different pools of P in the northern GOM shelf, slope and deep-sea sediments. Therefore, there are no data from this region to directly compare with our results. However, our results are consistent with the dominant distribution of Ca/Mg-P in the

Table A5.1. Pearson product-moment correlation coefficients for different species of P and TOC in the Gulf of Mexico sediments. The P-values for significant correlation coefficient ($P < 0.05$) are presented in parentheses.

	Available-P	Fe/Al-P	Alkali ext. organic-P	Ca/Mg-P	Residual-P	Total-P
Available-P	-					
Fe/Al-P	0.15	-				
Alkali ext. organic-P	0.37(0.04)	0.18	-			
Ca/Mg-P	-0.10	-0.29	-0.32	-		
Residual-P	0.31	-0.20	0.27	-0.03	-	
Total-P	-0.02	-0.25	-0.17	0.99(<0.001)	0.08	-
TOC	0.17	0.68(<0.001)	0.48(0.01)	-0.06	0.30	0.04

Mississippi River sediments deposited in the Lake Pontchartrain estuary (Nguyen, 2014), coastal GOM estuaries (Huanxin et al., 1994), other GOM shelf sediments (Sutula et al., 2004), and sediments from Florida Bay (Zhang et al., 2004). In contrast, the distributions of P fractions observed in this study are different from Mississippi River bed sediments which were dominated by Fe/Al-P (47%) (Sutula et al., 2004). Areas with high terrigenous and organic matter deposition, such as coastal regions and continental margins, generally have higher rates of apatite minerals formation which could explain the abundance of Ca/Mg-P found in our study (Froelich et al., 1982; Ruttenberg and Berner, 1993). In addition, the diatom-derived polyphosphates can play a key role in apatite formation in the marine sediments (Diaz et al., 2008). Therefore, co-precipitation of DIP and Ca/Mg minerals due to early diagenesis, or polyphosphates formation, could be the mechanisms responsible for the higher distribution of Ca/Mg-P in the GOM sediments (Froelich et al., 1982; Ruttenberg and Berner, 1993; Diaz et al., 2008). A high

percentage of residual-P may be related to terrestrial-derived river inputs or higher benthic and water column productivity (Zhang et al., 2004).

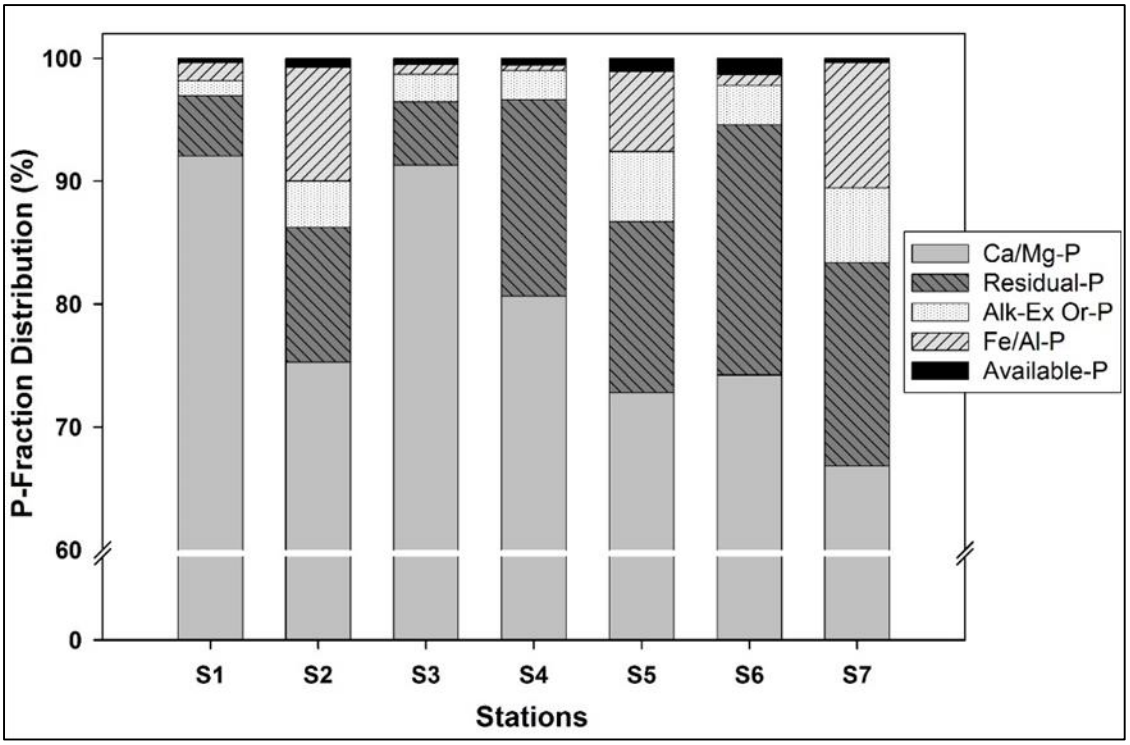

Figure A5.4: Distribution of different phosphorus fractions in the northern Gulf of Mexico sediments.

The Fe/Al-P and alkali ext. organic-P comprised 0.5-10% and 1.2-6.0% of TP, respectively (Figure A5.4). The stations along the Atchafalaya River transect (S3, S4 and S6) and closest to the Mississippi River (S1) had lowest abundance of Fe/Al-P. Available-P represented the smallest (0.3-1.3%) fraction of TP (Figure A5.4). The percentage of available-P observed in this study is lower than the values reported by: Sutula et al. (2004) in the lower Mississippi River and GOM shelf sediments (7-13%); Zhang et al. (2004) in Florida Bay (8.2 ± 2.2%); and Reddy et al. (1998) in Florida Everglades (1-4%). However, available-P is higher in this study than in Lake Pontchartrain estuarine sediments, 0.16-0.29% (Nguyen, 2014). Available-P can be readily

released in to the water column via desorption processes. Therefore, this loosely adsorbed P is an important pool of sedimentary P that can respond to the P concentrations in overlying water column, primarily during sediment resuspension, and plays an important role in primary production (Reddy et al., 1998; Zhang et al., 2004).

Sutula et al. (2004) demonstrated that as the Mississippi River sediments travel further and are deposited on the GOM shelf-floor, the relative proportion of Ca/Mg-P (16% in river sediment and 39% in shelf sediment) and residual-P (10% in river sediment and 19% in shelf sediment) increases, while available-P (13% in river sediment and 4% in shelf sediment) and Fe/Al-P decreases (38% in river sediment and 19% in shelf sediment). All our stations had lower Fe/Al-P than river sediments which suggests that the river-derived shelf sediments likely lose Fe-bound P due to anoxic conditions brought on by burial and hypoxia. In contrast, the proportions of Ca/Mg-P and available-P in our study showed an opposite trends (lower Ca/Mg-P and higher available-P at the furthest stations). The stations located furthest from the mouth of the Mississippi River are under direct influence of the discharge of the Atchafalaya River which contains a flood plain of hydrologically connected marshes with high organic matter soils and may also influence sediments in this area (Scott et al., 2014).

A5.3.2. Sedimentary P-release during anaerobic incubation

The P-release rate during the 30 d incubation period varied between 0.02 to 4.4 mg kg^{-1} d^{-1} (Figure A5.5a and 5b). The rates were significantly higher in stations S2, S5, and S7 (0.6-4.4 mg kg^{-1} d^{-1}) than at other stations (0.02-0.32 mg kg^{-1} d^{-1}) (Figure A5.5a and 5b). The initial concentration of DIP in the overlying water column was 0.006 ± 0.005 mg L^{-1} which increased to 0.77 ± 0.87 mg L^{-1} (range 0.06 to 2.27 mg L^{-1}) by the end of the incubation. This result indicates that a significant amount of DIP can be released from the sediments into the overlying water

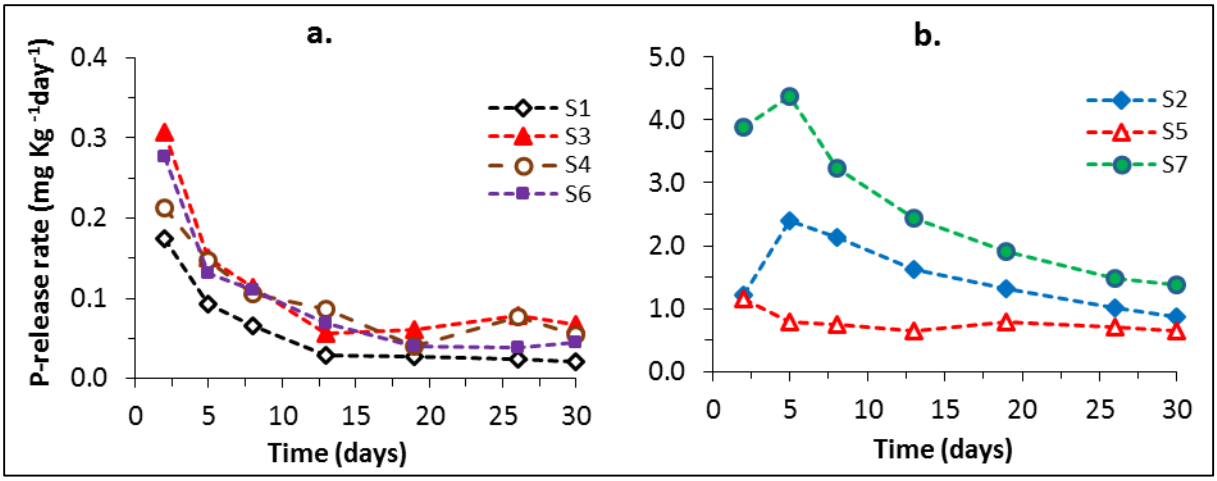

Figure A5.5. Phosphorus-release rates from the northern Gulf of Mexico sediments plotted against incubation time (a) for stations S1, S3, S4 and S6, (b) for stations S2, S5 and S7.

column under anaerobic conditions and is consistent with previous anaerobic sediment incubation studies on Mississippi River-derived sediments in estuaries (Roy et al., 2012; Zhang et al., 2012). A month of anaerobic incubation released ~0.1 to 6.9% of the TP in the sediments (Figure A5.6a). The sediment from stations S2, S5, and S7 released higher percentages of TP than the sediments from other stations (Figure A5.6a). These are the stations with high Fe/Al-P (Figure A5.3c) and TOC (17918 to 21279 mg kg^{-1}). This result implies that the Fe/Al-P and organic content of the coastal sediments can play a dominant role in P-release from these sediments.

The P-release rates were significantly positively correlated with Fe/Al-P (Figure A5.6b) which suggests that the anoxic sediment conditions primarily releases P bound in Fe/Al-P fraction associated with Fe in the GOM sediment. Zhang et al. (2012) also found that P-releases were correlated with Fe due to the release of Fe-bound P by the reduction of Fe^{3+} to Fe^{2+}, a consequence of the lower redox conditions in the bottom sediments. The P-release rates were significantly (P=0.01) positively correlated with the TOC content in the sediments (R=0.86),

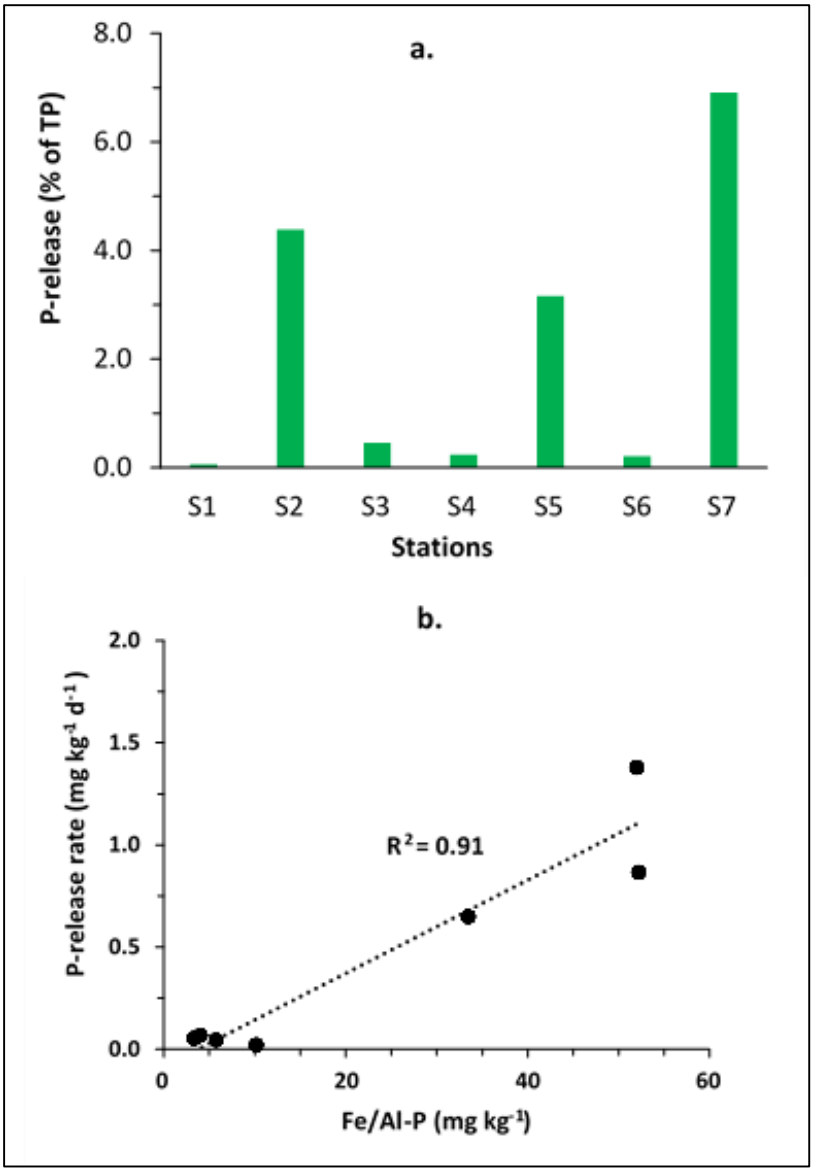

Figure A5.6. Total amount of phosphorus released (% of TP) from the northern Gulf of Mexico sediments after 30 days of incubation, and (b) Phosphorus-release rates after 30 days of anaerobic incubation plotted against Fe/Al-P.

indicating P-release from anaerobic decomposition of OM or solubilization of Fe-coated organic P (Canfield et al., 1993; Kristenesen et al., 1995; Zhang et al., 2012). In general, the rate of the sedimentary P-release decreased with incubation time however, for two stations (S2 and S5) P-release rates increased up to 5 d of incubation followed by a gradual decrease in release rates similar to other stations. Phosphorus is generally released relatively quickly upon the onset of

anaerobic conditions (Malecki et al., 2004; Zhang et al., 2012), however amorphous Fe-bound P solubilizes more rapidly than the crystalline Fe-bound P (Lia and Lam, 2008; Lindstrom and White, 2011). The potential presence of more crystalline forms of Fe in the sediments could be the reason of delayed peak in P-release rates for stations S2 and S7, though we did not quantify amorphous and crystalline forms of Fe in this study.

The hypoxia formation in the northern GOM can remobilize Fe from the bottom sediments (Jones et al., 2015). Therefore, hypoxic conditions can cause *in situ* releases of Fe/Al-P into the water column, decreasing the concentrations of Fe/Al-P in the sediment, over time, resulting a lower percentage of Fe/Al-P in the sediment in areas prone to low bottom water DO. This preferential release of the Fe/Al-bound P pool may explain the significant difference in P fractions between the Mississippi River bedload sediments, which is high in Fe/Al-P and the shelf sediments sampled in this study, much lower in Fe/Al-P. During the sampling cruise, water column DIP concentrations at the sampling locations increased with water depth under hypoxia condition (Figure A5.7). This pattern suggests a bottom source of P to the overlying water column and supports the assertion that a significant amount of DIP can be potentially released during low oxygen water column events.

A5.3.3. Implications to the Gulf of Mexico Hypoxia

The results from this study may have important implications on the assessment and control of the coastal eutrophication, and particularly on the Action Plan for Reducing, Mitigating, and Controlling Hypoxia in the northern Gulf of Mexico, implemented by the Mississippi River/Gulf of Mexico Watershed Nutrient Task Force. The Action Plan primarily focuses on reducing external N loading, mainly the Mississippi River inputs, into the northern GOM waters. This strategy aims to reduce the area of the GOM 'Dead Zone' to an average of

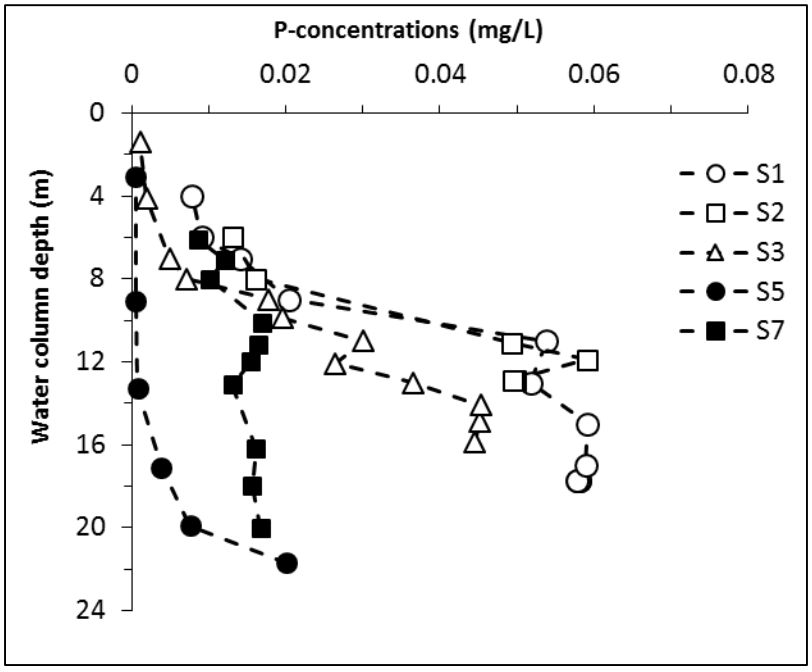

Figure A5.7. Vertical profiles of water column dissolved inorganic P (DIP) concentrations measured during the sediment sampling cruise in the Gulf of Mexico.

5000 km^2 or less by summer 2015, thereby providing a better quality ecosystem for the benthic organisms present in the sediments (EPA, 2015). The size of the 'Dead Zone' in 2014 was measured to be 13,080 km^2 (LUMCON, 2014). This measure indicates that we are still far away from achieving the goal of the Action Plan by summer 2015. The Action Plan and a number of hypoxia related studies have been primarily focusing on reducing external N load into the Gulf waters (Rabalais et al., 2002a, 2002b; Justic et al., 2003; Scavia et al., 2003), with few studies on external P load (Sylvan et al., 2006; Scavia and Donnelly, 2007; Turner et al., 2008). However, none of these studies focused on the internal P load released from the sediment in the northern GOM.

The elemental ratios of dissolved inorganic N to dissolved inorganic P (DIN:DIP) in the Mississippi and Atchafalaya river waters during spring and early summer can be as high as 50 (EPA, 2004; Mize and Demcheck, 2009; Roy et al, 2013). This ratio is significantly higher than

the Redfield ratio (Redfield, 1958). Therefore, the available-P in the inflowing river water can be rapidly assimilated in phytoplankton (Bargu et al., 2011), quickly leading to P-limitation in the river-dominated coastal GOM (Figure A5.8). Similar results have been reported for the Mississippi River water and sediments in an estuarine lake (Mize and Demcheck, 2009; Roy et al., 2013). The rapid phytoplankton blooms are followed by organic matter deposition in bottom sediments. Biological activities in deposited sediments either directly releases P into the overlying water column or creates anoxic conditions favorable for Fe reduction. Sedimentary P is preferentially remobilized relative to N under anoxic conditions (Ingall et al., 2005), primarily releasing Fe/Al-P from the sediments (Figure A5.6b). Our results illustrate that a significant amount of P can be released via anaerobic sediment conditions which can play an important role in controlling the concentrations of bioavailable-P in the northern GOM water column. Enhanced release of available-P into the N-rich overlying water column can provide substantial additional P for biological production that could extend the peak of primary productivity in the P-limited Gulf waters (Figure A5.8), thereby further increasing favorable conditions for the onset of hypoxia (Colman and Holland, 2000; Sylvan et al., 2006; Paytan and McLaughlin, 2007; Roy et al., 2012). This finding is consistent with findings from previous studies conducted in other coastal areas (Benitez-Nelson, 2000; Malecki et al., 2004; Paytan and McLaughlin, 2007; Roy et al., 2012; Zang et al., 2012).

Given that we have established a linear regression equation for Fe/Al-P vs P-release rates (Figure A5.6b), such a relationship can be used to estimate the amount of P-release during hypoxia in the GOM, if we have a more detailed map of the Fe/Al-P concentrations in the sediments. Although, Fe/Al-P is the primary source of released sediment P to the overlying water

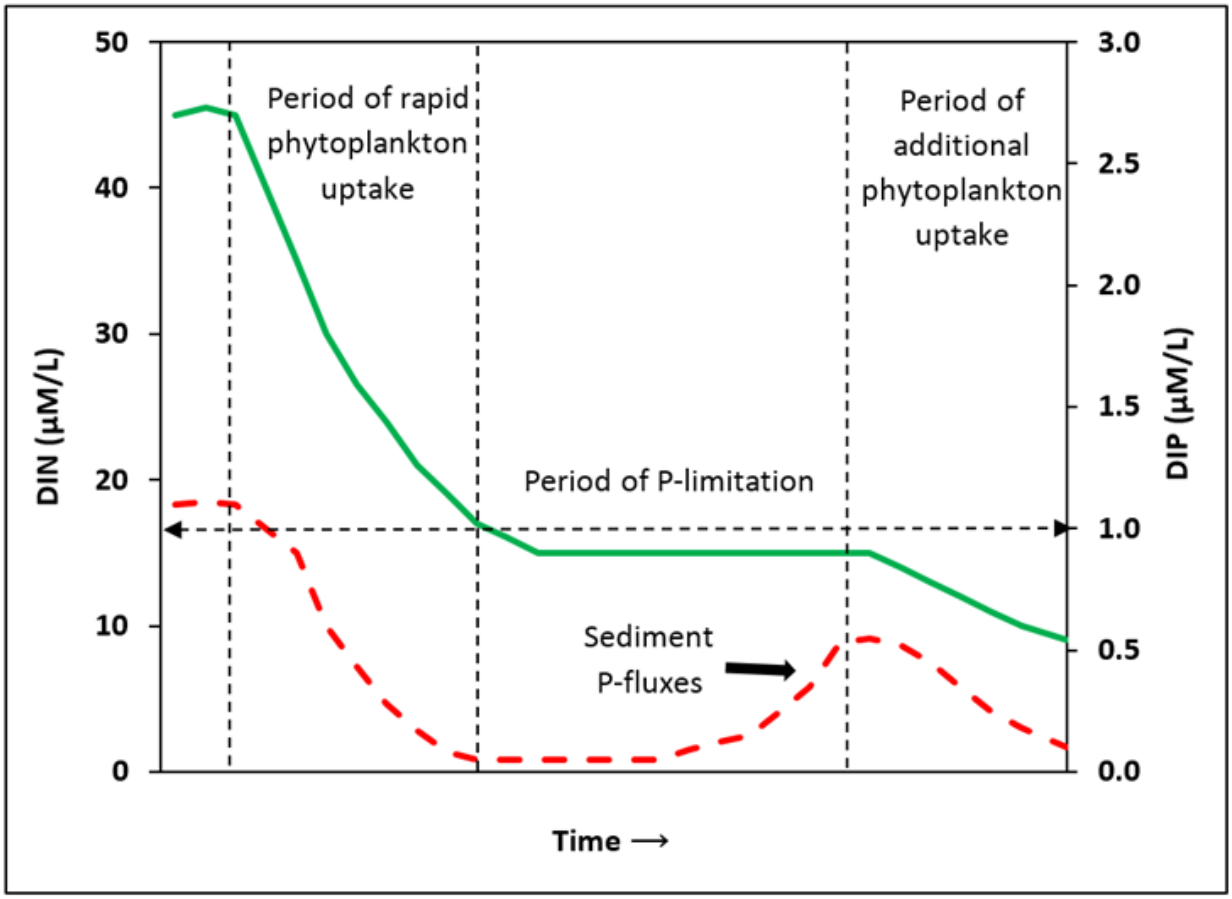

Figure A5.8. A conceptual model showing how the available-P (dissolved inorganic P; DIP) and dissolved inorganic nitrogen (DIN) in inflowing waters from the Mississippi and Atchafalaya Rivers can be quickly utilized by the phytoplankton creating highly P-limited ecosystem, and the sedimentary P-fluxes to sustain the primary productivity in the river-dominated coastal Gulf of Mexico. The solid and dotted lines represent water column concentrations of DIN and DIP, respectively.

column under anoxic conditions (Figure A5.6b), it represents only ~4% of TP (Figure A5.4), implying a relatively small fraction of sedimentary P pool is being remobilized. However,sedimentary P-release is not a simple mechanisms as several other factors such as dissolution of Ca/Mg-P, organic matter decomposition under both aerobic and anaerobic conditions, and release of bacterial P can modify the P regeneration process (Ku et al., 1999; Hupfer and Lewandowski, 2008). Therefore, more extensive laboratory and *in situ* P incubation

and P fractionation studies, including other parameters that can potentially effect P remobilization, need be conducted in this region to develop and validate such relationship

The continual sedimentary fluxes of bioavailable-P can stimulate and extend eutrophic conditions in the N-rich and P-limited Gulf waters, even after external P loads are reduced (Colman and Holland, 2000; Malecki et al., 2004; Lia and Lam, 2008). It has been well established in lakes and estuaries therefore consequently needs to be accounted for in any management plans to reduce coastal eutrophication (Lia and Lam, 2008; Reddy et al., 2011; Roy et al., 2012). This can lead to further enhanced biological production, potentially increasing the size or intensity of the hypoxic "Dead Zone" in the northern GOM. Therefore, the internal sediment P load can limit the effectiveness of upstream watershed efforts aimed at reducing the external nutrient loading in order to mitigate coastal eutrophication and associated GOM hypoxia. Consequently, the presence of such large internal loads of bioavailable-P should be accounted for in any watershed nutrient management plans aimed at reducing the areal extent of the GOM hypoxia zone.

A5.4. Conclusion

The total sedimentary P in northern GOM sediments were separated into five operationally-defined pools. The largest proportion (79.0 ± 9.4%) of the P pool was associated with Ca and Mg (Ca/Mg-P), while the readily available P was the least abundant form of P, accounting for 0.7 ± 1.0% of TP. The residual-P, Fe/Al-P and alkali ext. organic-P contributed 12.6 ± 5.6%, 4.2 ± 4.4% and 3.5 ± 2.4%, respectively. Total P and the P-fractions were variable among the sampling stations and did not show a consistent pattern along the coast by the distance from the mouth of the Mississippi River. Sediment incubations demonstrated the potential anaerobic release of sediment P load can be a significant source of bioavailable-P to the

overlying water column in the northern GOM and was supported by field water column data, releasing 0.02 to 4.4 (mean 0.76 ± 1.0) mg $kg^{-1}d^{-1}$ of DIP. Such a significant amount of internal loading of available P from the anoxic sediments can supply additional P into the P-limited Gulf waters (Sylvan et al., 2006; Laurent et al., 2012) and help to trigger or extend primary production peaks creating a positive feedback to the maintenance of the GOM hypoxic zone. Therefore, any plan to mitigate coastal eutrophication in order to reduce the area of the northern GOM hypoxia requires taking into account the internal loadings of bioavailable-P from the coastal sediments. The P-release rates were positively correlated with Fe/Al-P, and TOC, indicating the Fe reduction and organic matter under anaerobic condition to be the major sources of released available P. The Fe/Al-P comprised only a relatively small fraction (4.2 ± 4.0%) of TP implying that only a small pool of the sedimentary P is being remobilized. However, it is likely that much of the P pool had been previously mobilized prior to sample collection during previous periods of hypoxia. This idea is supported by a comparison on Fe/Al-P pool of P (~4% of TP in this study) in coastal sediments with the Fe/Al-P pool of P (~47%) in the Mississippi River bed sediments which is the source of the coastal shelf sediments (Sutula et al., 2004).

A5.5. Acknowledgement

This research was made possible by a research grants from the Louisiana Board of Regents (Grant # LEQSF (2011–13-RD-A-10 to K.M.) which provided funding for sample collection and the Bureau of Ocean Energy Management (Grant# M14AC00030 to KM and JRW) which provided student support and analysis. We would like to thank the captain and crew of the *R/V Endeavor*. Special thanks to Dr. Jim McManus and Jesse Muratli at Oregon State University for their help with sediment core collection and water column nutrient analysis. We

would also like to thank the associate editor and two anonymous reviewers for their valuable comments.

A5.6. References

Anderson, L.D., Delaney, M.L., 2000. Sequential extraction and analysis of phosphorus in marine sediments: streamlining of the SEDEX procedure. Limnology and Oceanography 45, 509-515.

Bargu, S., White, J.R., Li, C.Y., Czubakowski, J., Fulweiler, R.W., 2011. Effects of freshwater input on nutrient loading, phytoplankton biomass, and cyanotoxin production in an oligohaline estuarine lake. Hydrobiologia 661, 377-389.

Benitez-Nelson, C.R., 2000. The biogeochemical cycling of phosphorus in marine systems. Earth-Science Reviews 51, 109-135.

Bianchi, T.S., DiMarco, S.F., Cowan Jr, J.H., Hetland, R.D., Chapman, P., Day, J.W., Allison M.A., 2010. The science of hypoxia in the Northern Gulf of Mexico: a review. Science of the Total Environment 408, 1471-1484.

Brunner, C.A., Beall, J.M., Bentley, S.J., Furukawa Y., 2006. Hypoxia hotspots in the Mississippi Bight. The Journal of Foraminiferal Research 36, 95-107.

Canfield, D.E., Thamdrup, B., Hansen J.W., 1993. The anaerobic degradation of organic matter in Danish coastal sediments: iron reduction, manganese reduction, and sulfate reduction. Geochimica et Cosmochimica Acta 57, 3867-3883.

Colman, A.S., Holland H.D., 2000. The global diagenetic flux of phosphorus from marine sediments to the oceans: Redox sensitivity and the control of atmospheric oxygen levels: SEPM Special Publication 66, 53–75.

Conley, D.J., Smith, W.M., Cornwell, J.C., Fisher T.R., 1995. Transformation of particle-bound phosphorus at the land-sea interface. Estuarine, Coastal and Shelf Science 40, 161-176.

DeGroot, C.J., Golterman, H.L., 1990. Sequential fractionation of sediment phosphate. Hydrobiologia, 192, 143-148.

Delaney, M.L., 1998. Phosphorus accumulation in marine sediments and the oceanic phosphorus cycle. Global Biogeochemical Cycles 12, 563-572.

Diaz, J., Ingall, E., Benitez-Nelson, C., Paterson, D., de Jonge, M.D., McNulty, I., Brandes J.A., 2008. Marine polyphosphate: a key player in geologic phosphorus sequestration. Science 320, 652-655.

EPA (Environment Protection Agency), 2004. Evaluation of the role of nitrogen and phosphorus in causing or contributing to Hypoxia in the northern Gulf. U.S. Environmental Protection Agency Region 4: Atlanta, Georgia.

EPA (Environment Protection Agency), 2015. Mississippi River/Gulf of Mexico Watershed Nutrient Task Force. Action Plan for Reducing, Mitigating, and Controlling Hypoxia in the Northern Gulf of Mexico; Office of Wetlands, Oceans, and Watersheds, U.S. Environmental Protection Agency: Washington DC, 2001.

Filippelli, G.M., 2008. The global phosphorus cycle: past, present, and future. Elements 4, 89-95.

Filippelli, G.M., Delaney M.L., 1996. Phosphorus geochemistry of equatorial Pacific sediments. Geochimica et Cosmochimica Acta 60, 1479-1495.

Fisher, M.M., Reddy K.R., 2001. Phosphorus flux from wetland soils affected by long-term nutrient loading. Journal of Environmental Quality 30, 261-271.

Froelich, P.N., Bender, M.L., Luedtke, N.A., Heath, G.R., Devries T., 1982. The marine phosphorus cycle. American Journal of Science 282, 474–511.

Golterman, H.L., 1996. Fractionation of sediment phosphate with chelating compounds: a simplification, and comparison with other methods. Hydrobiologia, 335, 87-95.

Goolsby, D.A., Battaglin, W.A., Aulenbach, B.T., Hooper R.P., 2001. Nitrogen input to the Gulf of Mexico. Journal of Environmental Quality 30, 329-336.

Guo, L., Zhang, J.Z., Gueguen C., 2004. Speciation and fluxes of nutrients (N, P, Si) from the upper Yukon River. Global Biogeochemical Cycles 18(1).

Harris, D., Horwath, W.R., van Kessel, C., 2001. Acid fumigation of soils to remove carbonates prior to total organic carbon or carbon-13 isotopic analysis. Soil Science Society of America Journal, 65, 1853-1856.

Hedges, J.I., Stern, J. H., 1984. Carbon and nitrogen determinations of carbonate-containing solids1. Limnology and Oceanography, 29, 657-663.

Howarth R.W., Jensen, H.S., Marino, R., Postma H., 1995. Transport to and processing of P in nearshore and oceanic waters. In: Tiessen H (ed) Phosphorus in the global environment. Wiley, New York, 323–328.
http://water.epa.gov/type/watersheds/named/msbasin/zone.cfm.

Huanxin, W., Presley, B.J., Armstrong, D., 1994. Distribution of sedimentary phosphorus in Gulf of Mexico estuaries. Marine Environmental Research 37, 375-392.

Hupfer, M., Lewandowski J., 2008. Oxygen Controls the Phosphorus Release from Lake Sediments–a Long-Lasting Paradigm in Limnology. International Review of Hydrobiology 93, 415-432.

Ingall, E., Jahnke R., 1994. Evidence for enhanced phosphorus regeneration from marine sediments overlain by oxygen depleted waters. Geochimica et Cosmochimica Acta 58, 2571-2575.

Ingall, E., Kolowith, L., Lyons, T., Hurtgen M., 2005. Sediment carbon, nitrogen and phosphorus cycling in an anoxic fjord, Effingham Inlet, British Columbia. American Journal of Science 305, 240-258.

Jickells, T., 2005. External inputs as a contributor to eutrophication problems. Journal of Sea Research 54: 58-69.

Jones, P., Maiti, K., and McManus, J., 2014. Lead-210 and Polonium-210 disequilibria in the Northern Gulf of Mexico Hypoxic Zone. Marine Chemistry 169, 1-15.

Justic, D., Rabalais, N.N., Turner, R.E., 2003. Simulated responses of the Gulf of Mexico hypoxia to variations in climate and anthropogenic nutrient loading. Journal of Marine Systems 42, 115-126.

Kristensen, E., Ahmed, S.I., Devol, A.H., 1995. Aerobic and anaerobic decomposition of organic matter in marine sediment: which is fastest? Limnology and Oceanography 40, 1430-1437.

Ku, T.C.W., Walter, L.M., Coleman, M.L., Blake, R.E., Martini, A.M., 1999. Coupling between sulfur recycling and syndepositional carbonate dissolution: Evidence from oxygen and sulfur isotope composition of pore water sulfate, South Florida Platform, USA. Geochim. Cosmochim. Acta 63, 2529-2546.

Lai, D.Y.F., Lam, K.C., 2008. Phosphorus retention and release by sediments in the eutrophic Mai Po Marshes, Hong Kong. Marine Pollution Bulletin 57, 349-356.

Laurent, A., K. Fennel, J. Hu, and R. Hetland. 2012. Simulating the effects of phosphorus limitation in the Mississippi and Atchafalaya River plumes. Biogeosciences 9, 4707-4723.

Lebo, M.E., Sharp, J.H., 1992. Modeling phosphorus cycling in a well-mixed coastal plain estuary. Estuarine, Coastal and Shelf Science 35, 235-252.

Lin, P., Chen, M., Guo, L., 2012. Speciation and transformation of phosphorus and its mixing behavior in the Bay of St. Louis estuary in the northern Gulf of Mexico. Geochimica et Cosmochimica Acta 87, 283-298.

Lindstrom, S.M., and J.R. White. 2011. Reducing phosphorus flux from organic soils in surface flow treatment wetlands. Chemosphere 85, 625-629.

LUMCON (Louisiana Universities Marine Consortium), 2014. Press release, August 4, 2014. http://www.gulfhypoxia.net/Research/Shelfwide%20Cruises/2014/Hypoxia_Press_Release_2014.pdf.

Malecki, L.M., White, J.R., Reddy, R., 2004. Nitrogen and phosphorus flux rates from sediment in the lower St. Johns River estuary. Journal of environmental quality 33, 1545-1555.

Meybeck, M., 1982. Carbon, nitrogen, and phosphorus transport by world rivers. Am. J. Sci 282, 401-450.

Meybeck, M., 1993. C, N, P and S in rivers: from sources to global inputs. "Interactions of C, N, P and S Biogeochemical cycles and global change. Springer Berlin Heidelberg 163-193.

Mize, S.V., Demcheck, D.K., 2009. Water quality and phytoplankton communities in Lake Pontchartrain during and after the Bonnet Carre Spillway opening, April to October 2008, in Louisiana, USA. Geo-Marine Letters 29, 431-440.

Nguyen, N.T., 2014. Legacy phosphorus implications in the Lake Pontchartrain estuary sediment due to the 2011 Bonnet Carre Spillway opening. M.S. Thesis, Department of Oceanography and Coastal Science, Louisiana State University, Baton Rouge, Louisiana.

NOAA (National Oceanic and Atmospheric Administration), 2011. National Coastal Data Development Center, Gulf of Mexico Hypoxia Watch Bottom Dissolved Oxygen Contours for June and July SEAMAP Cruise of 2011. http://www.ncddc.noaa.gov/hypoxia/products/.

Paytan, A., McLaughlin, K., 2007. The oceanic phosphorus cycle. Chemical Reviews 107, 563-576.

Rabalais, N.N., Turner, R.E., Diaz, R.J., Justic, D. 2009. Global change and eutrophication of coastal waters ICES J. Mar. Sci. 66, 1528–1537.

Rabalais, N.N., Turner, R.E., Scavia, D., 2002a. Beyond Science into Policy: Gulf of Mexico Hypoxia and the Mississippi River Nutrient policy development for the Mississippi River watershed reflects the accumulated scientific evidence that the increase in nitrogen loading is the primary factor in the worsening of hypoxia in the northern Gulf of Mexico. BioScience 52, 129-142.

Rabalais, N.N., Turner, R.E., Wiseman Jr, W.J., 2002b. Gulf of Mexico hypoxia, AKA" The dead zone". Annual Review of ecology and Systematics 33, 235-263.

Reddy, K.R., Newman, S., Osborne, T.Z., White, J.R., Fitz, H.C., 2011. Phosphorous cycling in the greater Everglades ecosystem: Legacy phosphorous implications for management and restoration. Critical Reviews in Environmental Science and Technology 41, 149-186.

Reddy, K.R., Wang, Y., DeBusk, W.F., Fisher, M.M., Newman, S., 1998. Forms of soil phosphorus in selected hydrologic units of the Florida Everglades. Soil Science Society of America Journal 62, 1134-1147.

Redfield, A.C., 1958. The Biological Control of Chemical Factors in the Environment. American Scientist 46, 1- 221.

Roy, E.D., Nguyen, N.T., Bargu, S., White, J.R., 2012. Internal loading of phosphorus from sediments of Lake Pontchartrain (Louisiana, USA) with implications for eutrophication. Hydrobiologia 684, 69-82.

Roy, E.D., White, J.R., Smith, E.A., Bargu, S., Li, C., 2013. Estuarine ecosystem response to three large-scale Mississippi River flood diversion events. Science of the Total Environment 458, 374-387.

Ruttenberg, K.C., 1992. Development of a sequential extraction method for different forms of phosphorus in marine sediments. Limnology and Oceanography, 37, 1460-1482.

Ruttenberg, K.C., Berner. R.A., 1993. Authigenic apatite formation and burial in sediments from non-upwelling, continental margin environments. Geochimica et cosmochimica acta 57, 991-1007.

Ruttenberg, K.C., Goni, M.A., 1997. Phosphorus distribution, C:N:P rations, and $\delta^{13}C_{oc}$ in artic, temperature, and tropical coastal sediments: tools for characterizing bulk sedimentary organic matter. Marine Geology 139, 123-145.

Ruttenberg, K.C., Tamburini, N.O., Ogawa, F., Briggs, A.A., Colasacco, N.D., Joyce, E., 2009. Improved, high-throughput approach for phosphorus speciation in natural sediments via the SEDEX sequential extraction method. Limnology and Oceanography: Methods 7, 319-333.

Scavia, D., Donnelly, K.A., 2007. Reassessing hypoxia forecasts for the Gulf of Mexico. Environmental science & technology 41, 8111-8117.

Scavia, D., Justic, D., Bierman, V.J., 2004. Reducing hypoxia in the Gulf of Mexico: advice from three models. Estuaries 27, 419-425.

Scavia, D., Rabalais, N.N., Turner, R.E., Justic, D., Wiseman Jr, W.J., 2003. Predicting the response of Gulf of Mexico hypoxia to variations in Mississippi River nitrogen load. Limnology and Oceanography 48, 951-956.

Scott, D.T., Keim, R.f., Jones, C.N., Edwards, B.L., Kroes, D.E., 2014. Floodplain biogeochemical processing of floodwaters during the Mississippi River flood of 2011. Journal of Geophysical Research 119, 537-546.

Suess, E., 1980. Particulate organic carbon flux in the oceans-surface. Nature 288, 260-263.

Sutula, M., Bianchi, T.S., McKee, B.A., 2004. Effect of seasonal sediment storage in the lower Mississippi River on the flux of reactive particulate phosphorus to the Gulf of Mexico. Limnology and Oceanography 49, 2223-2235.

Sylvan, J.B., Dortch, Q., Nelson, D.M., Maier Brown, A.F., Morrison, W., Ammerman, J.W., 2006. Phosphorus limits phytoplankton growth on the Louisiana shelf during the period of hypoxia formation. Environmental science & technology 40, 7548-7553.

Turner, R.E., Rabalais, N.N., Justic, D., 2008. Gulf of Mexico hypoxia: Alternate states and a legacy. Environmental Science & Technology 42, 2323-2327.

Turner, R.E., Rabalais, N.N., Justic, D., Dortch, Q., 2003. Global patterns of dissolved N, P and Si in large rivers. Biogeochemistry 64, 297-317.

Van Cappellen, P., Ingall, E.D., 1994. Benthic phosphorus regeneration, net primary production, and ocean anoxia: A model of the coupled marine biogeochemical cycles of carbon and phosphorus. Paleoceanography 9, 677-692.

Wang, G.P., Liu, J.S., Wang, J.D., Yu, J.B., 2006. Soil phosphorus forms and their variations in depressional and riparian freshwater wetlands (Sanjiang Plain, Northeast China). Geoderma 132, 59-74.

White, J.R., Reddy, R., Moustafa, M.Z., 2004. Influence of hydrologic regime and vegetation on phosphorus retention in Everglades stormwater treatment area wetlands. Hydrological processes 18, 343-355.

Zhang, J.Z., Fischer, C.J., Ortner, P.B., 2004. Potential availability of sedimentary phosphorus to sediment resuspension in Florida Bay. Global Biogeochemical Cycles 18(4).

Zhang, W., White, J.R., DeLaune, R.D., 2012. Diverted Mississippi River sediment as a potential phosphorus source affecting coastal Louisiana water quality. Journal of Freshwater Ecology 27, 575-586.

VITA

Puspa Lal Adhikari was born to Giri Prasad Adhikari and Maya Adhikari in a rural area of Parbat district of Nepal. When he was 12, his family migrated to the capital city of the country, Kathmandu. He attended Tri-Chandra College in Kathmandu and graduated with a B.S. degree in Environmental Science with minors in Chemistry and Biology. A keen interest on teaching led him to work as a high school science and environment teacher at Eureka High School for several years. Puspa earned his first M.S. degree in Environmental Science from Tribhuvan University in 2006, and continued his teaching career until 2009. In 2009, he moved to the United States of America to pursue his second master's degree in Aquaculture and Fisheries at University of Arkansas at Pine Bluff. After receiving his second M.S. degree, he joined the Marine Geochemistry lab at Louisiana State University to pursue his doctorate degree in the Department of Oceanography and Coastal Sciences under the supervision of Dr. Kanchan Maiti. The major focus of his PhD dissertation was to study the Polycyclic Aromatic Hydrocarbon dynamics in the northern Gulf of Mexico.